

**UNIVERSIDADE FEDERAL DO RIO GRANDE DO SUL
INSTITUTO DE GEOCIÊNCIAS
PROGRAMA DE PÓS-GRADUAÇÃO EM GEOCIÊNCIAS**

**TRANSPOSIÇÃO DE SEDIMENTOS NOS PROMONTÓRIOS DA
COSTA NORTE DA ILHA DE SANTA CATARINA**

GUILHERME VIEIRA DA SILVA

ORIENTADOR – Prof. Dr. Elírio Ernestino Toldo Júnior

CO-ORIENTADORES: Prof. Dr. Antônio Henrique da Fontoura Klein

Prof. Dr. Andrew D. Short

Prof. Dr. Colin Woodroffe

Porto Alegre – 2016

**UNIVERSIDADE FEDERAL DO RIO GRANDE DO SUL
INSTITUTO DE GEOCIÊNCIAS
PROGRAMA DE PÓS-GRADUAÇÃO EM GEOCIÊNCIAS**

**TRANSPOSIÇÃO DE SEDIMENTOS NOS PROMONTÓRIOS DA
COSTA NORTE DA ILHA DE SANTA CATARINA**

GUILHERME VIEIRA DA SILVA

ORIENTADOR – Prof. Dr. Elírio Ernestino Toldo Júnior

CO-ORIENTADORES: Prof. Dr. Antônio Henrique da Fontoura Klein

Prof. Dr. Andrew D. Short

Prof. Dr. Colin Woodroffe

BANCA EXAMINADORA:

Prof. Dr. Antonio Fernando Härter Fetter Filho - Departamento de Geociências -
Universidade Federal de Santa Catarina - UFSC

Prof. Dr. Lauro Júlio Calliari - Instituto de Oceanografia - Universidade Federal do Rio
Grande - FURG

Prof. Dr. Wiliam Correa Marques - Instituto de Matemática, Estatística e Física -
Universidade Federal do Rio Grande - FURG

Tese de Doutorado apresentada como
requisito parcial para a obtenção do
título de Doutor em Ciências

Porto Alegre – 2016

UNIVERSIDADE FEDERAL DO RIO GRANDE DO SUL

Reitor: Carlos Alexandre Netto

Vice-Reitor: Rui Vicente Oppermann

INSTITUTO DE GEOCIÊNCIAS

Diretor: André Sampaio Mexias

Vice-Diretor: Nelson Luiz Sambaqui Gruber

Silva, Guilherme Vieira da

Transposição de sedimentos nos promontórios da costa norte da Ilha de Santa Catarina . / Guilherme Vieira da Silva. - Porto Alegre: IGEO/UFRGS, 2016.

[130 f.] il.

Tese (Doutorado).- Universidade Federal do Rio Grande do Sul. Programa de Pós-Graduação em Geociências. Instituto de Geociências. Porto Alegre, RS - BR, 2016.

Orientador(es):Elírio Ernestino Toldo Júnior
Coorientador(es):Antonio Henrique da Fontoura Klein

1. Linha de costa 2. Modelagem numérica 3. Balanço Sedimentar
4. Transporte de Sedimentos I. Título.

CDU 551.468.1

Catálogo na Publicação

Biblioteca Instituto de Geociências - UFRGS

Renata Cristina Grun

CRB 10/1113

Dedicatória

*À Aninha, minha esposa,
com amor.*

AGRADECIMENTOS

Não se constrói uma tese de doutorado sozinho. Muita gente ajuda de diversas maneiras, seja inspirando, ensinando, compartilhando ideias, apoiando ou financiando. Por esse motivo, gostaria de registrar meus agradecimentos especiais aos que de alguma forma contribuíram para a conclusão desta tese:

- À minha esposa e grande incentivadora. Obrigado por estares do meu lado e por me apoiares incondicionalmente. Eu te amo!

- À minha família, em especial à minha mãe, meu pai, meus irmãos, meus avós e ao nino que me inspiraram, serviram de exemplo e deram forças para seguir a caminhada. Vocês são demais!

- À querida família Polli que passou a ser minha também. Obrigado pelo apoio e acolhimento;

- Ao professor Antônio Klein, que acompanho desde 2005, pelos ensinamentos, revisões e portas abertas;

- Ao professor Elírio Toldo Jr., orientador de mestrado e doutorado e pela confiança e incentivo;

- Ao professor Andrew Short por acompanhar esse trabalho desde o início dando sempre um excelente *feedback*, foi um prazer e uma honra tê-lo como meu co-orientador;

- Ao professor Colin Woodroffe, ao pessoal do "*coastal coffee*" e aos pós graduandos da UOW por me receberem na Austrália, pelas conversas e ensinamentos;

- À família Bonetti pela parceria na Austrália. Foi muito bom conviver com vocês (também) por lá. À Carla por toda a ajuda estatística e ao Jarbas pelas conversas e ideias;

- Aos meus irmãos de Porto Alegre, em especial Gabriel e Miojo por me acolherem tantas vezes em suas casas.

- Ao pessoal que ajudou nos trabalhos de campo: Cultura Subaquática, Charline Dalinghaus, Diego Porpilho, Maiara Werner, Paula Gomes, Rafael Sartori, vocês foram show!

- À Mariela Muller e ao Michel Franco pelo esforço no levantamento de dados e georreferenciamento das imagens aéreas;
- Ao pessoal do LOC pelas trocas de ideias relacionadas (ou não) com a tese;
- À galera da CB&I por todo o conhecimento que obtive no tempo que estive aí;
- Aos pós-graduandos do CECO;
- À CB&I, à CASAN e ao MMA - Fundo Clima por disponibilizarem dados utilizados nessa tese;
- Projeto MMA-Riscos - Termo de cooperação MMA/UFSC: 010/2011- Contrato UFSC/FAPEU: 035/2012
- CNPq processos: 471879/2013-4, 400302/2012-8, 140738/2012-6
- CAPES processo BEX nº 5809/14-2

RESUMO

Esta tese teve o objetivo de identificar e quantificar os processos geradores da transposição de sedimentos entre praias de enseada e propor um modelo conceitual da dinâmica sedimentar para o norte da Ilha de Santa Catarina, entre as praias arenosas de Santinho, Ingleses, Brava, Lagoinha, Ponta das Canas, Canasvieiras, Jurerê, Forte e Daniela. Para isso, foi dividida em três partes. Nos estudos geomorfológicos do sistema praial, na primeira parte, foram utilizadas imagens aéreas (1957, 1978, 1998, 2002 e 2010), levantamentos da linha de costa com RTK-GPS (2012) e topo-batimetria da área emersa e submersa adjacente, além de dados de maré. As imagens foram retificadas, as posições das linhas de costa foram vetorizadas e os erros do processo de retificação relacionados à maré foram calculados. Duas metodologias foram utilizadas: 1) método de regressão linear (tendências) e 2) distâncias Euclidianas em conjunto com análise ano-a-ano. Os resultados indicam o transporte entre as praias no sentido anti-horário, sendo este responsável pelo desenvolvimento de três pontais arenosos ao longo da área, possivelmente alimentados pelo transporte subaquoso de sedimentos das praias a barlar. O pontal de Ponta das Canas controla a disponibilidade de sedimentos a sotamar. E, quando está se desenvolvendo atua como uma armadilha de sedimentos e as praias a sotamar regridem, quando o pontal se une à costa disponibilizando sedimento, as praias a sotamar progradam. Para a análise do balanço de sedimentos, na segunda parte, foram adquiridos dados de batimetria de detalhe, perfis de praia, transporte de sedimentos, ondas, correntes e marés. Os dados mostram que o volume de sedimentos trapeados decrescem em direção à porção protegida da área de estudo com distribuição de tamanho de grão compatível, suportando a hipótese de conexão entre as praias. Um modelo numérico foi configurado, calibrado e validado através de medições *in situ*. Três formulas de transporte de sedimentos foram testadas e comparadas com os dados medidos, e aquela que melhor reproduz o processo na área de estudo foi identificada. Ainda, foi realizada uma simulação anual com a intenção de identificar como e onde ocorre o transpasse de sedimentos. Os resultados indicam o sentido anti-horário de transporte na área de estudo. A terceira e última parte consistiu em estudar a contribuição das forçantes; marés, ventos e ondas na indução da transposição de sedimentos, gerando um modelo conceitual para o processo. Foram simulados 26 cenários incluindo diversas condições de marés, ventos e ondas. As ondas representam a principal forçante da transposição entre as praias estudadas, transportando sedimentos com taxas entre duas e três ordens de magnitude acima do transportado por marés ou vento. A transposição de sedimentos ocorre preferencialmente no sentido anti-horário, podendo ocorrer inversões dependendo das condições oceanográficas vigentes. Nas praias voltadas para leste a maior parte da transposição de sedimentos no sentido anti-horário ocorre sob condições de ondas entre sul e leste. Nas praias voltadas para norte, as ondas de nordeste ditam o transporte ao redor dos promontórios. Esta tese contribuiu para o entendimento da dinâmica sedimentar da costa norte da Ilha de Santa Catarina. Foi demonstrado e documentado que a transposição de sedimentos ocorre mesmo quando o padrão cíclico descrito na literatura não está presente. Além disso, foram identificadas as condições necessárias para que o processo ocorra, gerando um modelo conceitual para a área. A transposição de sedimentos é fundamental para o balanço sedimentar, destacando-se a importância da compreensão do todo ao invés de considerar praias de enseada como células fechadas.

ABSTRACT

This thesis aims to identify and quantify of the process that generate headland sand bypassing, and in doing so develop a conceptual model of these process around the north coast of Santa Catarina island. The research project was divided into three parts: Part 1: Aerial images (1957, 1978, 1998, 2002 e 2010) and a RTK-GPS survey (2012) were used together with a topo-bathymetric data and a tide time-series. The images were rectified, the shoreline extracted and the rectification and tide-related errors were calculated. Two methods were used: 1) linear regression (general trend) and; 2) Euclidean distances together with a year-to-year analyzis. The results indicate the anticlockwise sediment transport which is also responsible for developing three spits along the study area, possibly nourished by the updrift beaches. Ponta das Canas spit, for example, controls the sediment availability of the downdrift areas. When it is growing it acts as a sediment trap and the downdrift areas retreat, when it merges to the coast it spreads the sediment towards the downdrift areas that then progrades; Part 2 is a dataset composed of detailed bathymetry, beach profiles, sediment transport, waves, currents and tides. The data showed that the volume of sediment trapped decreases towards the protected area while maintaining the grain size distribution, supporting the hypothesis of connections between beaches. A numerical model was set up, calibrated and validated (waves, currents and tides). Three sediment transport formulas were tested and compared with measured transport and the one that best reproduce the process was identified. An annual simulation was performed aiming to identify if/where the headland bypassing occurs. The results indicate the anticlockwise sediment transport in the study area; Part 3 consists of a study of the contribution of the driving forces (waves, tides, wind) to headland bypassing, generating a conceptual model for the entire process. Twenty-six scenarios were simulated using several waves, tides and wind conditions. Waves were found to be the main driving force for headland bypassing, transporting sediments in rates two to three orders of magnitude above the transported by tides or winds. The headland bypassing occurs mainly in anticlockwise direction but it can also occur in the opposite direction depending on the wave-tide-wind conditions. In the east-facing beaches, most of the headland bypassing is anticlockwise under waves from the south to east. On the sheltered north-facing beaches, northeast waves dictate the headland sediment transport. The present thesis contributed for the knowledge of the headland sediment bypassing, demonstrated that the process occur in the study area and documented it even when the pulsative cycle described in literature is not present. It is highlighted the importance of the "big picture" comprehension rather than consider embayed beaches as closed cells.

LISTA DE FIGURAS

Figura 1: Esquematisação do processo de transposição sedimentar. fonte: Short (1999).....	2
Figura 2: Área de estudo: região norte da Ilha de Santa Catarina.	4
Figura 3: Modelo conceitual da transposição contínua de sedimentos gerado pela ação das ondas (seta alaranjada), e o ingresso de sedimentos eólicos pelo campo de dunas do Santinho (seta vermelha).	7
Figura 4: Modelo conceitual de transporte de sedimentos induzido por ondas na região Norte de da Ilha de Santa Catarina	8
Figura 5: Modelo conceitual de transporte de sedimentos induzido por marés na região norte de Florianópolis.....	9

Figure 1: Location of the study area on the southern of Brazil and morphological details between the beaches in the north area of the Santa Catarina Island. Background image: ESRI Basemap imagery. ESRI World Imagery (ArcGIS 10).	16
Figure 2: HWL frequency - 95% of the central frequency occurrence was assumed as the HWL range - note that both tails (<2.5 and >97.5%) of the distribution were not considered.....	21
Figure 2: Bathymetry of the study area (top) and bathymetric profiles (bottom) vertical <i>datum</i> mean sea level. Note that the measured bathymetry was completed with nautical charts. Bar: Barra da Lagoa- Moçambique; Sant: Santinho; Ing: Ingleses; Br: Brava; Lag: Lagoinha; Pta: Ponta das Canas - Canasvieiras; Jur: Jurerê; For: Forte and; Dan: Daniela. The profiles presented at the bottom are shown on the top from A (land) to B (offshore). Background image: ESRI World Imagery (ArcGIS 10). See Figure 1 for location of beaches.....	24
Figure 3: a) Maximum shoreline displacement (m); b) Shoreline changes trend at the study area by Linear Regression Rate method ($m\ yr^{-1}$) - changes lower than the calculated error are represented in white.	26
Figure 4: a) Dunefield migrating from Santinho to Ingleses Beach; b) Ponta das Canas spit developing - notice the eroded portion downdrift of the spit as well as the downdrift spreading of the former spit; c) minor sand wave migration at east Jurerê; d) Forte beach at bottom presenting the sand wave pattern and Daniela spit. Photos by Andrew Short, Mariela Muler and Raphael Ribeiro.....	28

Figure 5: a) Euclidean distance matrix indicating similarities (blue) and differences (yellow-red) among the beach transects at every 50 m - the arrows (bottom and the left side) represent the direction indicated on figure b. b) the arrow indicates the direction of the Euclidean matrix presented on the left (a). Bar = Barra - Moçambique, Sant = Santinho, Ing = Ingleses, Br = Brava; Lag = Lagoinha; Pta = Ponta das Canas - Canasvieiras, Jur = Jurerê, For = Forte and; Dan = Daniela.	29
Figure 6: Shoreline changes (m yr^{-1}) along the temporal series analysed by End Point Rate (EPR) - changes lower than the calculated error are represented in white.	30
Figure 7: Schematic sediment path at the study area. It is highlighted the migrating dunefield from Santinho to Ingleses as well as the spit development at Ponta das Canas, Jurerê and Forte indicating the anticlockwise net sediment transport. Background image: ESRI World Imagery (ArcGIS 10); Santinho dunefield photo by A D Short.	32
Figure 8: Location of the study area on the southern coast of Brazil and location of the measured data. STs : ADCP locations; HSs: Helley-Smith trapping locations. Background image source: ESRI World Imagery (ArcGIS 10).	48
Figure 9: Flow diagram illustrating the methods of sediment trapping experiment and data processing (left) and modelling procedures (right) as well as the connection between both methods.	50
Figure 10: Numerical model wave grids, location of WW3 wave data, CFSv2 wind data, TPXO predicted tides and Armação tide gauge. Background image source: ESRI World Imagery (ArcGIS 10).	54
Figure 11: Environmental conditions measured at ST17 (see Figure 8) during the sediment trap experiment (wl: water level; U: zonal velocity; V: meridional velocity; Hs: significant wave height; Tp: peak wave period; Dirp: peak wave direction). The rectangles indicate the trapping period for each location - 20 samples were collected within the time encompassed by each rectangle.	59
Figure 12: Measured sediment transport rates (m^2s^{-1}) for four locations at field work 1 (top panel) and field work 2 (bottom panel). * represent the median sediment transport, the rectangles are the quartiles (25 and 75%), the lines indicate the maximum values not considered outliers and the circle is the outlier value. Values presented here encompass all 140 samples (20 samples / location / FW). Note different vertical scales.	60

Figure 13: Grain size distribution for 6 samples of each location / field work. The highlighted picture shows the presence of coarser composition due biotritic (shell pieces) material at Brava FW1.	61
Figure 14: Hydrodynamic and wave model calibration and mean absolute error (MAE) - austral summer. From top to bottom: Hs: Significant wave height; Tp: peak wave period; Dirp: peak wave direction; wl: water level; U: depth average zonal velocity; V: depth average meridional velocity. From left to right: ST15, ST16 and ST17 - see Figure 8.....	63
Figure 15: Hydrodynamic and wave model validation and mean absolute error (MAE) - austral winter. From top to bottom: Hs: Significant wave height; Tp: peak wave period; Dirp: peak wave direction; wl: water level; U: depth average zonal velocity; V: depth average meridional velocity. From left to right: ST15, ST16 and ST17 - see Figure 8.	63
Figure 16: Sediment transport formula comparison. The diagonal solid line represent perfect agreement between measured and simulated bedload transport, the dashed lines represent a factor of 0.5 and 2 of the perfect agreement indicating a good agreement buffer as described by Camenen and Larroudé (2003).....	64
Figure 17: Mean direction of sand transport during the simulated year (2014). Arrows are indicative of the direction of transport, colours indicate the magnitude (m^2yr^{-1}). Background image source: Landsat 7.	65
Figure 18: Predicted sediment transport in $\text{m}^3 \text{yr}^{-1}$ at the study area. A, B, C and D represent a zoom of the Figure 17 including the transport rates at specific locations. A) headland between Santinho (south) and Ingleses (north); B) headland between Ingleses (south) and Brava (north); C) headlands between Brava (east) and Lagoinha (north) and between Lagoinha (north) and Ponta das Canas (west) and; D) protected areas, including Ponta das Canas - Canasvieiras, Jurerê, Forte and Daniela beaches as well as the headland between them. Background image source: Landsat 7.	66
Figure 19: Study area, dataset location, numerical grids, transect location where the transport rates were integrated for every simulation.	86
Figure 20: Transport ($\text{m}^3 \text{yr}^{-1}$) during tide scenario simulation per location (see Figure 19). + indicate sediment transport in clockwise direction (exiting bay); - indicate anticlockwise direction of sediment transport (towards the bay). Magnitudes lower than $50 \text{ m}^3 \text{yr}^{-1}$ are suppressed of the figure.....	91

- Figure 21: Transport ($\text{m}^3 \text{yr}^{-1}$) during wind scenario simulation per location (see Figure 1). Av=Average; Ex=extreme; NW=Northwest; N=North; NE=Northeast, E=East, SE Southeast; S=South and SW=Southwest. + indicate sediment transport in clockwise direction (exiting bay); - indicate anticlockwise direction of sediment transport (towards the bay). Magnitudes lower than $50 \text{ m}^3 \text{y}^{-1}$ are suppressed of the figure. 92
- Figure 22: Transport ($\text{m}^3 \text{yr}^{-1}$) during wave scenario simulation per location (see Figure 1). Av=Average; Ex=extreme; NE=Northeast, E=East, SE Southeast and S=South. + indicate sediment transport in clockwise direction (exiting bay); - indicate anticlockwise direction of sediment transport (towards the bay). Magnitudes lower than $50 \text{ m}^3 \text{y}^{-1}$ are suppressed of the figure..... 94
- Figure 23: Conceptual model of conditions that generate headland sand bypassing in anticlockwise (A) and clockwise directions (C) *press*). Hollow circles indicate that sediment transport does not occur in this direction. The arrows represent the sediment transport based on Vieira da Silva (*in press*) for anticlockwise (net) and the opposite of the authors suggestions for clockwise. Colours represent the magnitude of the sediment transport for each scenario in $\text{m}^3 \text{y}^{-1}$ 100

LISTA DE TABELAS

Table 1: Images sources, resolution and scale.....	18
Table 2: Errors related to rectifying process (1957 to 2010), to RTK- GPS survey (2012) and to tidal variations (μ = mean; σ = standard deviation) per beach.	22
Table 3: General trend summary per beach.	25
Table 4: Wave model calibration parameters.....	56
Table 5: FLOW model calibration parameters.	56
Table 6: Mean absolute error (MAE) in percentage. Note that excepting the peak wave direction on ST17 and zonal velocity during validation on ST15 (bold) all the errors are lower than 15%. Hs: Significant wave height; Tp: peak wave period; Dirp: peak wave direction; wl: water level; U: zonal current velocity; V: meridional current velocity.	62
Table 7: Summary of physical settings (Truccolo et al., 2004; Nobre et al., 1996; Truccolo, 2011 and Araújo et al., 2003).	87
Table 8: Modelled scenarios.....	90

SUMÁRIO

INTRODUÇÃO	1
1.1 Área de Estudo	3
1.2 Objetivo Geral	5
1.2.1 Objetivos Específicos	5
1.3 Hipóteses	6
1.4 Sobre a Estrutura desta Tese:.....	9
SHORELINE CHANGE ANALYSES AND INSIGHT INTO THE SEDIMENT TRANSPORT PATH ALONG SANTA CATARINA ISLAND NORTH SHORE, BRAZIL	11
1 INTRODUCTION.....	14
2 Regional Settings.....	16
3 METHODS	18
3.1 Dataset.....	18
3.2 Shoreline Indicator	19
3.3 Shoreline Position Error Quantification	20
3.4 Shoreline Changes.....	22
4 RESULTS.....	23
4.1 Spit formation.....	27
4.2 Beach rotation.....	31
5 DISCUSSION.....	31
5.1 Barra-Moçambique.....	32
5.2 Santinho-Ingleses	33
5.3 Ingleses-Brava	33
5.4 Brava-Lagoinha.....	34
5.5 Lagoinha-Ponta das Canas.....	34
5.6 Jurerê and Forte spits	34

5.7 Daniela spit	35
6 CONCLUSIONS.....	35
HEADLAND SAND BYPASSING - QUANTIFICATION OF NET SEDIMENT TRANSPORT IN EMBAYED BEACHES, SANTA CATARINA ISLAND NORTH SHORE, SOUTHERN BRAZIL.....	43
1 Introduction	46
2 Regional Settings.....	47
3 Materials and Methods.....	50
3.1 Sediment Trapping and Samples Processing.....	50
3.2 Numerical Modelling.....	53
3.2.1 Wave Model.....	53
3.2.2 Flow Model	54
3.2.3 Model Calibration and Validation Procedure.....	55
3.2.4 Sediment Transport	56
4 Results.....	58
4.1 Sediment Trapping Experiment.....	58
4.2 Numerical modelling.....	61
5 Discussion.....	68
5.1 Numerical Modelling.....	69
6 Conclusions	73
IDENTIFICATION OF DRIVING FORCES AND THEIR IMPORTANCE FOR HEADLAND SAND BYPASSING ON THE NORTH SHORE, SANTA CATARINA ISLAND, SOUTHERN BRAZIL.....	82
1 Introduction	84
2 Regional Settings.....	85
3 Materials and Methods.....	88
4 Results.....	90
5 Discussion.....	95

5.1	Santinho - Ingleses (T1 to T5).....	95
5.2	Ingleses - Brava (T7-T9)	95
5.3	Brava - Lagoinha (T10-T14).....	96
5.4	Lagoinha-Ponta das Canas - Canasvieiras - (T14-T16).....	96
5.5	Ponta das Canas - Canasvieiras - Jurerê (T17-T18).....	97
5.6	Jurerê - Forte (T19-T20)	97
5.7	Forte - Daniela - North Bay (T21-T23)	97
5.8	Conceptual model of headland bypassing	98
6.	Conclusions.....	100
	TRABALHOS FUTUROS	108
	CONSIDERAÇÕES FINAIS	109
	REFERÊNCIAS BIBLIOGRÁFICAS.....	112

INTRODUÇÃO

Promontórios, desembocaduras e estruturas construídas pelo homem atuam como um obstáculo ao transporte de sedimentos ao longo da costa. O fluxo de água e sedimentos é interrompido (ou reduzido) implicando em um acúmulo de sedimentos a sotamar. Desta maneira, a total compreensão da transposição de sedimentos e dos fatores que a geram são de fundamental importância para o entendimento do balanço de sedimentos na região costeira.

O conhecimento das taxas de transporte de sedimentos em uma determinada área, em geral, está restrito à praias retilínea ou embaiamentos, muitas vezes considerados células fechadas. Alguns estudos, entretanto, descreveram conceitualmente o processo de transposição de sedimentos no entorno dos promontórios (Evans, 1943; Short e Masselink, 1999 e Smith, 2001). Apesar de poucos estudos terem se dedicado ao estudo da transposição sedimentar ao redor de promontórios, muitos outros (Silvester, 1985; FitzGerald *et al.*, 2000; FitzGerald e Pendleton, 2002; Cheung *et al.*, 2007; Mariani, 2010; Eslami *et al.* 2010; Ab Razak *et al.* 2013; Garel *et al.* 2015) descrevem o mecanismo de transposição em estruturas construídas pelo homem (e.g. molhes) ou em desembocaduras.

Mais recentemente, as investigações buscaram entender o processo com base em dados medidos em campo e modelos numéricos, os quais incluem variações batimétricas da plataforma antepraia (Goodwin *et al.*, 2013) que relacionaram a transposição de sedimentos com a variabilidade do clima de ondas; uso de imagens de satélite e dados de RTK-GPS (Ribeiro *et al.*, 2014); uso de sedimentos marcados Duarte *et al.*, (2014); George *et al.* (2015) que desenvolveram uma classificação e investigaram as células costeiras associadas com diferentes tipos de promontórios; Ab Razak (2015), reproduziu e estudou esta mecânica numericamente. Apesar do crescente interesse nesse tópico, George *et al.* (2015), destaca que estudos que conectam os processos oceanográficos às taxas de transporte de sedimentos e mudanças morfológicas ainda são escassos.

O modelo de transposição de sedimentos mais aceito na literatura foi apresentado por Short e Masselink (1999). Segundo os autores, a transposição de sedimentos se manifesta em duas etapas. A primeira é o acúmulo do sedimento na porção a barlar do promontório pelo processo de rotação praias. A segunda, é o movimento

aparente do sedimento ao redor do promontório, inicialmente identificável por um grande banco a barlar do promontório. Em seguida o banco se move em direção à costa podendo resultar em acresção significativa da praia, entretanto, a maior parte do sedimento permanece na porção subaquosa. Ondas de areia (*sandwaves*) migram na direção barlar, formando feições que variam entre pequenas ondas de areia a longos pontais arenosos. A onda em seu percurso de migração se move como um banco de fundo, largo, raso e ligado à praia, ou como um prolongamento de pontal arenoso que pode gerar uma laguna associada. As duas últimas formas de migração normalmente geram erosão a barlar imediatamente a frente do banco/pontal. Por fim, o banco/pontal se une a praia, não sendo mais possível sua identificação (Figura 1)

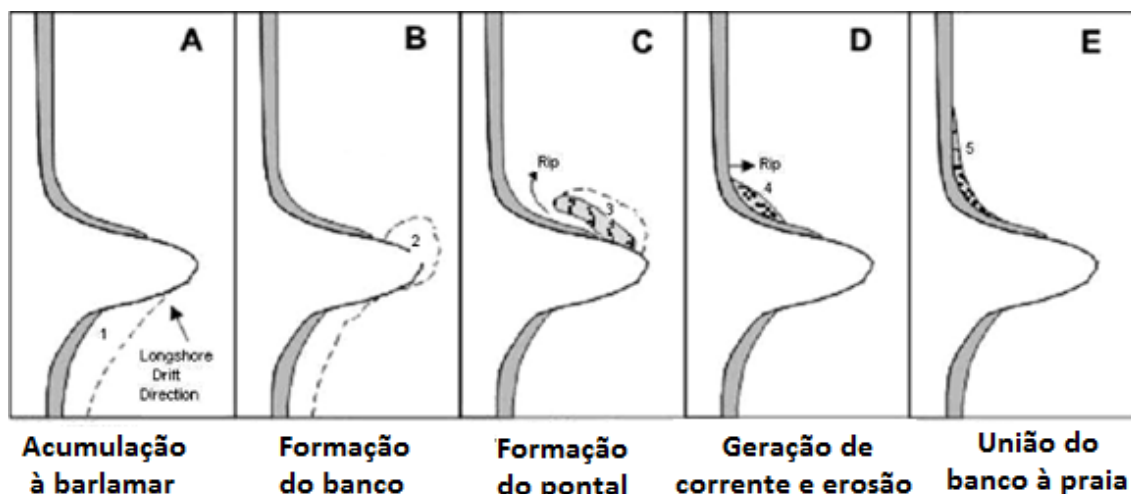


Figura 1: Esquematização do processo de transposição sedimentar. fonte: Short (1999).

A esquematização proposta por Short e Masselink (1999), ocorre principalmente associado ao processo de rotação praial. Entretanto, a transposição de sedimentos pode acontecer em praias que não experimentam esta dinâmica sedimentar. Segundo Silveira *et al.* (2010), se a extremidade do promontório está em profundidades inferiores à profundidade de fechamento, pode haver a transposição de sedimentos. Neste caso, se não existir a rotação praial, o transporte pode ocorrer de forma contínua. O sedimento pode ainda transpor um promontório através de dunas migratórias ou ainda na face da praia, durante marés altas.

Maior parte dos estudos sugerem que a principal forçante para a transposição de sedimentos são as ondas (i.e. Evans, 1943; Short e Masselink, 1999, Smith, 2001, Goodwin *et al.*, 2013 Ab Razak, 2015). Contudo, Masselink e Pattiaratchi (1998) descreveram a importância dos ventos em ambientes de baixa energia, enquanto

Lessa *et al.* (2001), sugerem que as correntes de maré são importantes componentes do transporte longitudinal de sedimentos em áreas próximas à grandes baías. Apesar disso não havia até o momento um registro na literatura da influência das correntes geradas por ventos e marés no processo de transposição de sedimentos.

Este trabalho tem o intuito de: identificar a transposição de sedimento nos promontórios, inferindo os processos e agentes que causam e facilitam a dinâmica sedimentar, e também gerar modelos conceituais da transposição sedimentar para a área de estudo.

1.1 Área de Estudo

A área compreende a região norte da Ilha de Santa Catarina, com enfoque nos promontórios entre as praias de Ingleses, Brava, Lagoinha, Ponta das Canas - Cachoeira do Bom Jesus, Canasvieiras, Jurerê, Forte e Daniela (Figura 2), localizada na cidade de Florianópolis- SC, região sul do Brasil. De acordo com Simó e Horn Filho (2004), em uma análise sobre ressacas ocorridas entre os anos de 1991 e 2001 apontam entre as onze praias mais atingidas por ressacas as praias de Canasvieiras, Ingleses, e Ponta das Canas, indicando a importância do transporte sedimentar em momentos de alta energia de ondas, mesmo em se tratando de praias com baixa energia (Canasvieiras e Ponta das Canas). Além dessas praias, os autores encontraram evidências erosivas nas praias Brava, Jurerê.



Figura 2: Área de estudo: região norte da Ilha de Santa Catarina.

Na região, o clima é do sub-tipo clima temperado chuvoso (Cfa), sem estações de seca e com verões quentes (GAPLAN, 1986). De acordo com o IBGE (2010), a região da grande Florianópolis apresenta clima temperado de categoria Sub-quente, com temperaturas médias entre 15 e 18°C no inverno e entre 24 e 26°C no verão, a média anual de temperatura é de 20,4°C, com pequena amplitude térmica devido a influências marinhas.

Na região, os ventos de sul apresentam as maiores velocidades médias e podem soprar em rajadas que atingem 80 km/h ocorrendo em geral associados ao Anticiclone Polar e os ventos do quadrante nordeste associados ao Anticiclone Tropical Atlântico e possuem velocidades médias de 12 km/h (Monteiro, 1992).

Araújo *et al.* (2003), identificaram que as ondas mais freqüentes na área de estudo provém do quadrante sul com período de 12 s, seguidas pelas vagas de Leste com período de 8 s. A maior energia de onda provém de sul e sudeste, com períodos acima de 11 s e ondas que ultrapassam 4 m de altura em águas profundas. Durante os meses de outono e inverno, as ondulações de sul prevalecem sobre as vagas de

Leste, no outono há um equilíbrio entre ambas já durante a primavera as vagas de Leste são predominantes.

As marés no Porto de Florianópolis são do tipo micromarés com desigualdades diurnas, com número de forma de 0,44. As variações entre a média das baixa-mares e a média das preamares de sizígia de 0,85 m (FEMAR, 2000).

A granulometria das praias estudadas, segundo Horn Filho (2006), é bastante homogênea. Todas as praias são compostas de areias finas, bem selecionadas ou muito bem selecionadas, com diâmetro médio variando de 0,22 mm, próximo ao costão norte de Canasvieiras e 0,16 mm próximo ao costão norte da praia da Daniela.

CPE (2010), estudou através de modelagem numérica o impacto de ondas e correntes gerados pela instalação de um terminal de cruzeiros em Florianópolis. Os resultados apresentados indicam a intensificação das correntes junto aos promontórios da área de estudo (resultados abrangem da praia Brava à Daniela, a praia dos Ingleses não está contemplada pelas grades numéricas do estudo). Esta intensificação se apresenta de forma expressiva entre as praias Brava e Lagoinha e Lagoinha e Ponta das Canas, chegando a velocidades de 0,7 m/s em condições de marés de sizígia. A intensificação de correntes longitudinais pela ação das marés corrobora com o modelo proposto por Lessa *et al.* (2001), em estudo na Baía de Todos os Santos.

1.2 Objetivo Geral

Identificar e quantificar os processos associados a ondas, marés e ventos geradores da transposição de sedimentos entre praias de enseada, a fim de propor um modelo conceitual da dinâmica sedimentar para a costa norte da Ilha de Santa Catarina.

1.2.1 Objetivos Específicos

1. Analisar as variações da linha de costa em escala de ano e décadas, identificando potenciais caminhos do transporte de sedimento;
2. Medir o transporte de sedimentos nas proximidades dos promontórios;
3. Identificar a equação de transporte de sedimentos que, pela ação combinada de ondas e correntes, melhor reproduz o processo na área de estudo;

4. Quantificar o transporte líquido anual de sedimentos no entorno dos promontórios;
5. Quantificar e identificar as condições das ondas, vento e marés que geram o transporte líquido de sedimentos no entorno dos promontórios da área de estudo;
6. Gerar um modelo conceitual da transposição de sedimentos na costa norte da Ilha de Santa Catarina.

1.3 Hipóteses

A hipótese desta tese consiste na verificação dos mecanismos responsáveis pela transposição de sedimentos que ocorre entre as praias dos Ingleses, Brava, Lagoinha, Ponta das Canas, Canasvieiras, Jurerê e Daniela, tendo como forçante principal o padrão de ondulação regional. Na porção subaérea do sistema Ingleses - Brava a dinâmica sedimentar ocorre de modo contínuo (Figura 3) sendo a mecânica das ondas a principal forçante do transporte. E, na área abrigada entre Lagoinha e Daniela, a transposição ocorre pela atuação conjunta das correntes induzidas por ondas, marés e ventos.

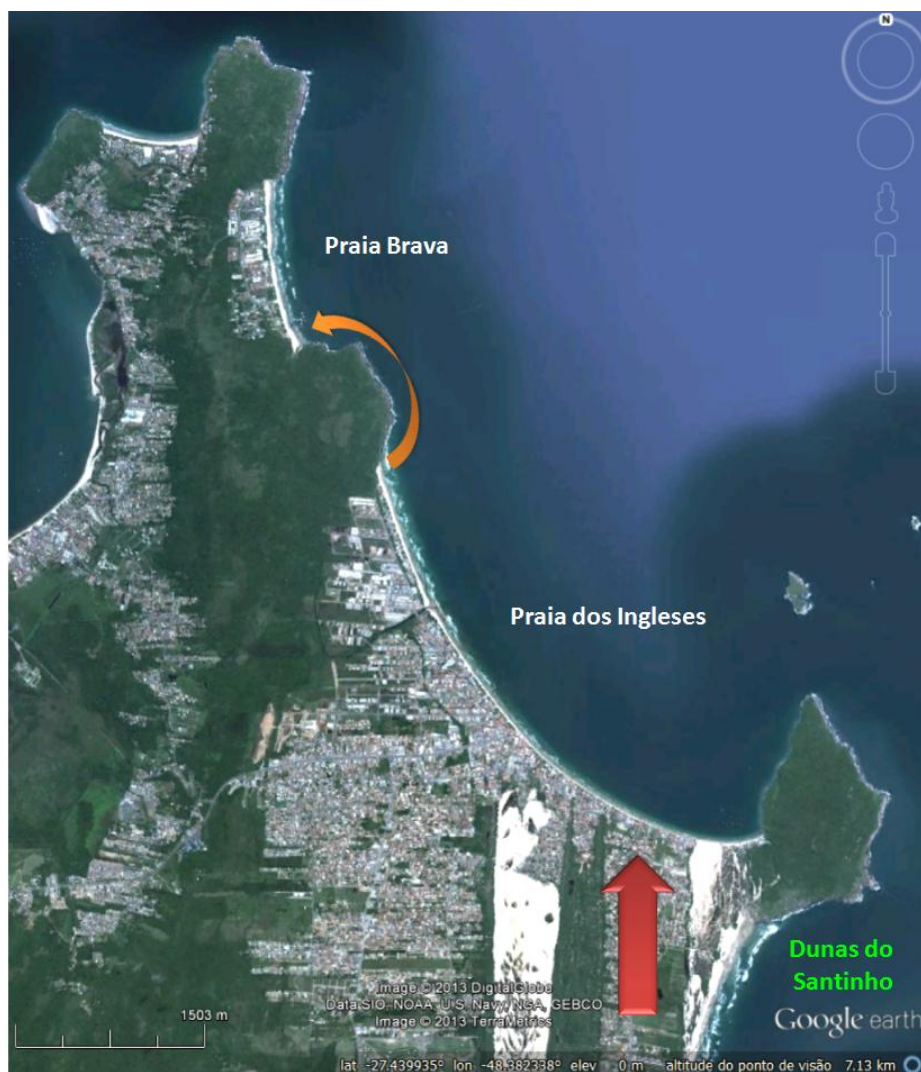


Figura 3: Modelo conceitual da transposição contínua de sedimentos gerado pela ação das ondas (seta alaranjada), e o ingresso de sedimentos eólicos pelo campo de dunas do Santinho (seta vermelha).

A Figura 4 apresenta um modelo conceitual da geração de correntes por ondas na região Norte da Ilha de Santa Catarina. Ao sofrerem os processos de refração e difração, as ondas atingem a costa Norte da Ilha de Santa Catarina obliquamente, gerando correntes e transporte de Leste para Oeste.



Figura 4: Modelo conceitual de transporte de sedimentos induzido por ondas na região Norte de da Ilha de Santa Catarina

Por outro lado, a ação das correntes geradas por marés e ventos podem atuar como um fator amplificador do transporte de sedimentos na área. Com a subida da maré (nível na região exposta mais alto que no interior da baía), são geradas correntes longitudinais às praias em direção à área mais abrigada (Figura 5). Devido à forma da entrada da baía (forma de "funil"), ocorreria a aceleração dessas correntes que podem ser responsáveis pela geração ou aumento do transporte induzido por ondas na região.

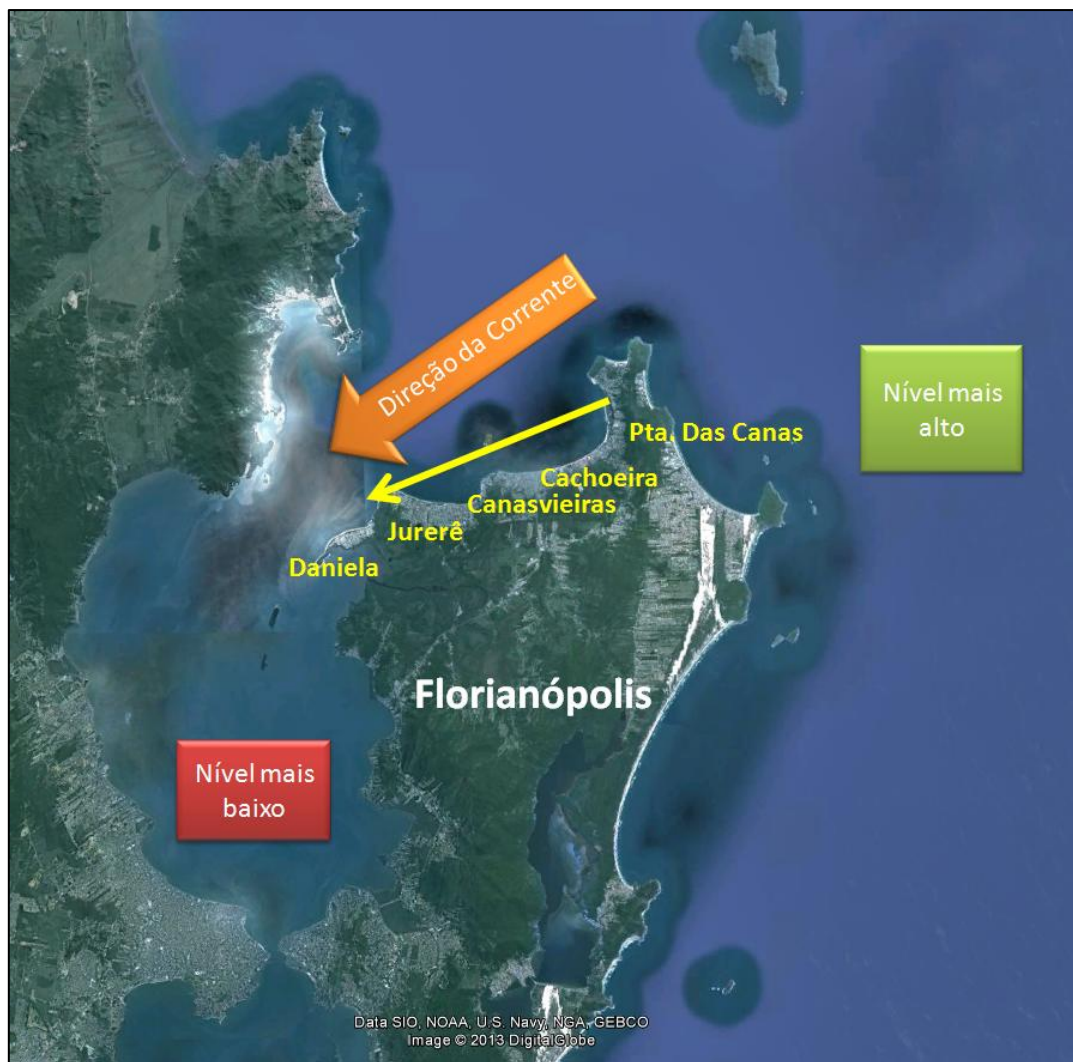


Figura 5: Modelo conceitual de transporte de sedimentos induzido por marés na região norte de Florianópolis.

1.4 Sobre a Estrutura desta Tese:

Esta tese de Doutorado está estruturada em torno de artigos publicados/submetidos em periódicos com corpo editorial permanente e revisores independentes escritos pelo autor durante o desenvolvimento de seu Doutorado. Conseqüentemente, sua organização compreende as seguintes partes principais:

- a) Introdução sobre o tema e descrição do objeto da pesquisa de Doutorado, onde estão sumarizados os objetivos e a filosofia de pesquisa desenvolvidos, o estado da arte sobre o tema de pesquisa (apresentada anteriormente);
- b) Artigo aceito para a publicação na *Journal of Coastal Research*:
Vieira da Silva, G.; Muler, M.; Prado, M.F.V.; Short, A.D.; Klein, A.H.F., and Toldo, E.E., Jr., 2016. **Shoreline change analyses and insight into the**

sediment transport path along Santa Catarina Island north shore, Brazil.

Journal of Coastal Research. Coconut Creek (Florida), ISSN 0749-0208;

c) Artigo submetido (em avaliação) para a *Marine Geology*:

VIEIRA DA SILVA, G; TOLDO JR. , E. E.; A. H. F. KLEIN, SHORT, A. D.;
WOODROFFE, C. D. Headland Sand Bypassing - **Quantification of Net
Sediment Transport in Embayed Beaches, Santa Catarina Island North
Shore, Southern Brazil;**

d) Artigo submetido (em avaliação) para *Coastal Engineering* :

VIEIRA DA SILVA, G; TOLDO JR., E. E.; A. H. F. KLEIN, SHORT, A.
D..**Identification of driving forces and their importance for headland
sand bypassing on the North Shore, Santa Catarina Island, Southern
Brazil;**

e) Conclusões gerais da tese.

SHORELINE CHANGE ANALYSES AND INSIGHT INTO THE SEDIMENT TRANSPORT PATH ALONG SANTA CATARINA ISLAND NORTH SHORE, BRAZIL

Este capítulo apresenta o conteúdo primeiro artigo que compõe esta tese e foi enviado à revista *Journal of Coastal Research* em 01/09/2015, aceito com revisões em 11/11/2015 e aceito em definitivo em 15/12/2015. Está disponível online (pre-print) desde 04/02/2016 em: <http://www.jcronline.org/doi/abs/10.2112/JCOASTRES-D-15-00164.1>. O conteúdo apresentado a seguir segue na íntegra o publicado na revista, mudando apenas a formatação do texto. A carta de aceite das revisões realizadas é apresentada na próxima página.



Guilherme Vieira da Silva <oc.guilhermevs@gmail.com>

Your Submission to Journal of Coastal Research

1 mensagem

The Journal of Coastal Research <em@editorialmanager.com>
 Responder a: The Journal of Coastal Research <cfinkl@cerf-jcr.com>
 Para: Guilherme Vieira da Silva <oc.guilhermevs@gmail.com>

11 de novembro de 2015 14:55

CC: cmakowski@cerf-jcr.com

Ref.: Ms. No. JCOASTRES-D-15-00164R1
 Shoreline Change Analyses and Insight into the Sediment Transport Path along Santa Catarina Island North Shore, Brazil
 Journal of Coastal Research

Dear Mr. Vieira da Silva,

This letter is to inform you that the revision of your manuscript was received in good condition. I have now completed my final adjudication of your contribution and am pleased to formally accept the paper for publication in the Journal of Coastal Research (JCR).

In due course you will receive page proofs, at which time it is highly recommended that you thoroughly check for errors. Please note that each author alteration (AA) will be assessed a \$5 USD revision charge. Printing errors are, of course, corrected free of charge.

I hope that you will be pleased with the final production of your work. Again, congratulations and thank you for choosing the JCR to publish your research. In order to expedite the publishing process for your paper, I wanted to bring to your attention several available options:

1. Order a professionally typeset PDF pre-print of your article. By doing so, an online publication date will be placed on the front page of the article and an electronic pre-print of the paper will be made available to current CERF members and JCR subscribers at <http://www.JCRonline.org>. By having a professionally typeset pre-print available online, authors can begin to cite a published version of their paper almost immediately. Current pricing for pre-prints are \$85.00 USD per article. To order a professional pre-print of your article, please email your request within 10 days to cmakowski@cerf-jcr.com

2. Help the Coastal Education & Research Foundation [CERF] and the Journal of Coastal Research by offering to pay voluntary page charges for your article. CERF depends, in large part, on the payment of these voluntary page charges for its operation in publishing the JCR. For current CERF members, a reduced (recommended) page charge of at least \$50.00 USD per estimated printed page is kindly requested. For non-CERF members, a recommended page charge of at least \$70.00 USD per estimated printed page is kindly requested. Even though these recommended prices are stated above, we understand that funding for publishing costs may be limited, and therefore, we will accept a reduced amount if that is all one can afford. The editors of the JCR graciously thank you when you contribute towards the payment of these voluntary page charges. Due to the heavy volume of professional papers published in the JCR, payment of these voluntary page charges will place an author's paper at the top of the JCR's printing queue, allowing the paper to be published in print much sooner than the average waiting time. The paper will also be published immediately online as a professionally typeset pre-print. If you would like to pay voluntary page charges for your article, please email your request within 10 days to cmakowski@cerf-jcr.com

Take care and I thank you again for being a contributing author to the JCR. If you have any questions, please do not hesitate to contact me at cfinkl@cerf-jcr.com.

With kind regards,

Charles W. Finkl, Ph.D.
 EIC
 Journal of Coastal Research

SHORELINE CHANGE ANALYSES AND INSIGHT INTO THE SEDIMENT
TRANSPORT PATH ALONG SANTA CATARINA ISLAND NORTH SHORE, BRAZIL

Guilherme Vieira da Silva^{1,2}, Mariela Muler³, Michel F. V. Prado⁴, Andrew D. Short⁵,
Antonio Henrique da Fontoura Klein⁴, Elírio E. Toldo Jr.¹

¹CECO, Instituto de Geociências

Universidade Federal do Rio Grande do Sul

Porto Alegre, RS, Brasil

oc.guilhermevs@gmail.com

²School of Earth and Environmental Sciences

University of Wollongong

Wollongong, NSW, Australia

³CETESB, Companhia Ambiental do Estado de São Paulo

Taubaté, SP, Brazil

⁴Laboratório de Oceanografia Costeira, Departamento de Geociências

Universidade Federal de Santa Catarina

Florianópolis, SC, Brazil

⁵School of Geosciences

University of Sydney

Sydney, NSW, Australia

LRH: Vieira da Silva, Muler, Prado, Short, Toldo Jr. and Klein

RRH: Shoreline Changes and Sediment Transport Path

ABSTRACT

This paper presents a shoreline change analysis applied to identify the sediment transport path involving nine adjoining beaches, including dunes and spits, located along the microtidal eastern and northern shores of Santa Catarina Island (Brazil) and extending 50 km from Barra-Moçambique to Daniela. A dataset comprising aerial images from 1957, 1978, 1998, 2002, 2007 and 2010 and the 2012 shoreline position measured with RTK-GPS; topo-bathymetric dataset; and a 60 year water level time series. The images were rectified and the shoreline position for each year was extracted. The average errors (ranging from 1 to 9.8 m) of the rectification process as well as the horizontal tide-related errors (varying from 8.3 ± 2.6 m to 14.9 ± 0.6 m) were calculated within a confidence level of 95%. Two complementary approaches were used: (1) general trends analysis using Linear Regression Rate method and; (2) shoreline behaviour statistically analysed by Euclidean distance and year-to-year analysis. The results indicate an anticlockwise longshore transport between a series of beaches with variable orientation and separated by headlands, including a dune *overpassing* from Santinho delivering $\sim 10,000 \text{ m}^3 \text{ yr}^{-1}$ to Ingleses; and headland bypassing leading to the development of three spits along the protected part of the study area that are possibly been nourished by subaqueous sand transport from the updrift beaches. During its development Ponta das Canas spit grew $\sim 7,000 \text{ m}^3 \text{ yr}^{-1}$, controlling the sediment availability downdrift. As the spit grows it traps sediment and the downdrift area retreats, on the other hand, when the spit merges to the coast the sand spreads and the downdrift beaches prograde.

ADDITIONAL INDEX WORDS: Shoreline evolution, historical trends, headland bypassing, spits, beach rotation, pocket beaches.

1 INTRODUCTION

Beaches are natural environments that fluctuate in response to changing physical processes. The knowledge of their fluctuations has evolved beyond an academic and scientific exercise to become a common objective of most coastal management programs (Moore, Ruggiero, and List, 2006) such as setback lines definition (Ferreira *et al.*, 2006). An effective approach to understanding these processes is through examination of historical shoreline change (Dolan *et al.*, 1980) in order to

determine shoreline stability, setback and hazards lines. It has been shown that shoreline changes analysis provides a good indication of erosion/accretion rates (Absalonsen and Dean, 2011; Farris and List, 2007; Jones *et al.*, 2009) as well as being used as regional and historical data points for calculating the sediment budget (Toldo *et al.*, 2013).

Despite of being bounded by headlands or man-made structures, embayed beaches are very dynamic, presenting a seasonal or event-related variation in width, morphodynamic state and orientation (beach rotation process) (Harley *et al.*, 2014; Klein, Benedet Filho, and Schumacher, 2002; Masselink and Pattiaratch, 2001; Ojeda and Guillén 2008; Ranasinghe *et al.* 2004; Short *et al.* 1995; Short and Masselink 1999; Turki *et al.* 2013). Because of their physical limits, embayed beaches and beaches bounded by hydrodynamic obstacles (such as inlets) have frequently been considered closed systems (without significant input/output of sediment). Although, several studies have reported obstacles bypassing and overpassing (Ab Razak *et al.* 2013, Boeyinga *et al.* 2010; Cheung, Gerritsen, and Cleveringa, 2007; Eslami *et al.*, 2010; Fitzgerald, Krauss, and Hands 2000;. Fitzgerald and Pendleton, 2002; Goodwin, Freeman, and Blackmore, 2013; Mariani, Carley, and Miller, 2010; Short and Masselink 1999; Silvester, 1985). A conceptual model of headland bypassing was presented by Short and Masselink (1999). According to the authors the process begins with the beach rotation when sand is accumulated on the updrift side of the headland, then moves subaqueously around the headland to emerge as an elongated spit at the lee of the headland and finally the spit merges the coast. Therefore, understanding and identifying beach rotation and spit development is essential to recognizing headland sand bypassing and understanding its role in longshore sediment transport.

The aims of this paper are: (1) analyse the shoreline changes along a section of the southern Brazilian coast; (2) interpret beach rotation and spit development using shoreline changes and; (3) use the shoreline changes, bathymetric measurements and current evidence to test the conceptual model of headland bypassing (Short and Masselink, 1999) and overpassing. This is the first time sand transport around a series of beaches and headlands via bypassing, overpassing and spits has been documented.

2 REGIONAL SETTINGS

The study area encompasses nine beaches located around the microtidal coast of eastern and northern shores of Santa Catarina Island. They extend for 50 km from Barra-Moçambique on the east coast to Daniela beach, which faces west into the North Bay entrance (Figure 1).

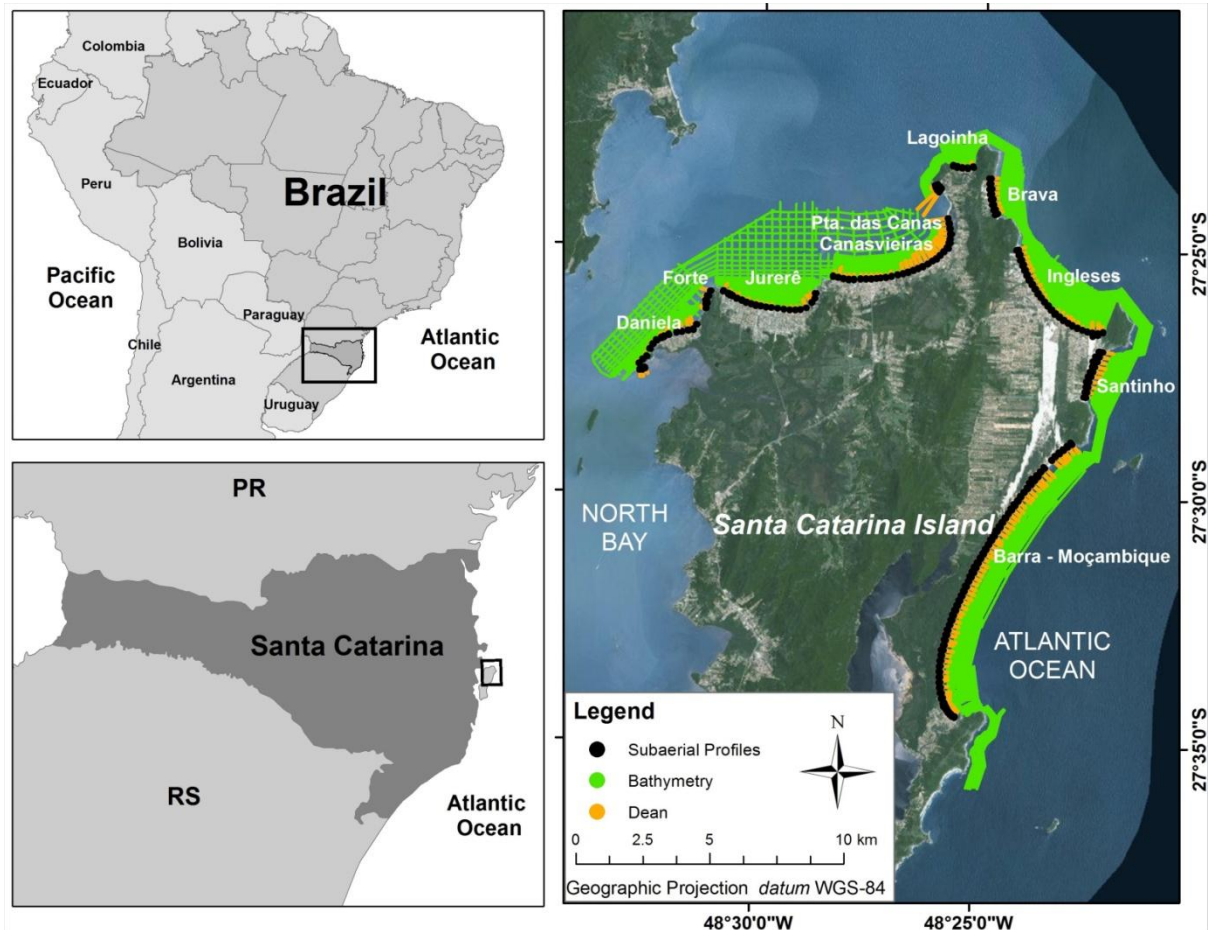


Figure 1: Location of the study area on the southern of Brazil and morphological details between the beaches in the north area of the Santa Catarina Island. Background image: ESRI Basemap imagery. ESRI World Imagery (ArcGIS 10).

Santa Catarina Island receives a dominance of northerly winds, with strong southerly winds accompanying the passage of cold-front systems (Nobre *et al.*, 1986; Truccolo, 2011). The most frequent waves arrive from the south with 12 s period, followed by sea from east with 8 s period and averaging 1-1.5 m in height (Araújo *et al.*, 2003). The highest waves comes from south and southeast, with a H_o (deep water wave height) greater than 4 m and periods above 11 s. During the autumn and winter, the swell waves from south prevail over easterly seas, while in summer there is a balance between both and during the spring easterly seas are predominant. The

astronomical tide is microtidal with a range between 0.4 and 1.2 m during neap and spring tide periods, respectively, while the low frequency oscillations (including storm surges) can be as high as 1 m (Truccolo, Franco, and Schettini, 2004).

Beach face sediment sampled at 189 points spaced at an average of 200 m by Federal University of Santa Catarina (UFSC) Coastal Oceanography Laboratory at the study area for MMA (Ministry of the Environment) showed a homogeneity of the sediment at the study area from Santinho to Daniela composed of moderately sorted medium sand and well sorted fine sand, with an average diameter ranging from 0.20 mm (near the southern Ingleses) and 0.30 mm (near the southern Brava). Barra-Moçambique beach had the greatest variations. In the southern sector 65% of the samples are composed by fine sand (0.20 mm to 0.25 mm) and 35% by medium sand (0.26 mm to 0.41 mm), ranging from moderately to well sorted. The central sector ranged from moderately to well sorted with 48% fine sand (0.23 mm to 0.25 mm), 48% by medium sand (0.26 mm to 0.43mm), only one sample (4%) classified as coarse sand (0.52mm), with slight increase in grain diameter from south to north. In the northern sector grain size decreased northward, with 32% of the samples were classified as fine sand (0.21 mm to 0.25 mm), 64% as medium sand (0.25 mm to 0.44 mm) and 4% as coarse sand, all ranging from moderately sorted to well sorted.

The beaches in the study area vary from sheltered reflective beaches in the north to predominantly rip-dominated transverse bar and rip to rhythmic bar and beach (TBR-RBB) also including a double bar system at Moçambique (Klein, Short, and Bonetti, *in press*) in the east.

Porpilho *et al.* (2015) used interferometric and current meter data to identify an intensification of the current in front of the headland between Moçambique and Santinho leading to a net northward sediment transport. CPE (2010) conducted a numerical modeling study at the study area and the results indicate the intensification of currents near the headlands of the study area (the results covers from Daniela to Brava beaches) was observed in Brava-Lagoinha and Lagoinha-Ponta das Canas headlands during flood tide condition. During ebb tides this intensification is not observed, suggesting a net transport toward the North Bay.

3 METHODS

This section is divided in four subsections. The first subsection will present the dataset used; the second defines the shoreline indicator; the third describes the shoreline position error quantification; and, finally the fourth presents the shoreline changes analysis.

3.1 Dataset

A set of aerial photos from 1957, 1978, 1998, 2002, 2007 and 2010 from multiple sources (Table 1), as well as a RTK-GPS field survey from 2012 was used to analyse the decadal shoreline changes along the north of Santa Catarina Island. The images were digitalized in variable resolution in order to standardize the pixel size representation of at least ~1 m as suggested by Araujo *et al.* (2009).

Table 1: Images sources, resolution and scale.

Year	Source	Scale	Scanning resolution (dpi)
1957	Secretaria de Planejamento e Gestão do Estado - SPG	1:25.000	600
1978	Departamento Nacional de Produção Mineral	1:25.000	600
1998	CELESC - Centrais Elétricas de Santa Catarina S.A. (e IPUF)	1:15.000	400
2002	Instituto de Planejamento Urbano de Florianópolis - IPUF	1:8.000	600
2007	Instituto de Planejamento Urbano de Florianópolis - IPUF	1:8.000	600
2010	Secretaria de Desenvolvimento Sustentável – Diretoria de Recursos Hídricos – Coordenação de Cartografia	1:10.000	600

Image rectification was performed in SIG environment by relating the image to actual coordinates. The coordinates can be obtained in the field or in digital cartographic databases. In this case, a digital 1:2,000 base map (Instituto de Planejamento Urbano de Florianópolis - IPUF) was used with its accuracy calculated by Muler *et al.* (2014) at 1.63 m. As the error was a systematic displacement of the base map it was corrected by subtracting the error of both east and north directions the corrected base map error tended to zero.

Beside the shorelines digitalized from aerial photos a set of *in situ* data were measured and are presented in Figure 1. It comprises subaerial beach profiles, bathymetric survey, as well as a shoreline position measured with a RTK-GPS.

Beach profiling and a bathymetric survey was carried out by UFSC Coastal Oceanography Laboratory at the study area for a MMA (Ministry of the Environment) in 2013. The beach profiling survey consisted on 189 transects lines perpendicular to the shoreline, spaced an average of 200 m apart encompassing all the studied beaches. It was conducted using a RTK-GPS Trimble R6 from the most onshore to the most offshore position where the RTK-GPS antenna was safe and dry. The data was real time corrected by a base station set in a known position. The bathymetric survey was conducted with interferometer Edge Tech® 4600 at a frequency of 540 kHz and a swath of 400 beams with 0.2 m diameter resulting in coverage swath corresponding to 3 times the water depth. The system has an integrated sound velocity sensor Teledyne Odom Hydrographic Digibar Pro for post-processing the bathymetry, two DGPS using an Omnistar XP to correct its position and identifying the boat heading, as well as a motion sensor SMC IMU-108 to correct the boat movements (pitch, roll and heave) all linked to a processing unit. A total of 865 km were mapped covering the whole study area from the most onshore depth the boat could safely navigate to below the closure depth. The gap between the subaerial beach profiles and the bathymetric data was completed using the equilibrium profile presented by Bruun (1954) and Dean (1977). For each measured profile an iterative process was used to identify the “A” factor that best fits the study area. This procedure was necessary because we found that at the swash zone and very shallow waters (*i.e.* < 1m) the beach slope vary considerably and the A parameter should be adapted for each case, so the gap between subaerial profiles and bathymetry was a smooth transition, avoiding abrupt bathymetric changes.

A 60 years (1948-2008) water level series developed by SMC-Brasil (Ministério do Meio Ambiente - MMA and Instituto de Hidráulica Ambiental of Universidade de Cantábria - IH Cantabria) was used to analyze the range of the high water line (HWL) in a timescale compatible to the shoreline change analysis. The series is composed by both astronomical (from TPXO - Egbert, Bennett, and Foreman, 1994; Egbert and Erofeeva, 2002) and meteorological effects from numerical simulation using wind and pressure fields as input.

3.2 Shoreline Indicator

Boak and Turner (2005) found that the best shoreline indicator depends on the study in question and the possibility of identification of an indicator. According to Araujo *et*

al. (2009) the high water line (HWL) is normally the most prevalent and easily identifiable in the images in Santa Catarina state. It is recognized in aerial photographs as a tonal contrast between the wet intertidal beach and the dry supratidal beach (Moore *et al.*, 2006) and it has been demonstrated to be the best indicator of the land-water interface for historical shoreline comparison studies (Crowell, Leatherman, and Buckley, 1991). Nevertheless it is important to know and quantify the errors related to the shoreline indicator. For this paper, the HWL indicator was chosen and traced in a SIG environment for further shoreline variation analysis

3.3 Shoreline Position Error Quantification

The main sources of errors on shoreline analysis using aerial images and HWL as shoreline indicators are related to image rectification process and to water level fluctuations (Moore, 2000). To quantify the errors related to these processes a 95% of confidence was used.

At the rectification process at least 20 control points distributed evenly throughout the image were used so that it is possible to calculate the 95% confidence interval error of the rectificated images based on its RMS errors according to FGDC-STD (1998), and Araujo *et al.*, (2009). Images from 2010 were already rectificated with the error presented in the metadata.

The RTK-GPS survey involved setting up a GPS base at a known position and walking with GPS rover attached to a wheel at the wet-dry sand interface and collecting one sample every 0.5 m. The processed data resulted in a constant error estimation of ~1 cm (0.01m).

The HWL delineates the landward extend of the last high tide (Crowell, Leatherman, and Buckley, 1991), including the swash effect and despite it being easily identified and prevalent on the analyzed images, it may vary from one day to another and so its error must be quantified. The 60 year of water level data was analyzed as follows: (1) HWL were identified on the series; (2) frequency of the HWL were computed; (3) the vertical tidal range of the HWL was considered as the 95% of modal levels - the 2.5% highest and 2.5% lowest tidal levels were not considered since they are very unlikely (5% of chance) to happen on the day when the image was obtained (Figure 2). A HWL varied in a range of 0.9 m at the study area for 95% of the time; 4) the

beach face slope at the 189 measured profiles was used to transform the vertical water level to a horizontal distance.

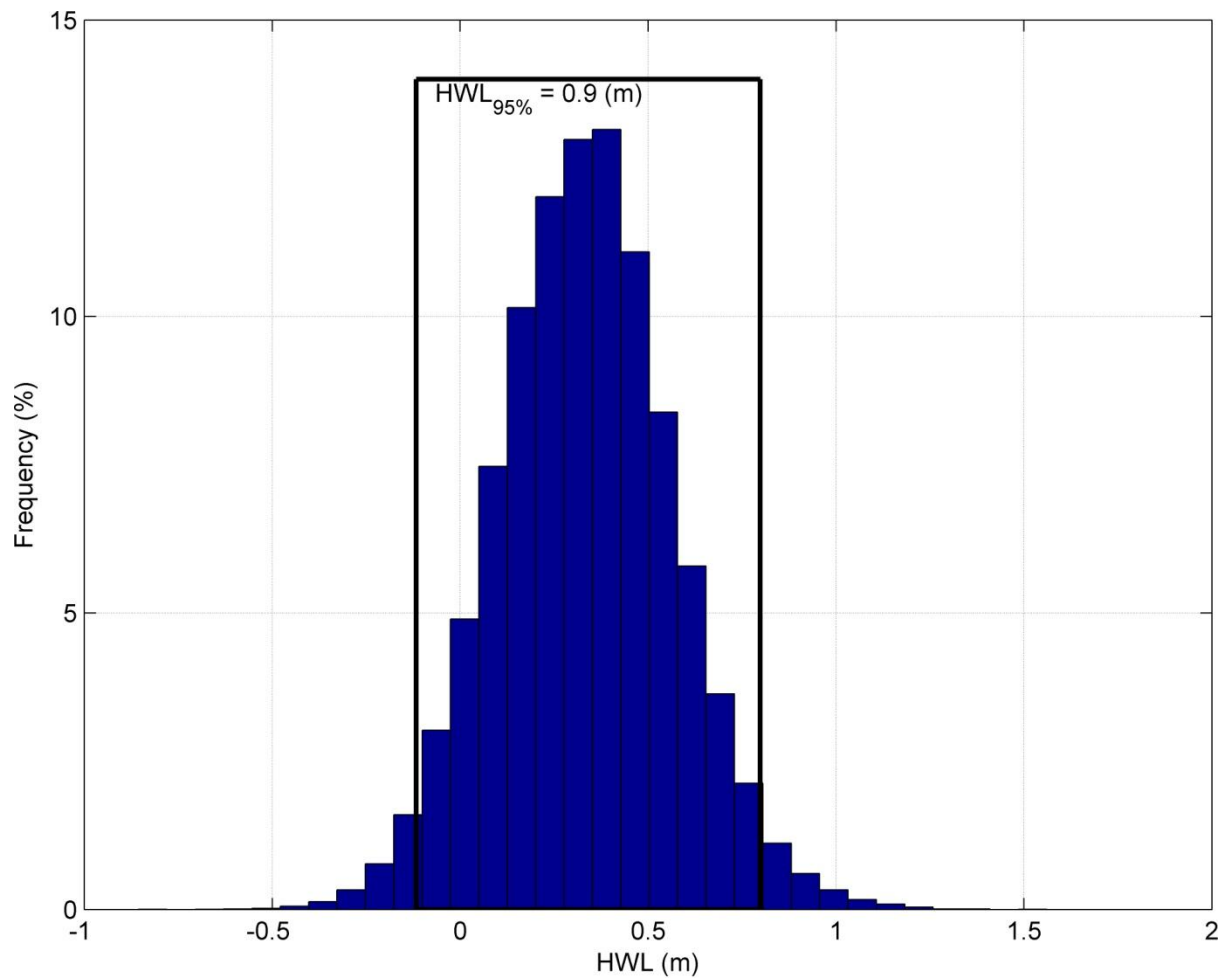


Figure 2: HWL frequency - 95% of the central frequency occurrence was assumed as the HWL range - note that both tails (<2.5 and >97.5%) of the distribution were not considered.

The errors related to rectifying process, RTK-GPS survey and tide-related (average horizontal tide error per beach) are presented in Table 2. Each source of error is assumed to be independent, thus, as presented by Crowell, Leatherman, and Buckley (1991), the total error estimation is calculated by the root mean square approach divided by the analyzed time frame. Note that as the beach slope varies along the beaches the tide related errors are also variable. Therefore, the errors were calculated for each transect (at every 50 m) and for each analyzed timeframe according to:

$$E_t = \frac{\sqrt{E_{im1}^2 + E_{im2}^2 + E_{hte}^2}}{t} \quad (\text{eq. 1})$$

where E_t is the total error per transect (m yr^{-1}); E_{im1} is the rectification related error of the image (aerial photo) 1 (m); E_{im2} is the rectification related error of the image (aerial photo) 2 (m); E_{hte} is the horizontal tide related error (m); and t is the time (yr) between the analyzed images. When more than two images (aerial photos) are compared (i.e. for general trend analysis), the errors of all images are included in the error calculation.

Table 2: Errors related to rectifying process (1957 to 2010), to RTK- GPS survey (2012) and to tidal variations (μ = mean; σ = standard deviation) per beach.

Beach/year	1957 (m)	1978 (m)	1998 (m)	2002 (m)	2007 (m)	2010 (m)	2012 (m)	Horizontal tide error $\mu \pm \sigma$ (m)
Barra - Moçambique	7.6	8.5	6.4	5.0	2.8	1.0	0.01	8.3 ± 2.6
Santinho	7.2	3.3	5.6	2.3	2.7	1.0	0.01	14.2 ± 1.5
Ingleses	7.4	3.3	3.7	2.3	2.7	1.0	0.01	11.7 ± 1.6
Brava	6.9	5.6	4.8	1.8	1.7	1.0	0.01	13.5 ± 0.4
Lagoinha	6.9	5.6	4.4	1.8	1.8	1.0	0.01	14.9 ± 0.6
Ponta das Canas - Canasvieiras	6.9	4.7	6.3	1.2	2.4	1.0	0.01	11.1 ± 3.0
Jurerê	9.8	4.8	3.2	1.2	2.3	1.0	0.01	8.6 ± 1.9
Forte	9.8	6.3	1.8	1.6	2.3	1.0	0.01	12.2 ± 0.3
Daniela	9.8	6.3	2.9	0.9	2.3	1.0	0.01	14.3 ± 5.2

3.4 Shoreline Changes

The Digital Shoreline Analysis System (DSAS) tool developed by Thieler *et al.* (2005) and improved by Thieler *et al.* (2009) was used to calculate the shoreline changes. By using the tool, lines orthogonal to the shoreline with pre-defined spacing (every 50 m) were generated and the distance between a base line and the traced shorelines was used to calculate shoreline changes rates based on statistical regression fits. To smooth changes in shoreline position from transect to transect, and to minimize measurements errors or uncertainties, Ferreira *et al.* (2006) suggested the use of a moving average corresponding to 750 m. For the present paper it was found that the 550 m was enough to filter the high frequency related to local shoreline position variations (such as beach cusps) without removing the actual shoreline changes. To analyze the general trends of the shoreline, the Linear Regression Rate (LLR) was used. Changes less than the shoreline position errors were assumed as stable. The shoreline changes comparison between every transect for the whole study area was carried out by computing a Q-mode association matrix.

The Q-mode resemblance functions are used to measure similarity or dissimilarity between samples (Ludwig and Reynolds, 1988). The resemblance function method chosen was the Euclidean distance. Matrix based upon Euclidean distance can lead to unique insights in data interpretation (Elmore and Richman, 2001), in the case of the present paper it shows how similar (or dissimilar) the shoreline changes are between each analyzed transect and all the rest of the area. The Euclidean distance is defined by the hypotenuse of a right triangle whose other two legs are parallel to the two data axes (Wilks, 2006) according to:

$$\|x - y\| = \sqrt{\sum_{k=1}^k (x_k - y_k)^2} \quad (\text{eq. 2})$$

To do so the cases (transects) were organized in the similarity matrix anti-clockwise orientated from Barra-Moçambique (bottom right) to Daniela (top left). Each row represent one transect. Lower values indicate that shoreline position behaves similarly (*i.e.* preset similar trends along time series data), while higher values indicate the transects have different behaviour (*i.e.* different shoreline displacement rates / inverse trends). The Euclidean distance values were considered indicators of significant differences when higher than 70 while coefficient values lower than 70 are interpreted as representing similar changes patterns.

To help the interpretation of the Euclidean distance analysis the End Point Rate (EPR) method was used for the year-to-year comparison. The method analyze the distance of the shorelines at every transect and divides it by the time between them given as a result the rate of change in m yr^{-1} .

4 RESULTS

Figure 3 presents the bathymetry at the study area. Areas not covered by topobathymetric dataset presented in Figure 1 were completed with nautical charts. Profiles in front of each headland are presented at the bottom of the figure. The profiles vary in steepness from 1:30 in front of Ingleses and Brava headland to a very gentle slope (1:170) at Daniela.

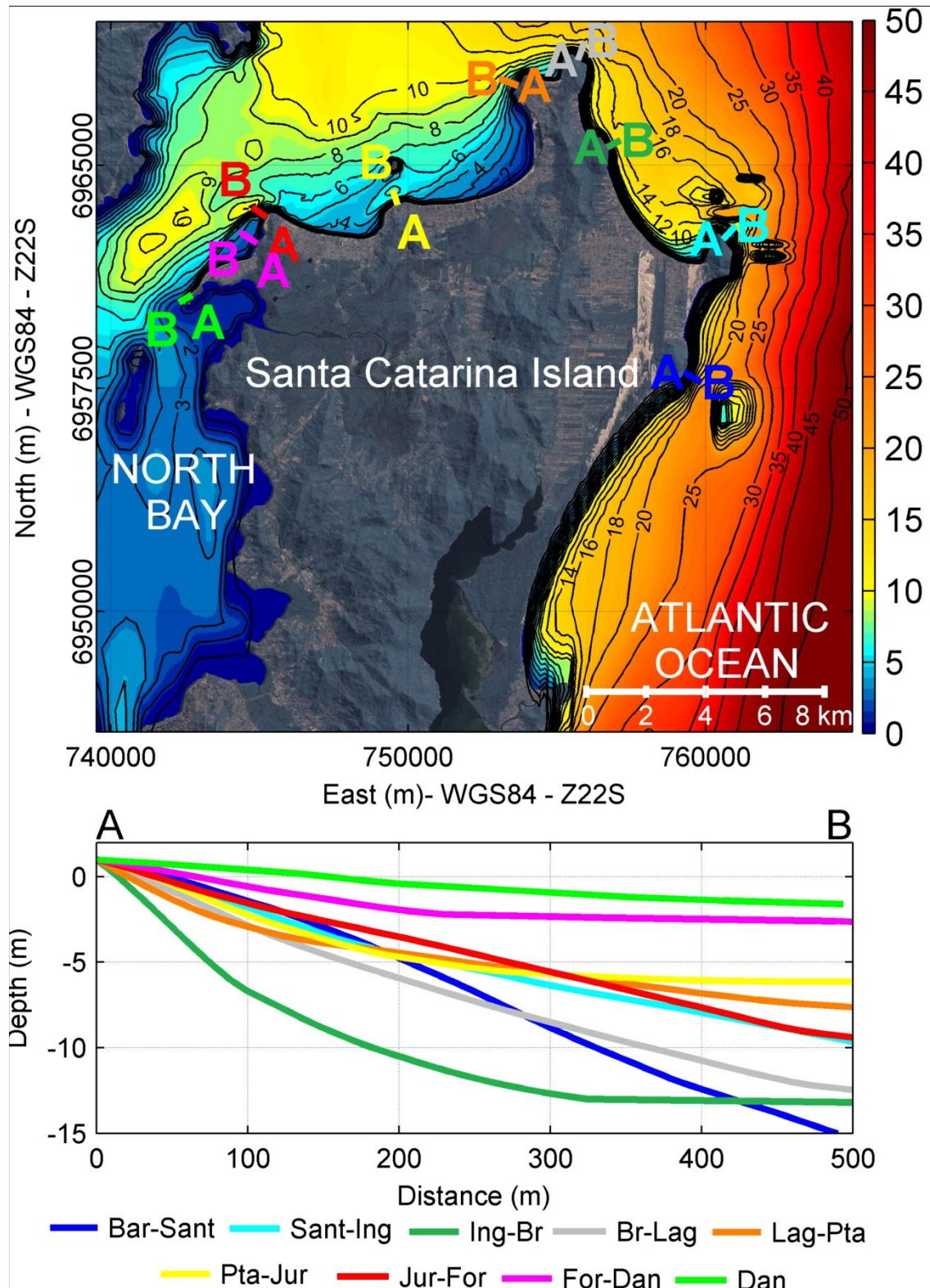


Figure 3: Bathymetry of the study area (top) and bathymetric profiles (bottom) vertical *datum* mean sea level. Note that the measured bathymetry was completed with nautical charts. Bar: Barra da Lagoa-Moçambique; Sant: Santinho; Ing: Ingleses; Br: Brava; Lag: Lagoinha; Pta: Ponta das Canas - Canasvieiras; Jur: Jurê; For: Forte and; Dan: Daniela. The profiles presented at the bottom are shown on the top from A (land) to B (offshore). Background image: ESRI World Imagery (ArcGIS 10). See Figure 1 for location of beaches.

The maximum shoreline displacement at the study area - over the 55 years - is presented in Figure 4a. The most dynamic portion of the study area is in the northeast at Ponta das Canas - Canasvieiras beach, which had a maximum variation of 330 m. The central portion of Barra-Moçambique beach is the most stable area, with a maximum shoreline variation of 12 m where the beach rotation pivotal point is located. The results presented in Figure 4b and Table 3 shows that most of the study area is either stable or retreating. Exceptions are accretion at Santinho beach (0.24 ± 0.38 m), northeast of Ponta das Canas - Canasvieiras (2.13 ± 1.47 m), Forte (0.38 ± 0.69 m) and Daniela (0.06 ± 0.81 m).

Table 3: General trend summary per beach.

Beach	Number of Transects	$\mu \pm \sigma$ (m yr ⁻¹)	min (m yr ⁻¹)	max (m yr ⁻¹)
Barra-Moçambique	244	-0.26 ± 0.29	-0.86	0.48
Santinho	39	0.24 ± 0.38	-0.48	0.94
Ingleses	103	-0.61 ± 0.16	-0.93	0.00
Brava	34	-0.06 ± 0.19	-0.35	0.44
Lagoinha	20	-0.03 ± 0.13	-0.35	0.12
Ponta das Canas - Canasvieiras	161	0.40 ± 2.16	-5.96	5.81
Jurerê	95	-0.27 ± 0.12	-0.43	0.10
Forte	25	0.38 ± 0.69	-0.78	1.47
Daniela	63	0.06 ± 0.81	-1.94	1.88

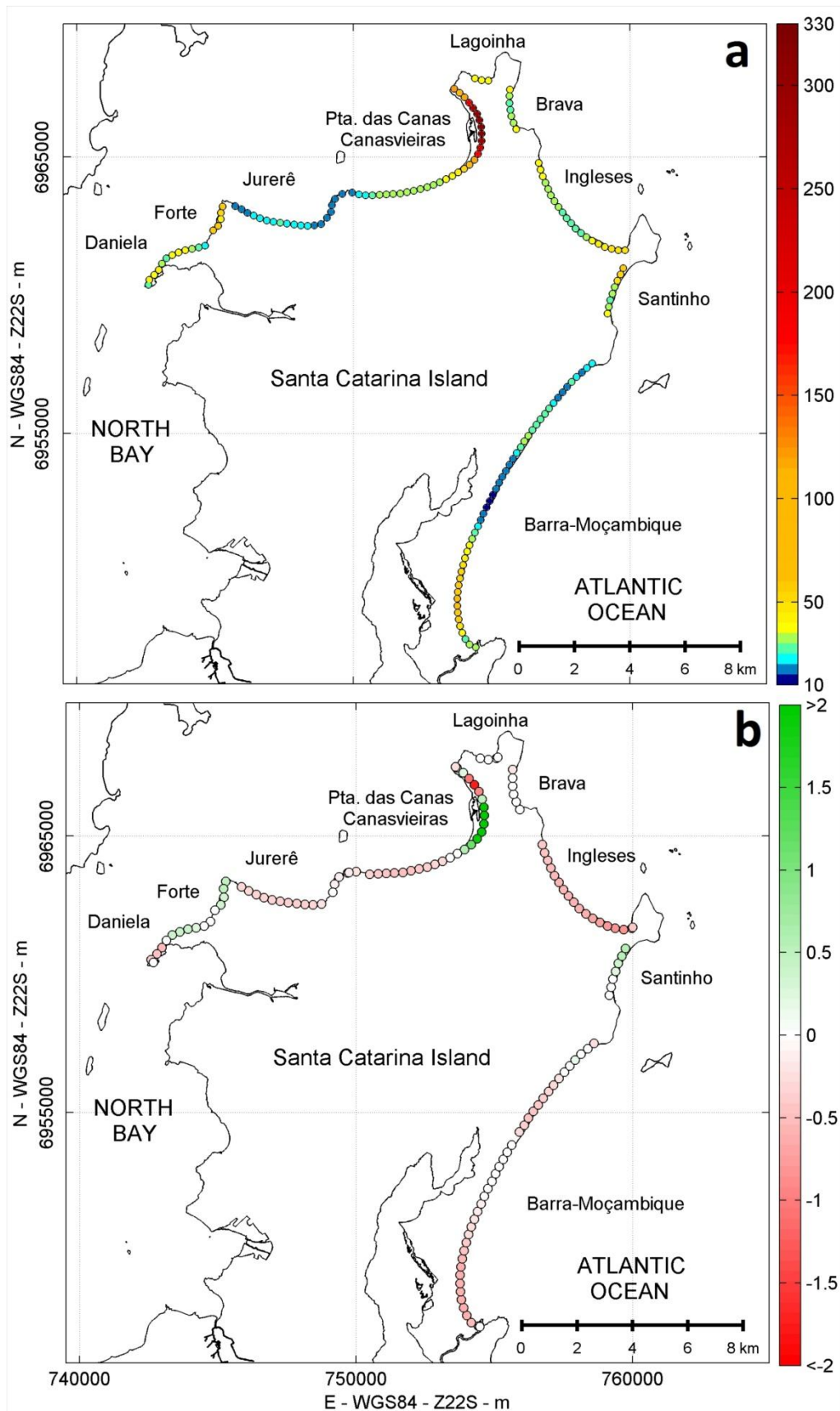


Figure 4: a) Maximum shoreline displacement (m); b) Shoreline changes trend at the study area by Linear Regression Rate method (m yr^{-1}) - changes lower than the calculated error are represented in white.

4.1 Spit formation

The northeast headlands of Ponta das Canas-Canasvieiras and Forte have very dynamic spits which go through a cycle of downdrift growth; the attachment of the spit to the beach (usually impounding small lagoons) with a rip exiting the lagoon or downdrift side of the sand wave and causing downdrift erosion of the beach; and finally the merging of the spit with the beach and gradually dissipating downdrift, following the model described by Short and Masselink (1999). The average rate of Ponta das Canas spit migration is 60 m yr^{-1} with an volume increase of $\sim 7,000 \text{ m}^3 \text{ yr}^{-1}$ (differences of spit area times the spit height $\sim 1.2 \text{ m}$). Forte spit migrates at an average of $40 \text{ m yr}^{-1} \sim 4,600 \text{ m}^3 \text{ yr}^{-1}$. In both cases the migration is faster at the beginning of the migration and slow down as it migrates and merges. At Jurerê a minor spit is present and its formation and migration happens at a smaller scale where it acts as a sand wave and does not impound a lagoon. The presence of these features are an indication of net transport towards North Bay. They also follow the model of Short and Masselink (1999) and suggest that sediment may be bypassing the headlands to initiate the spits. Daniela beach is also prograding with the beach extending as a sand spit 3 km into the bay entrance (Figure 5), with bathymetric data (Figure 3) showing that the spit extends underwater. The large spit can only have been supplied through westerly longshore sediment transport. This spit also represents the final terminus or sink for the northern Santa Caterina island shore.



Figure 5: a) Dunefield migrating from Santinho to Ingleses Beach; b) Ponta das Canas spit developing - notice the eroded portion down-drift of the spit as well as the down-drift spreading of the former spit; c) minor sand wave migration at east Jurerê; d) Forte beach at bottom presenting the sand wave pattern and Daniela spit. Photos by Andrew Short, Mariela Muler and Raphael Ribeiro.

The northern part of Santinho beach has a significant Euclidean distance (Figure 6) when compared with Ingleses beach, which can be explained by the inverse pattern presented by both beaches - when north of Santinho is prograding, Ingleses is retreating and vice-versa (Figure 7). Similar patterns are also observed between: Ingleses and Brava beaches; Lagoinha and north of Ponta das Canas - Canasvieiras bay. The latter case may indicate that at least part of the sand that builds Ponta das Canas spit is coming from Lagoinha beach. The northeast of Ponta das Canas - Canasvieiras has the highest distance values (Figure 6), differing from all the other beaches (Figure 6). It is the most distinct environment within study area in terms of shoreline change patterns. These differences occur because of the presence of the headland bypassing process identified by the cyclic development and migration of the spit.

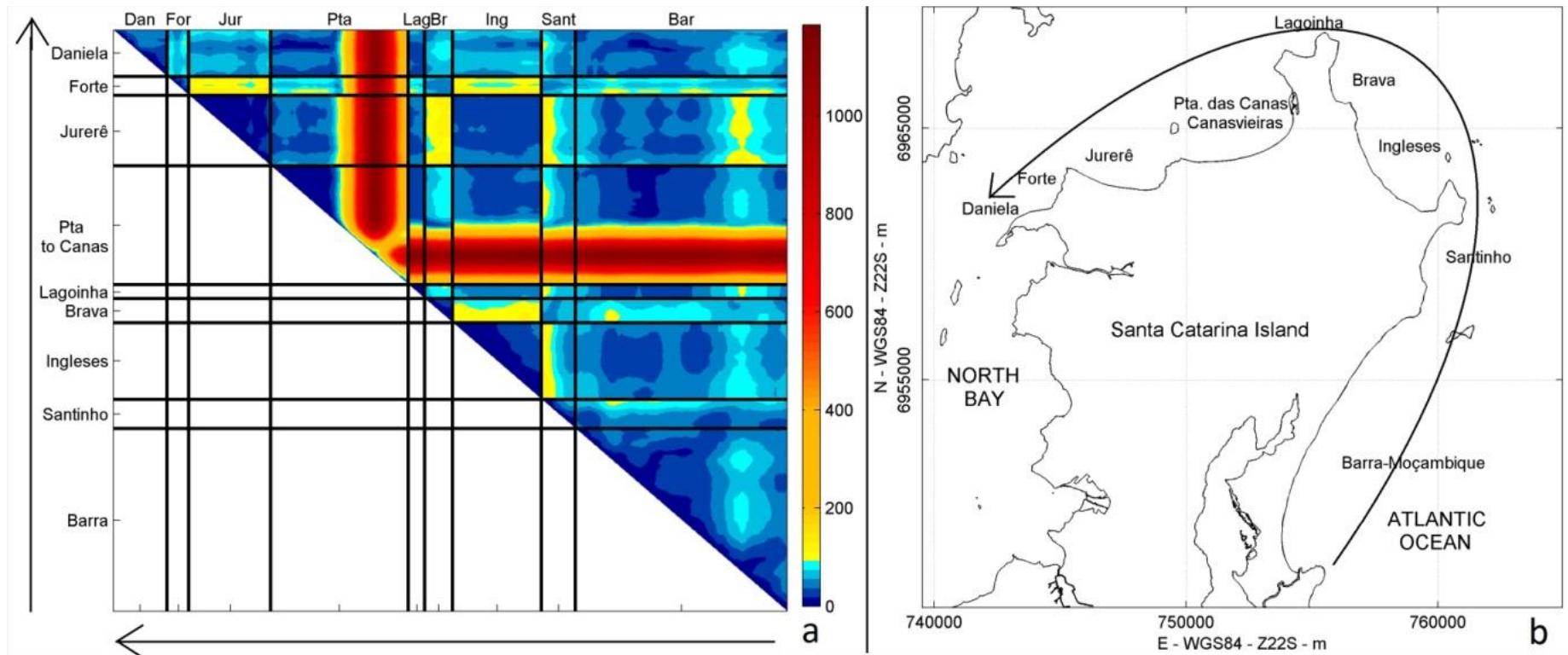


Figure 6: a) Euclidean distance matrix indicating similarities (blue) and differences (yellow-red) among the beach transects at every 50 m - the arrows (bottom and the left side) represent the direction indicated on figure b. b) the arrow indicates the direction of the Euclidean matrix presented on the left (a). Bar = Barra - Moçambique, Sant = Santinho, Ing = Ingleses, Br = Brava; Lag = Lagoinha; Pta = Ponta das Canas - Canasvieiras, Jur = Jurerê, For = Forte and; Dan = Daniela.

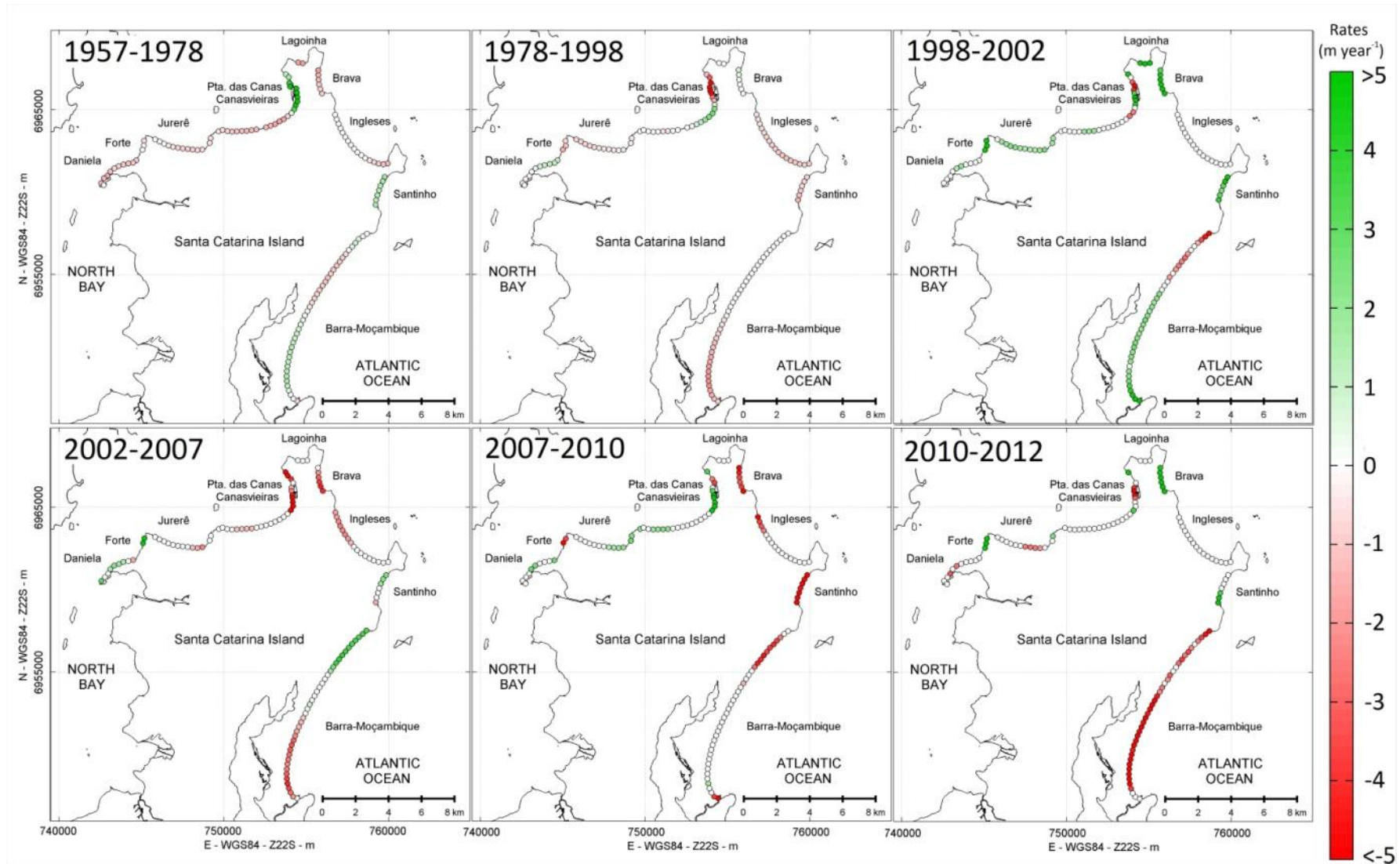


Figure 7: Shoreline changes (m yr⁻¹) along the temporal series analysed by End Point Rate (EPR) - changes lower than the calculated error are represented in white.

Figure 7 shows that when Ponta das Canas spit is growing it traps sediment and the downdrift area (towards North Bay) is deprived of sediment and retreats, on the other hand, when the spit merges to the coast (retreating) and start to spread the downdrift beaches prograde. This is part of the pulsative cycle of sediment initiated by the spit and manifest as it moves downdrift and merges with the beach.

Forte beach is also a very dynamic area (see Figure 5c) and undergoes a cyclic pattern of spit formation, growth, erosion downdrift and merging to shoreline. By analysing Figure 7 it seems that the process that happens at Ponta das Canas - Canasvieiras is also happening at Forte, which explains the difference when compared to Jurerê. In this case, Jurerê is providing sand by headland bypassing to Forte beach.

4.2 Beach rotation

Figure 7 illustrates the rotational behaviour of some of the beaches. Barra-Moçambique (1957-1978, 1998-2002 and 2002-2007) and Santinho (2002-2007) experience erosion at one end while the other end accretes, suggesting beach rotation. This process may be linked to sediment bypassing between Barra-Moçambique and Santinho, and between Santinho and Ingleses, with northerly rotation providing sand for headland bypassing, as suggested by Short and Masselink (1999). In addition it may increase the sand availability from Santinho beach to supply the dune, which in turn delivers sand by overpassing to Ingleses.

5 DISCUSSION

Based on presented shoreline analysis as well as other authors observations a sediment path has been identified along the northern coast of Santa Catarina Island. The path extends for 50 km from Barra-Moçambique to Daniela, including beach rotation and spit migration which are evidences of headland bypassing presented by Short and Masselink (1999) in their conceptual model. Close to the study area there is no large drainage systems or eroding cliffs that suggest the main source of sediment is through longshore transport as well as from the inner shelf. A schematic map based on the results and other authors is presented in Figure 8. This Discussion will commence at Barra-Moçambique beach and work counter-clockwise around the northern part of the island in the direction of sediment transport.

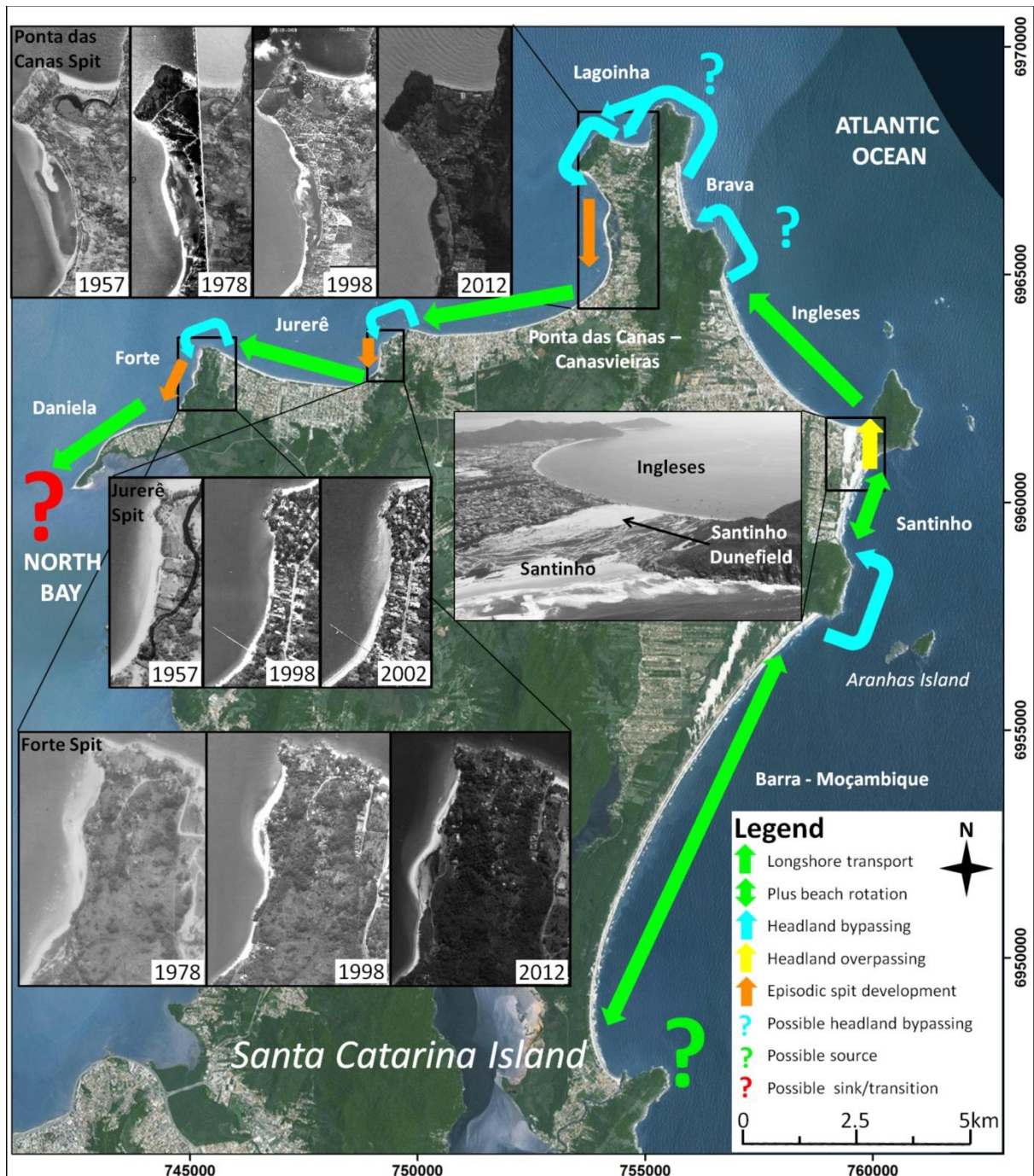


Figure 8: Schematic sediment path at the study area. It is highlighted the migrating dunefield from Santinho to Ingleses as well as the spit development at Ponta das Canas, Jurerê and Forte indicating the anticlockwise net sediment transport. Background image: ESRI World Imagery (ArcGIS 10); Santinho dunefield photo by A D Short.

5.1 Barra-Moçambique

Although the temporal scale of beach rotation process has a higher frequency (< decadal) that could not be recorded by the present dataset (> decadal), the very stable central portion Barra-Moçambique beach bordered by more dynamic north and south sectors may indicate a transitional-fulcrum area of the rotation process as described by Short, Trembanis, and Turner (2001), and Klein, Benedet Filho, and Schumacher (2002). Therefore, there is a strong indication that Barra-Moçambique

beach undergoes a rotational process, which could result in sediment accumulation at its northern end, providing sand for headland bypassing to the adjoining Santinho. The bathymetric data (Figure 3) shows that the profile in front of the headland present a convex shape to ~6 m depth and then becomes concave, suggesting sediment accumulation in front of the headland (Figure 3). In addition Porpilho *et al.* (2015) observed the northerly migration of sand waves past the headland confirming sediment is moving northward around the headland as part of the headland bypassing process.

5.2 Santinho-Ingleses

It has been shown that a reduction in sand input from Santinho dunefield to Ingleses beach has lead to a retreat of Ingleses shoreline that may indicate it is losing sediment downdrift (northward - eventually to Brava). According to Boeyinga *et al.* (2010), Santinho beach is supplying a dunefield that migrates northward and delivers $10,000 \text{ m}^3 \text{ yr}^{-1}$ to Ingleses beach via headland overpassing. Pinto *et al.* (2015) found the migration rate of the dunefield has decreased during the last 60 years due to urbanization and increasing vegetation cover. This may explains the recent propagation of Santinho as well as indicate the importance of the dunefield to nourish Ingleses, which is now retreating. Porpilho *et al.* (*in press*) indicate the formation of a shoreface sand body (SSB) in front of the Santinho-Ingleses headland, which is also observed in bathymetric data (see Figure 3). According to the authors, the formation of the SSB has occurred due to the convergence of bi-directional currents and associated sediment transport. Therefore, while the beach experiences beach rotation (Figure 7) no significant headland bypassing is expected to occur around this headland and the main path of sediment is via dunefield.

5.3 Ingleses-Brava

While the headland between Ingleses and Brava has the steepest profile (Figure 3), the first 70 m from the headland lies in depths shallower than 5 m where sand can be transported by waves. The more energetic southerly waves (Araujo *et al.*, 2003) may be able to transport sand around this headland. Also, Ingleses and adjoining Brava beaches behave differently (see Figure 6 and Figure 7) with unrelated rates of shoreline changes (*i.e.* Brava prograding and Ingleses stable between 1998 and 2002 as well as 2010 and 2012). However, sediment transport between the beaches has not been verified.

5.4 Brava-Lagoinha

There is no evidence of sediment bypassing between Brava and Lagoinha and they show similar behaviour as shown in Figure 6 (Euclidean distance <70) and Figure 7 (*i.e.* Brava and Lagoinha retreating between 1957 and 1978, stable between 1978 and 1998 and prograding between 1998 and 2002), however the bathymetry in front of the headland (Figure 3) indicate that at least a 150 m wide strip close to the headland lies in depths less than 5 m where wave-driven sediment transport may be occurring. Between Ingleses and Lagoinha is a gap in our knowledge of the sediment path, although it is possible that the sand bypasses both headlands and finally reaches Lagoinha. CPE (2010) and Porpilho *et al.* (2015) showed that the intensification of the currents and associated shore perpendicular northward migrating megaripples around the headlands of the study area that may indicate sediment transport in these areas and contribute to sand bypassing around both headlands.

5.5 Lagoinha-Ponta das Canas

Sand is apparently moving from Lagoinha to the Ponta das Canas spit through headland bypassing. Ponta das Canas spit controls the sediment availability downdrift as far as Daniela. In front of the headland between Lagoinha and Ponta das Canas (Figure 3) a gentle bathymetry (~1:100) is observed, indicating an accumulation of sand. The average rate of spit migration is 60 m yr⁻¹ represents an increase of 7,000 m³ yr⁻¹ (based on the spit height of 1.2 m). The spit undergoes initial rapid accumulation then slows down as it migrates. As the spit grows it traps sediment and the downdrift area (towards Daniela) retreats, on the other hand, when the spit merges to the coast (retreating) and start to spread the downdrift beaches prograde. The cyclic development and migration of the spit corroborates with Short and Masselink (1999) model of headland sand bypassing.

5.6 Jurerê and Forte spits

Beside the major spit formation at Ponta das Canas, two minor spit were identified at Jurerê and Forte beaches. The shoreline changes presented in Figure 4 also support the hypothesis of sediment bypassing at both Jurerê and Forte beaches which are prograding due to sediment accumulation and westward migration as indicated by Almeida *et al.* (1991); CPE (2010); Diehl (1997). From the aerial photos (Figure 5) as well as the bathymetry (Figure 3) the presence of sand bars close to the headlands and spits (Ponta das Canas, Jurerê and Forte) are apparent and it is clear that the

headlands are not capable of trapping all sediment but they are part of the longshore transport path. The small spit at Jurerê is nourished by longshore sediment transport from Ponta das Canas - Canasvieiras. The Jurerê spit is also the main source of sediment to Forte spit that in its turn delivers sand to Daniela. The average migration rate of Forte spit is 40 m yr^{-1} representing a volume increase rate of $4,600 \text{ m}^3 \text{ yr}^{-1}$.

5.7 Daniela spit

According to Almeida *et al.* (1991), westerly longshore drift is responsible for developing the sandy spit at Daniela. In addition the bathymetry at the end of Daniela spit (Figure 3) has a very gentle slope, indicating sediment accumulation. According to Diehl (1997), this development is due to net sediment transport from the exposed area of the island westward towards the North Bay. Based on its plan form, Silveira, Klein, and Tessler (2010) classified Daniela beach as being in dynamic equilibrium, with the coastline being seaward of its equilibrium position, which may lead the shoreline to migrate towards its equilibrium as the sediment supply reduces. This would explain the erosional trend along the western part of Daniela beach - as the sediment is trapped at Forte and the east of Daniela beach which is presently prograding, while the western part of Daniela retreats. The development of the sandy spits are strong indicators of sediment transport into North bay, and the process of sediment bypass on updrift beaches is therefore an important mechanism for such development.

The spit formation and migration are strong indicators of the direction of the net sediment transport and support the anticlockwise path of sediment presented in this paper. Also the formation and migration of spits are dependent on sediment availability. Considering that the prevailing direction of the longshore transport is anticlockwise as well as the episodic formation of the spits along the study area it is very likely that the headland bypassing is the main source of the spit formation and grow. The anticlockwise transport is supplying sediment to downdrift of the study area - either a sink of sediment or a transitional area to the continuation of the sediment path.

6 CONCLUSIONS

This paper presented a shoreline change analysis used to identify the sediment transport path and headland bypassing involving nine beaches, extending 50 km from Barra-Moçambique to Daniela and including dunes and spits located along the

microtidal coast of eastern and northern shores of Santa Catarina Island – Brazil. While longshore sand transport is well documented and headland bypassing and overpassing has been reported, this is the first time sand transport around a series of beaches and headlands via bypassing, overpassing and spits has been documented.

Beach rotation was identified at Barra-Moçambique and Santinho beaches. The accumulation of sand by beach rotation may be the first step to sand to the bypassing. It was also demonstrated that Santinho beach is prograding while Ingleses is retreating, indicating the importance of the dunefield to supply sediment to Ingleses.

It was not possible to identify a sediment transport (bypassing) between Ingleses and Brava beaches as well as between Brava and Lagoinha. The stretch of the coast between Ingleses and Lagoinha is therefore the main gap in our knowledge of the sediment path.

A major spit develops at northeast of Ponta das Canas and cyclically grows, migrates, merges and releases the sediment to downdrift areas, indicating the occurrence of headland bypassing process. As Ponta das Canas spit grows it traps sediment and the downdrift beaches (west of Ponta das Canas - Canasvieiras, Jurerê, Forte and Daniela) retreat. On the other hand, when the spit erodes releasing the trapped sediment, the downdrift areas prograde.

An anticlockwise longshore transport was identified and described between a series of beaches with variable orientation and separated by headlands, including evidence of beach rotation (Barra-Moçambique and Santinho), headland overpassing (Santinho-Ingleses dunefield), together with three locations (Ponta das Canas, Jurerê and Forte) with cyclically spit formation. The estimated volume input from Ingleses ($10,000 \text{ m}^3 \text{ yr}^{-1}$) is similar to the volume trapped at Ponta das Canas spit as it grows ($7,000 \text{ m}^3 \text{ yr}^{-1}$) while a smaller volume is trapped as Forte spit grows ($4,600 \text{ m}^3 \text{ yr}^{-1}$). It is very likely that the headland bypassing is the main source of sand for the spit formation and growth. Studies using *in situ* sediment transport data (such as sediment traps or tracers) and/or modeling tools may fill the gap of sediment transport knowledge between Ingleses and Lagoinha beaches as well quantifying the volume of sediment bypassing the headlands.

Acknowledgements

The authors would like to thank to Prof. Carla Bonetti, Rafael Sartori, Diego Porpilho, Fundo Clima – MMA (Process number: 3520120), CNPQ [Process numbers: 400302/2012-8, 303550/2012-0 and 140738/2012-6], PRH-PB240 (Process number: 48610.002443/2013-14), CAPES (Process number: 005809/2014-02), SMC-BRASIL (MMA-IHC) and the Journal of Coastal Research reviewers for their suggestions.

References

Ab Razak, 2015. Natural Headland Sand Bypassing: Towards Identifying and Modelling the Mechanisms and Processes: Delft University of Technology. CRC Press/Balkema. the Netherlands. Ph.D. Thesis. 186 p.

Absalonsen, L. and Dean, R.G., 2011. Characteristics of the shoreline change along Florida sandy beaches with an example for Palm Beach County. *Journal of Coastal Research*, 27(6A), 16–26.

Almeida, E.S.; Abreu de Castilhos, J.J.; Simon, A. F.; Avila, E.L.; Aumond, J.J.; Pinto, N.L.C.; Dal Santo, N.A., and Infante, N., 1991. Observações geomorfológicas na praia do Forte - Ilha da Santa Catarina, município de Florianópolis - SC. *Geosul*, 11(4), 38-54.

Araújo, C.E.S.; Franco, D.; Melo Filho, E., and Pimenta, F., 2003. Wave regime characteristics of southern Brazilian coast. *Proceedings of the 6^o International Conference on Coastal and Port Engineering in Developing Countries, COPEDEC* (Colombo, Sri Lanka), Paper 97, 15p.

Araujo, R.S.; Silva, G.V.; Freitas, D., and Klein, A.H.F., 2009. Georreferenciamento de fotografias aéreas e análise da variação da linha de costa. *In: Alcántara-Carrió, J.; Correa, I.D.; Isla, F.; Alvarando, M. ; Klein, A.H.F., and Cabrera, J.A. (eds.). Metodologías en Teledetección Aplicada a la Prevención de Amenazas Naturales en el Litoral*. Valencia: Programa Iberoamericano de Ciencia y Tecnología para el Desarrollo (PICTD), pp. 237-257.

Boak, E.H. and Turner, I.L., 2005. Shoreline definition and detection: A review. *Journal of Coastal Research*, 21(4), 688-703.

- Boeyinga, J.; Dusseljee, D.W.; Pool, A.D.; Schoutens, P.; Verduin, F.; Van Zwicht, B.N.M., and Klein, A.H.F., 2010. The effects of a bypass dunefield on the stability of a headland bay beach: A case study. *Coastal Engineering*, 57(1), 152–159.
- Bruun, P., 1954. *Coast erosion and the development of beach profiles*. Washington DC: US Army Corps of Engineers, *Technical Memorandum No. 44*, 79p.
- Cheung, K.F.; Gerritsen, F., and Cleveringa, J., 2007. Morphodynamics and sand bypassing at Ameland Inlet, The Netherlands. *Journal of Coastal Research*, 23(1), 106-118.
- CPE Staff, 2010. *Análise de alternativas para o terminal de cruzeiros de Florianópolis - possíveis alterações nos padrões de circulação e taxa de sedimentação no canal de acesso ao porto de canasvieiras*. Florianópolis, SC Brazil: Coastal Planning and Engineering do Brazil, 55p.
- Crowell, M.; Leatherman, S.P., and Buckley, M.K., 1991. Historical shoreline change: Error analysis and mapping accuracy. *Journal of Coastal Research*, 7(3), 839-852.
- Dean, R.G., 1977. *Equilibrium Beach Profiles: U.S. Atlantic and Gulf Coasts*. Newark, Delaware: University of Delaware, Department of Civil Engineering, Ocean Engineering Report No. 12, 45p.
- Diehl, F.L., 1997. Aspectos Geoevolutivos, Morfodinâmicos e Ambientais do Pontal da Daniela, Ilha de Santa Catarina, Brasil. Florianópolis, Santa Catarina: Universidade Federal de Santa Catarina. Master's thesis, 111p.
- Dolan, R.; Hayden, B.P.; May, P., and May, S., 1980. The reliability of shoreline change measurements from aerial photographs. *Shore & Beach*, 48(4), 22–29.
- Egbert, G.D., Bennett, A., and Foreman, M., 1994. TOPEX/ Poseidon tides estimated using global inverse model. *Journal of Geophysical Research*, 99(12), 821–852.
- Egbert, G.D., and Erofeeva, S.Y., 2002. Efficient inverse modelling of barotropic ocean tides. *Journal of Atmospheric Oceanic Technology*, 19(1), 183–204.
- Elmore, K.L., and Richman, M.B., 2001. Euclidean distance as a similarity metric for principal component analysis. *Monthly Weather Review*, 129(3), 540-549.

Eslami, S.; Van Rijn, L.; Walstra, D.; Luijendijk, A., and Stive, M., 2010. A Numerical study on design of coastal groins. *Proceedings of International Conference on Scour and Erosion* (San Francisco, CA, USA), pp. 501-510.

Farris, A.S., and List J.H., 2007. Shoreline change as a proxy for subaerial beach volume change. *Journal of Coastal Research*, 23(3), 740-748.

Ferreira, O., Gargia, T., Matias, A.; Taborda, R., and Alveririnho Dias, J. 2006. An integrated method for the determination of set-back lines for coastal erosion hazards on sandy beaches. *Continental Shelf Research*, 26(1), 1030-1044.

FGDC-STD Staff, 1998. *Geospatial Positioning Accuracy Standards (part 3): National Standard for Spatial Data Accuracy*. Washington, DC: Federal Geographic Data Committee, FGDC-STD-007.3-1998, 25p.

Fitzgerald, D.M. and Pendleton, E., 2002. Inlet formation and evolution of the sediment bypassing system: New Inlet Cape Cod, Massachusetts. *In: Cooper and Jackson (eds.), Proceedings of International Coastal Symposium*. *Journal of Coastal Research*, Special Issue No. 36, pp. 290-299.

Fitzgerald, D.M., Krauss, N.C., and Hands, E.B., 2000. *Natural Mechanisms of Sediment Bypassing at Tidal Inlets*. Vicksburg, Mississippi: US Army Corps of Engineering, *Report ERDC/CGL CHETN-IV-30*, 10p.

Goodwin, I.D., Freeman, R., and Blackmore, K., 2013. An insight into headland sand bypassing and wave climate variability from shoreface bathymetric change at Byron Bay, New South Wales, Australia. *Marine Geology*, 341(1), 29-45.

Harley, M.D., Turner, I.L., Short, A.D., Ranasinghe, R., 2011. A reevaluation of coastal embayment rotation: The dominance of cross-shore versus alongshore sediment transport processes, Callaroy-Narrabeen Beach, southeast Australia. *Journal of Geophysical Research*. 116 (F04033). 16p.

Jones, B.M.; Arp, C.D.; Jorgenson, M.T.; Hinkel, K.M.; Schmutz, J.A., and Flint, P.L., 2009. Increase in rate and uniformity of coastline erosion in arctic Alaska. *Geophysical Research Letters*, 36(1). 5p.

- Klein, A.H.F.; Benedet Filho, L., and Schumacher, D.H., 2002. Short-term beach rotation processes in distinct headland bay beach systems. *Journal of Coastal Research*, 18(3), 442-458.
- Klein, A.H.F., Short, A.D., Bonetti, J. *in press*. Santa Catarina beach systems. *In: Short, A.D and Klein, A.H.F. (eds), Brazilian Beach Systems*. Springer Coastal Research Library.
- Ludwig, J.A., and Reynold, J.F. 1988. *Statistical Ecology: A Primer in Methods and Computing*. New York: John Wiley & Sons, 368p.
- Mariani, A.; Carley, J.T., and Miller, B.M., 2010, Infilling and sand bypassing of coastal structures and headlands by littoral drift. *Proceedings of 19º NSW Coastal Conference* (Batemans Bay, NSW, Austrália), 8p.
- Masselink, G., Pattiaratchi, C.B., 1998. Seasonal changes in beach morphology along the sheltered coastline of Perth, Western Australia. *Marine Geology*. 172, 243-263.
- Moore, L.J. 2000. Shoreline mapping techniques. *Journal of Coastal Research*, 16(1), 111-124.
- Moore, L.J.; Ruggiero, P., and List, J.H., 2006. Comparing mean high water and high water line shorelines: Should proxy-datum offsets be incorporated into shoreline change analysis? *Journal of Coastal Research*, 22(4), 894–905.
- Muler, M.; Prado, M.F.V.; Rocha, R.S.; Camargo, R.S.V., and Klein, A.H.F. 2014. Verificação da Precisão de Bases Cartográficas da Região de Florianópolis, SC. *Proceedings of Congresso Brasileiro de Cartografia* (Gramado, RS, Brazil), 15p.
- Nobre, C.A.; Cavalcanti, M.A.G.; Nobre, P.; Kayano, M.T.; Rao, V.B.; Bonatti, J.P.; Satyamurti, P.; Uvo, C.B., and Cohen, J.C. 1986. Aspectos da climatologia dinâmica do Brasil. *Climanálise Special Issue* (no number), 124p.
- Ojeda, E. and Guillén, J. 2008. Shoreline dynamics and beach rotation on artificial embayed beaches. *Marine Geology*. 253, 51-62.
- Pinto, M.W.; Meireles, R.; Cooper, A., and Klein, A.H.F. 2015. Santinho/Ingleses transgressive dunefield system - Santa Catarina Island (Brazil): temporal variability in

vegetation, manmade structures and dune migration. *Proceedings of Coastal Sediments'15* (San Diego, CA, USA), 14p.

Porpilho, D.; Klein, A.H.F.; de Camargo, R.S.V.; Prado, M.F.V.; Short, A. D.; Vieira da Silva, G., and Toldo Jr., E. E., 2015. Bedform classification in front of santinho headland, Santinho beach - Santa Catarina Island, Brazil. *Proceedings of Coastal Sediments'15* (San Diego, CA, USA), 10p.

Porpilho, D.; Klein, A.H.F.; de Camargo, R.S.V.; Prado, M.F.V.; Short, A.D. and Vieira da Silva, G., *in press*. Ingleses headland bedform characterization through interferometric data, Santa Catarina Island, southern Brazil. In: Vila-Concejo, A.; Bruce, E.; Kennedy, D.M., and McCarroll, R.J. (eds.), *Proceedings of the 14th International Coastal Symposium* (Sydney, Australia). *Journal of Coastal Research*, Special Issue, No. 75, Coconut Creek (Florida), ISSN 0749-0208.

Ranashinghe, R., McLoughlin, R., Short, A., Symonds, G., 2004. Southern Oscillation Index, wave climate and beach rotation. *Marine Geology*. 204, 273-287.

Short, A.D.; Cowell, P.J.; Cadee, M.; Hall, W.; and Van Dijk, B., 1995. Beach rotation and possible relation to southern oscillation. In: Aung, T.H. (ed.), *Proceedings of Ocean Atmosphere Pacific Conference* (Adelaide, SA, Australia), 329-334.

Short, A.D. and Masselink, G. Eds. 1999. Embayed and structurally controlled beaches, *In: Short, A.D.(ed), Handbooks of Beach and Shoreface Hydrodynamics*. New York: John Wiley and Sons, pp. 230–249.

Short, A.; Trembanis, A., and Turner, I, 2001. Beach oscillation, rotation and the southern oscillation, Narrabeen Beach, Australia. *Proceedings of the 27th International Conference on Coastal Engineering* (Sydney, NSW, Australia), pp. 2439-2452.

Silveira, L.F.; Klein, A.H.F., and Tessler, M.G., 2010. Headland-bay beach planform stability of Santa Catarina state and of the northern coast of São Paulo state. *Brazilian Journal of Oceanography*, 58 (2), 101-122.

Silvester, R., 1985. Sediment by-passing across coastal inlets by natural means. *Coastal Engineering*, 9, 327-346.

Thieler, E.R.; Himmelstoss, E.A.; Zichichi, J.L., and Miller, T.L., 2005. *Digital Shoreline Analysis System (DSAS) version 3.0: An ArcGIS Extension for Calculating Shoreline Change*. U.S. Geological Survey Open-file Report 1304.

Thieler, E.R., Himmelstoss, E.A., Zichichi, J.L., and Ayhan, E., 2009, *Digital Shoreline Analysis System (DSAS) version 4.0—An ArcGIS extension for calculating shoreline change*: U.S. Geological Survey Open-File Report 2008-1278.

Turki, I., Medina, R., Gonzales, M. and Coco, G., 2013. Natural variability of shoreline position: observations at three pocket beaches. *Marine Geology*. 338, 67-89.

Toldo Jr., E.E.; Motta, L.M.; Almeida, L.E.S.B., and Nunes, J.C.R., 2013. Large morphological change linked to sediment budget in the Rio Grande do Sul coast. *Proceedings of Coastal Dynamics 2013*, (Arcachon, France), pp. 1687-1696.

Truccolo, E.C.; Franco, D., and Schettini, C.A.F., 2004. The low frequency sea level oscillations in the northern coast of Santa Catarina, Brazil. *In*: Klein, A.H.F., Finkl, C.W., Sperb, R.M., Beaumord, A.C., Diehl, F.L., Barreto, A.S., Abreu, J.C.N., Bellotto, V.R., Kuroshima, K.N., Carvalho, J.L.B., Resgala Jr.,C., Fernandes, A.M.R. (eds.), *Proceedings of International Coastal Symposium*. Journal of Coastal Research, Special Issue No. 39, pp. 547-552.

Truccolo, E.C., 2011. Assessment of the wind behaviour in the northern coast of Santa Catarina. *Revista Brasileira de Meteorologia*. 26(3), 450-460.

Wilks, D.S. 2006. *Statistical Methods in the Atmospheric Sciences*. San Diego: Elsevier, 704p.

HEADLAND SAND BYPASSING - QUANTIFICATION OF NET SEDIMENT TRANSPORT IN EMBAYED BEACHES, SANTA CATARINA ISLAND NORTH SHORE, SOUTHERN BRAZIL

Este capítulo apresenta o conteúdo segundo artigo que compõe esta tese e foi enviado à revista *Marine Geology* em 12/11/2015. O artigo foi formatado para melhor apresentação nesta tese, contudo, o conteúdo segue na íntegra o submetido à revista:



Guilherme Vieira da Silva <oc.guilhermevs@gmail.com>

MARGO5950 - Notice of manuscript number

1 mensagem

Marine Geology <margo-eo@elsevier.com>

12 de novembro de 2015 11:10

Para: oc.guilhermevs@gmail.com, guivs84@yhao.com.br

Dear Mr. Vieira da Silva,

Your submission entitled "Headland Sand Bypassing - Quantification of Net Sediment Transport in Embayed Beaches, Santa Catarina Island North Shore, Southern Brazil" has been assigned the following manuscript number: MARGO5950.

Your paper will be considered as belonging to the category Research Paper. Please contact us if this is not correct.

When a decision has been taken we will contact you again.

Thank you for submitting your work to our journal.

Kind regards,

Marine Geology

HEADLAND SAND BYPASSING - QUANTIFICATION OF NET SEDIMENT TRANSPORT IN EMBAYED BEACHES, SANTA CATARINA ISLAND NORTH SHORE, SOUTHERN BRAZIL

Guilherme VIEIRA DA SILVA ^{a,b}, Elírio E. TOLDO JR. ^a, Antonio H. da F. KLEIN ^c, Andrew D. SHORT ^d, Colin D. WOODROFFE ^b

^a Centro de Estudos de Geologia Costeira e Oceânica, Instituto de Geociências, Universidade Federal do Rio Grande do Sul. Campus do Vale Av. Bento Gonçalves, 9500 Porto Alegre, RS, Brazil. CEP: 91501-970.

^b School of Earth and Environmental Sciences, University of Wollongong, Northfields Ave, Wollongong, NSW, Australia, 2522.

^c Laboratório de Oceanografia Costeira, Departamento de Geociências, Centro de Filosofia e Ciências Humanas Universidade Federal de Santa Catarina. Beco dos Coroas, Fundos, Barra da Lagoa - Florianópolis SC, Brazil – CEP: 88062-601.

^d School of Geosciences, University of Sydney, Sydney, NSW, Australia, 2006.

Corresponding author: Guilherme VIEIRA DA SILVA, e-mail: oc.guilhermevs@gmail.com

Elírio E. TOLDO JR., e-mail: toldo@ufrgs.br

Antônio H. da F. KLEIN, e-mail: antonio.klein@ufsc.br

Andrew D. SHORT, e-mail: andrew.short@sydney.edu.au

Colin D. WOODROFFE, e-mail: colin@uow.edu.au

Abstract

This paper presents a comprehensive study of headland bypassing comprising a series of seven headlands with different orientation and degree of wave and tide-induced current exposure, located on the northern shore of Santa Catarina island, southern Brazil. It encompasses an extensive dataset including detailed in situ measurements of bathymetry, beach profiles, sediment transport (traps), waves, currents and tides. The entrained sediment decreased in magnitude towards the protected area while maintaining compatible sediment grain distributions supporting the hypothesis of connection between beaches. Based on in situ measurements a

numerical model was calibrated (waves, currents and tides) and validated with errors representing 11% of the magnitude of the measurements. Furthermore, three sediment transport formulae were tested to identify the one that best reproduced the processes at the study area. An annual “brute force” model using tides, winds and full wave spectra as input was run to identify the general (net) trend of sediment transport in the study area aiming to identify if/where the headland bypassing occurs. The results show that headland sand bypassing does occur in the study area confirming the anticlockwise sediment transport path. The present work highlights the importance of understanding the "big picture" when studying headland bay beaches, which are usually considered to be closed cells.

key words: Sediment trapping; numerical modelling, Helley-Smith sampler; coastal cells.

1 INTRODUCTION

Headlands, estuaries and man-made structures act as obstacles to sediment transport by interrupting or stopping longshore sediment transport. The water and sediment flow are partially blocked resulting in accumulation of sediments on the updrift side of the obstacle. Therefore, it is not uncommon to consider (natural or artificially) embayed beaches as closed compartments (Hsu and Evans, 1989). However it is known that sediment can be transported around obstacles, and if this is the case understanding this process is essential for modelling sediment transport in coastal areas as well as in consideration of shoreline stability.

Sediment transport around obstacles such as man-made structures (e.g. jetties) or inlets has been described by several authors (Silvester, 1985; FitzGerald et al., 2000; FitzGerald and Pendleton, 2002; Cheung et al., 2007; Mariani, 2010; Eslami et al. 2010; Ab Razak et al. 2013). On the other hand, transport around headlands, despite the studies of Evans (1943), Short and Masselink (1999) and Smith (2001) that conceptually described the process (known as headland bypassing) has only recently been investigated in the field. Goodwin et al. (2013) related headland bypassing to the wave climate variability, based on shoreface bathymetric changes; Ribeiro et al. (2014) studied the process using Landsat images as well as RTK-GPS and ground-based photographic monitoring; Duarte et al. (2014) investigated the process using sand tracer experiments; Vieira da Silva et al. (in press) presented insights on headland bypassing based on statistical analysis of multi-decadal shoreline changes;

and Ab Razak (2015) used numerical modelling to reproduce and understand the process.

Regardless of the distinct methods of assessing headland bypassing there is not a standard or accepted best procedure. Each method has advantages and disadvantages. In situ measurements are limited in time and space; on the other hand, numerical models may be able to reproduce longer periods and cover larger areas but if not well calibrated / validated (with data collected in situ) may produce unreliable results. The present paper combined both in situ bedload transport measurements and numerical modelling to identify and quantify the headland bypassing at a complex study site encompassing a series of exposed and protected beaches influenced by waves, tidal currents, and winds, and separated by headlands. The present study is based on the hypothesis that there is a connection between adjacent beaches of the study area via headland bypassing. The aim of this research is to 1) measure sediment transport around headlands; 2) identify the sediment transport paths and Determine whether adjacent beaches can be considered closed cells or headland bypassing is occurring; 3) quantify the annual sediment transport around headlands.

2 REGIONAL SETTINGS

The central coast of Santa Catarina state (Brazil) classified by Klein et al. (2010) as rugged bedrock headland-strand plain coast. It has a relatively narrow discontinuous coastal plain that is bordered by crystalline rocks and where exposed granitic plutons form numerous low-relief headlands that dominate this section of the coast (FitzGerald et al. 2007). Santa Catarina Island is located on the central coast. Its north shore has seven beaches separated by headlands (Ingleses, Brava, Lagoinha, Ponta das Canas - Canasvieiras, Jurerê, Forte and Daniela) and are the subject of the present paper (Figure 9).

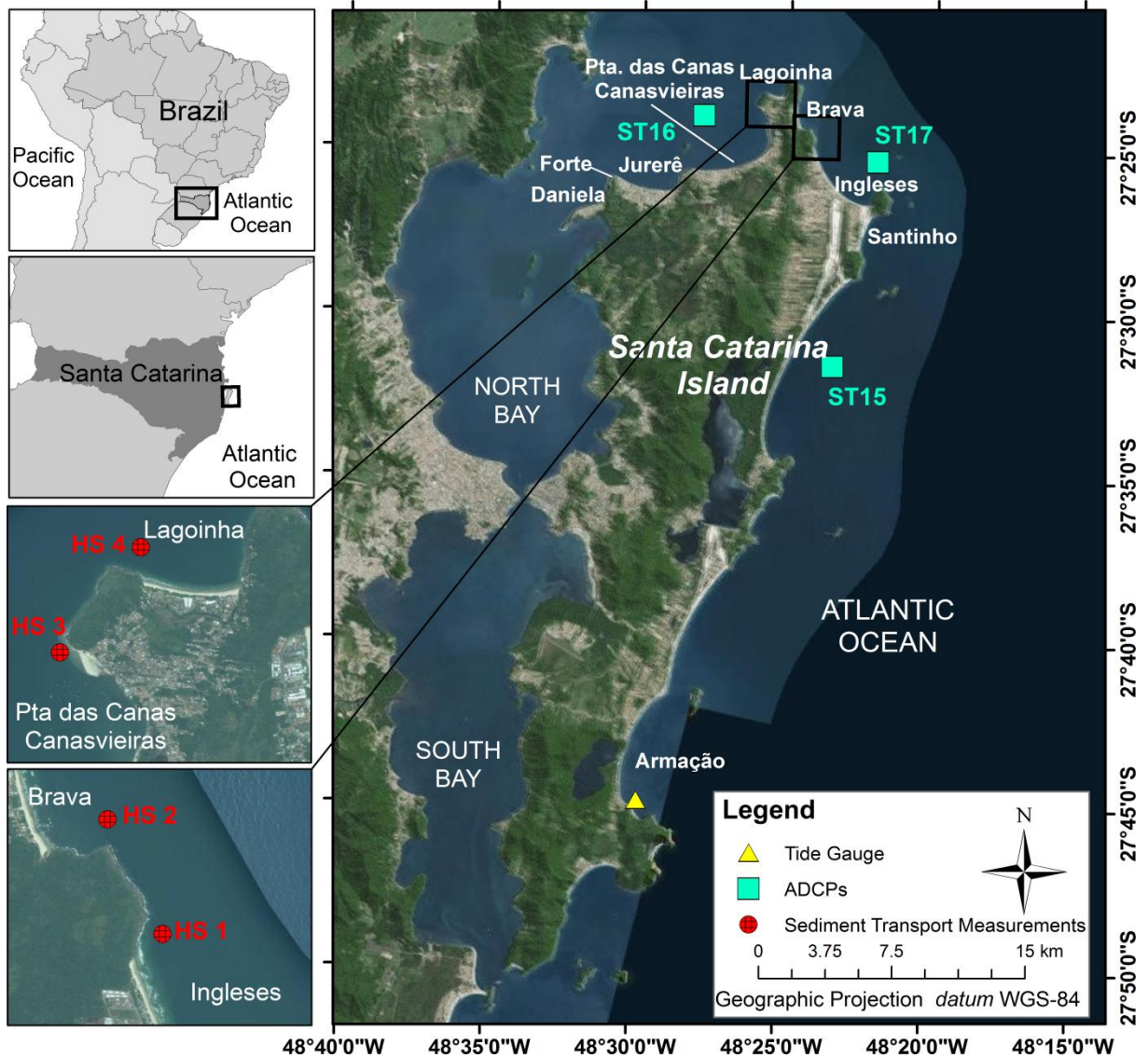


Figure 9: Location of the study area on the southern coast of Brazil and location of the measured data. STs : ADCP locations; HSs: Helley-Smith trapping locations. Background image source: ESRI World Imagery (ArcGIS 10).

The waves arrive predominantly from the south with periods of 12 s, followed by waves from the east with periods of 8 s, while >30% of the time bimodal (south and east) sea conditions occur. Wave height averages 1 to 1.5 m with the highest waves arriving from south and southeast, with H_o (deep water wave height) greater than 4 m and periods above 12 s (Araújo et al., 2003). During the austral autumn and winter (March to August), the swell waves from south prevail over easterly seas, while in summer (December to February) there is a balance between both, and during the spring easterly seas are predominant. The astronomical tide within Santa Catarina State is microtidal with a range between 0.4 m and 1.2 m during neap and spring tides, respectively, while lower frequency oscillations caused by meteorological forcing can be as high as 1 m (Truccolo et al. 2004). Based on

Relative Tide Range (RTR - Masselink and Short, 1993) the study area is mainly classified as wave-dominated, however, when wave breaking height (H_b) < 0.4 m it becomes tide-modified. This usually does not occur on the exposed east-facing part of the study area, while breaker wave height is frequently smaller in the protected area (Ponta das Canas to Daniela). The dominant winds come from the northwest with stronger southerly winds associated with the passage of cold-front systems (Nobre et al., 1996; Truccolo, 2011).

The beaches in the study area vary from sheltered reflective beaches in the north to predominantly rip-dominated Transverse Bar and Rip to Rhythmic Bar and Beach (TBR-RBB) beaches on the east coast (Klein, Short, and Bonetti, in press). H2 (2008) pointed out that the east-facing beaches are more exposed to the waves than north and west-facing beaches that receive only refracted/attenuated waves. Based on 189 beach face sediment samples, Vieira da Silva et al. (in press) describe the sediments of the study area beaches as homogeneous with an average diameter ranging from 0.20 mm (near the southern Ingleses) and 0.30 mm (near the southern Brava). The Santinho to Ingleses dunefield has a median grain size of 0.23 mm (Vintem et al., 2006). Porpilho et al. (in press) based on side scan sonar data showed that the inner shelf has similar sediments together with patches of coarser sediments.

A number of studies have investigated coastal processes and sediment transport in the study area. CPE (2010) observed the intensification of tidal currents near headlands (the study did not include Brava-Ingleses headland). This increase has a significant impact between Lagoinha e Ponta das Canas beaches during flood tide condition. Porpilho et al. (in press) showed that at Santinho-Ingleses headland there are two different sediment transport directions - on the eastern side of the headland with bedforms migrate northward, while on the northern side they migrate eastward into deeper water. Vieira da Silva et al. (in press) inferred an anticlockwise sediment transport path that begins at Ingleses and extends to Daniela. In addition the dunefield that extends northwards from Santinho to Ingleses delivers $\sim 10,000 \text{ m}^3 \text{ yr}^{-1}$ to Ingleses beach (Boeyinga et al. 2010) while Pinto et al. (2015) showed that the dunefield rate of migration has reduced during the last 60 years due to urbanization and increased vegetation coverage.

3 MATERIALS AND METHODS

The methods will be described in two sections. The first describes the field measurements and data processing. The second describes the model calibration; identification of the best sediment transport formula to describe the processes around headlands; and the procedure adopted to estimate the annual longshore sediment transport and headland bypassing. Figure 10 summarizes the methods adopted for this research.

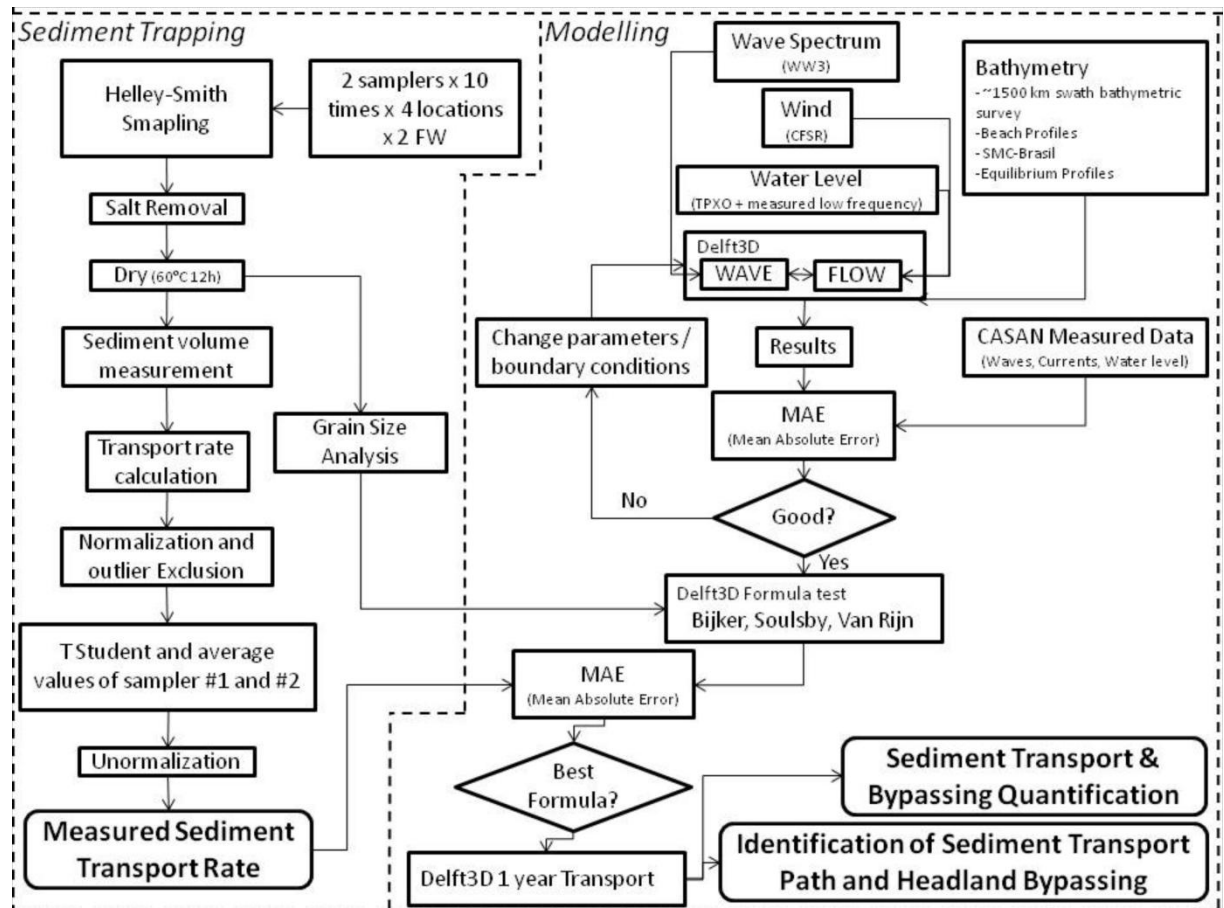


Figure 10: Flow diagram illustrating the methods of sediment trapping experiment and data processing (left) and modelling procedures (right) as well as the connection between both methods.

3.1 Sediment Trapping and Samples Processing

Two headlands were chosen for sediment transport experiment (see Figure 9): the exposed headland that separates Ingleses (south) and Brava (north) beaches and a protected headland located between Lagoinha (north) and Ponta das Canas (south) beaches where a spit develops and cyclically migrates (Vieira da Silva et al. in press). Two field experiments were carried out to quantify the bedload transport around the headlands; the first, between 16 and 17 of April 2014 (FW1) and the second between 18 and 19 of August 2014 (FW2). At each headland the sediment

transport was measured at different depths: 7.4, 10.9, 7.4 and 2.9 m for Ingleses, Brava, Lagoinha and Ponta das Canas, respectively.

The Helley-Smith sampler (Helley and Smith, 1971) was chosen for this fieldwork because it directly measures the sediment transport, it is the most widely used bedload transport measuring instrument, it is simple to operate and provides realistic values of sediment transport (Van Rijn, 1993).

Each field experiment consisted of: 1) navigating to the pre-defined sampling locations, positioning the boat with an RTK-GPS; 2) place and then recover at the bottom two samplers spaced ~1.5 m apart - the measurement time was 15 minutes and it was placed and taken off of the bottom by scientific divers avoiding any bottom disturbance drag or digging. The process was repeated 10 times so 20 samples were collected at each location; 3) labelling the samples; 4) at the laboratory each sample was washed on a 0.063 mm sieve (same size as the sediment trap mesh) for 5 minutes in running water to remove the salt, afterwards it was dried for 24 hours in a oven at 60° C (Fontoura, 2004); 5) the immersed volume of sediment catch was measured by filling a measuring cylinder with water, and adding the sample -the difference between the volume of water + sediment and the volume of water only is the immersed sediment volume; 6) calculate the sediment transport rate.

To calculate the sediment transport rate from the measured volume of sediment, Helley and Smith (1971) suggest a calibration coefficient of 0.5 for sediments finer than 0.5 mm. The authors observed an oversampling of fine material due to disturbance as the sampler is placed on the bottom as well as digging and dragging material as the sampler is pulled back. In the case of the present research, the oversampling was avoided by divers placing and retrieving the traps carefully rather than deploying it from the surface. Therefore, no digging or disturbance of the bottom was observed by the divers and it was assumed that only sediment that was actually being transported was trapped and the calibration coefficient was set to 1, avoiding underestimation of the sediment transport. The sediment transport was calculated as:

$$S_b = \frac{V}{tb} \quad \text{Eq.(01)}$$

where: S_b is the bedload sediment transport ($\text{m}^2 \text{s}^{-1}$); V is the immersed volume (m^3) of sediment trapped; t is the sampling interval (s) and b is the width (m) of the intake opening (0.0762 m).

A total of 140 samples were collected (20 / sampling point) - during FW1 it was not possible to sample at Ingleses due to technical problems. To avoid outliers that may be caused by several sources such as measuring method, natural fluctuations of concentration, velocity or transport (Van Rijn, 1993) a statistical procedure were carried out for each location/fieldwork. It consisted on:

1) normalization of the transport rates (a Shapiro Wilk test was carried out to confirm the normality of the dataset);

2) identification and exclusion of outliers:

$$q_1 - w(q_3 - q_1) > outlier > q_3 + w(q_3 - q_1) \quad \text{Eq.(02)}$$

where q_1 and q_3 are the 25th and the 75th percentiles, and w is 1.5 as according to Tukey (1977). Only one outlier was identified (at Brava FW1) and it was excluded from the dataset.

3) a series of 10 values of sediment transport measured by sampler #1 was compared to a series of 10 values of sediment transport measured by sampler #2 by applying a t Student test and for all fieldworks for both samplers presented statistically equal means.

4) for each location/fieldwork the series were reduced to 10 by averaging the series of sampler #1 and sampler #2 - each value of the series correspond to the average of the sediment transport measured by 2 samplers that were at the bottom at the same time.

5) series unnormalization (returning of the series to its original values) - the final series correspond to series of 10 values of sediment transport / location / fieldwork, a total of 70 values.

For each fieldwork and location six samples were randomly chosen for grain size analysis on a laser diffraction particle size analyser (Horiba LA-9500) to check the grain size compatibility between the samples. This procedure was used to identify any difference in grain composition between sites that would indicate that no headland bypassing occurs as well as to check if the sediment size trapped near the headlands is similar to the results presented by Vieira da Silva et al. (in press) at the beach face as well as to define the sediment characteristics to use as input for numerical modelling.

3.2 Numerical Modelling

To assess the sediment transport over macro timescale (years) (Kraus, 1991) the Delft3D model was used. It can integrate different modules, which allow the simulation of hydrodynamic flow, short wave propagation (fully spectral) and sediment transport (Lesser et al. 2004). For the present study two modules were used coupled - WAVE and FLOW. Both models were run in online mode.

A key point in numerical modelling is to obtain representative in situ data for running and calibrating the model. The topo-bathymetric data were measured by UFSC (Federal University of Santa Catarina) Coastal Oceanography Laboratory at the study area for a MMA (Ministry of the Environment - Klein et al., 2015) between 2013 and 2014 and covered 865 km of swath (3x the water depth) bathymetric lines covering the entire study area up to depths greater than the closure depth. Subaerial beach profiles (189 transects spaced ~200 m) were also measured and the small gaps between the subaerial profiles and the bathymetric survey filled with the best fit equilibrium profile presented by Bruun (1954) and Dean (1977). The bathymetry was undertaken using SMC-Brasil database (Instituto de Hidráulica Ambiental da Universidade de Cantábria - IH Cantabria) based on Brazilian Navy DHN/CHM nautical charts (www.mar.mil.br/dhn/chm/box-cartas-nauticas/cartas.html). For a detailed description of the adopted methods for data collection please refer to Klein et al. (2015), for the integration of the data as well as the bathymetric map, refer to Vieira da Silva et al. (in press).

3.2.1 Wave Model

Two nested numerical grids were used for the WAVE model. The first grid (Wave Regional) is a curvilinear grid with varying resolution (increasing towards the coast) designed to bring the waves from deeper to shallower water. It covers an area of 410 x 240 km and has a resolution of 10 x 6 km in deepwater and 1.7 x 1.7 km near the study area. A higher resolution grid was nested (Wave Local) on the first grid covering an area of 50 x 95 km with varying resolution (1.5 x 1.2 km offshore refining towards the study area where it has a resolution of 30 x 30 m). A time series of wave spectra obtained from a Wave Watch III (WW3) (Tolman, 1991; Tolman, 1997 and Tolman, 2009) model at 200 m depth at 27°30'S, 47°15'W (Figure 11) was used as boundary condition for the WAVE model.

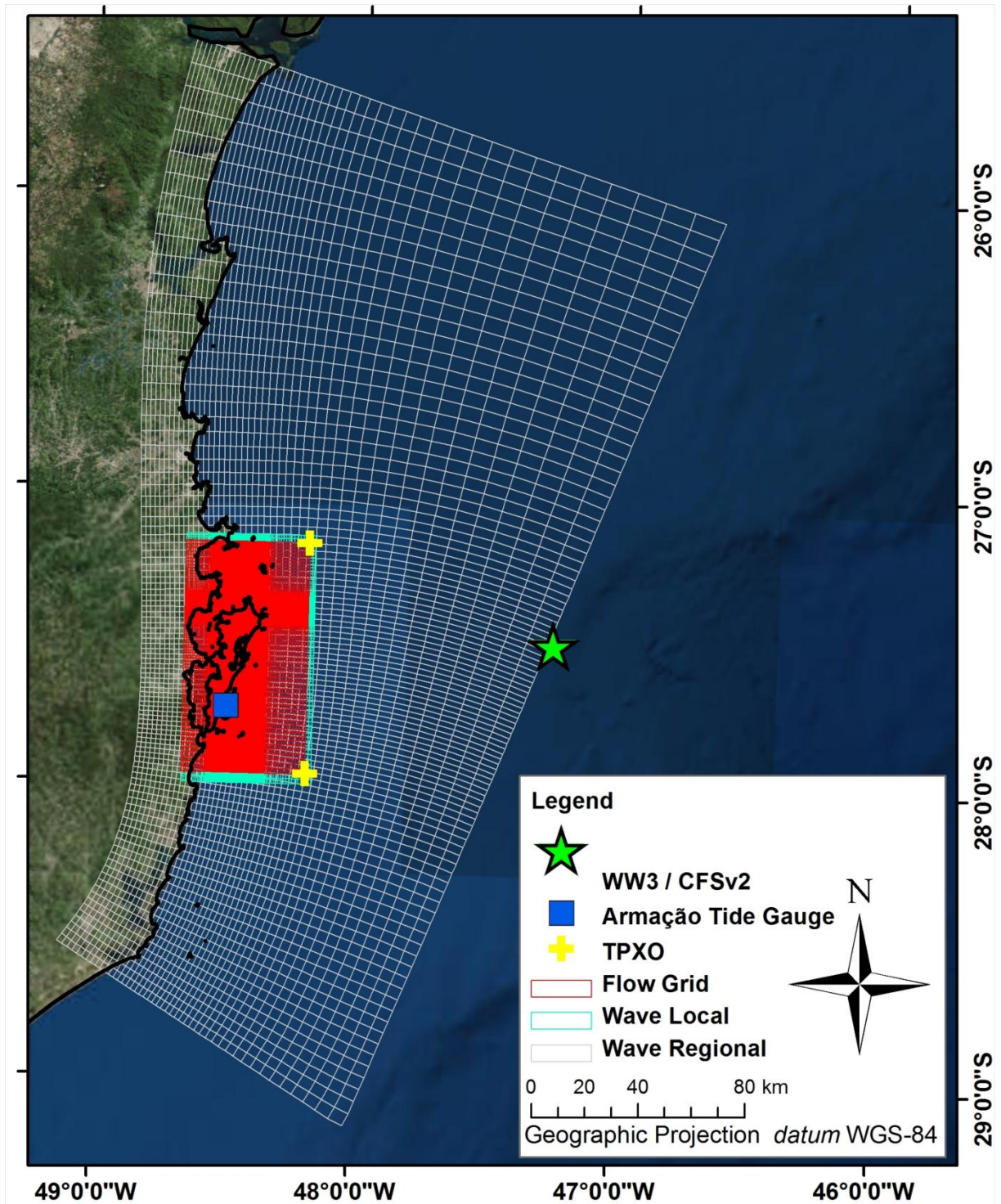


Figure 11: Numerical model wave grids, location of WW3 wave data, CFSv2 wind data, TPXO predicted tides and Armação tide gauge. Background image source: ESRI World Imagery (ArcGIS 10).

3.2.2 Flow Model

FLOW model was run with a grid (Figure 11) almost identical to the Wave Local, the differences are: 1) FLOW grid is two lines/rows smaller at the offshore, north and south boundaries to avoid any boundary instability and, 2) FLOW model was run in a 3D mode with five sigma vertical layers.

At the northernmost and southernmost offshore boundary (Figure 11) a water level time series was predicted using TPXO 7.2 model (Egbert et al. 1994; Egbert and Erofeeva, 2002) the predicted tide was summed to the residual sign of water level time series of the tide gauge located at Armação beach (Figure 11) installed by UFSC for MMA (Klein et al. 2015). The Armação water level time series was filtered using a Godin low pass filter (Godin, 1972) to obtain the residual low frequency signal.

To incorporate the wind effects on the model a wind time series from NCEP Climate Forecast System Version 2 (CFSv2 - Saha et al. 2014) was obtained at the same location as WW3 (see Figure 11). The north and south boundaries were set as gradient type (no gradient) boundary condition known as Neumann (Roelvink and Walstra, 2004) corresponding to an open boundary.

3.2.3 Model Calibration and Validation Procedure

To calibrate the wave model a wave, current and water level time series measured in situ by CASAN (Water and Sanitation Company of Santa Catarina) was used. It consists of time series obtained by three ADCPs AWAC moored in the study area (see Figure 9 - ST15, ST16 and ST17 at 21, 9.2 and 19.7 m respectively) of pressure, currents and wave parameters between 10/2013 to 09/2014. Several model setups/calibration parameters were tested. The model calibration consisted of comparing the modelled data against the measured data (see Figure 9) and adjusting the model so it could reproduce accurately the environment. The WAVE model calibration included tests on wave parameters, wave full spectrum, activation or deactivation of processes such as white-capping, diffraction, refraction and frequency shift. The FLOW model included tests with a range of parameters, number of vertical layers, boundary forcing type (water level - astronomic, water level - time series, Neumann). The calibration was carried out during a period of austral summer (21/01-18/02/2014) and the setup that best represented the environmental conditions was run for a period of austral winter (1-29/07-2014) to validate the model. Both, calibration and validation encompass approximately one lunar month to include both neap and spring tides as well as a range of different wind and wave conditions. In order to assess the model performance, the mean absolute error (MAE) was used as indicated by Willmott and Matsuura (2005). The calibration coefficients/parameters are presented in Table 4 for WAVE model and Table 5 for FLOW model.

Table 4: Wave model calibration parameters.

Parameter	Value
Gravity	9.81 m s ⁻²
Water density	1025 kg m ⁻³
Depth-induced breaking (Battjes and Janssen, 1978)	Alpha = 1; Gamma = 0.73
Bottom friction (Hasselmann et al., 1973)	0.067 m ² s ⁻³
Whitecapping	Komen et al. (1984)
Diffraction	Activated
Refraction	Activated
Frequency shift	Activated

Table 5: FLOW model calibration parameters.

Parameter	Value
Gravity	9.81 m s ⁻²
Water density	1025 kg m ⁻³
Air density	1 kg m ⁻³
Wind drag (Breakpoints: Coefficient / Wind Speed)	A: 0.00063/0m s ⁻¹ B: 0.00723/100m s ⁻¹ C: 0.00723/100 m s ⁻¹
Bottom roughness (Chézy)	U=65 $\sqrt{\text{ms}^{-1}}$ / V=65 $\sqrt{\text{ms}^{-1}}$
Horizontal eddy viscosity	1 m ² s ⁻¹
Horizontal eddy diffusivity	10 m ² s ⁻¹

3.2.4 Sediment Transport

Following the wave and hydrodynamic calibration of the numerical model, three sediment transport equations were tested in the on Delft3D model to identify the best to describe the processes around the headland. The test consisted of comparing the bedload transport predicted by each formula and the measured bedload transport at the study area. Bijker (Bijker 1967; 1971), van Rijn (van Rijn 1993; 2000), and Soulsby (Soulsby, 1997) formulae includes the effect of waves and calculate bedload and suspended load separately, since only the bedload was measured. The model was run for the period of both field experiment periods (FW1 and FW2) and the result were compared with the measured data. The sediment grain size was obtained from the trapped sediment and is composed of fine sand (0.22 mm). The specific density and the dry bed density were set to 2,650 and 1,600 kg m³. Discussion of the

differences between sediment transport formulations and methods of calculation is beyond the scope of this paper and has been discussed in detail by many authors (i. e. Wang et al., 1998, Bayram et al., 2001, Camenen and Larroudé, 2003, Silva et al. 2009; Cartier et al. 2012). There is no consensus in the literature regarding what is the best formulation to describe the process and a formula that best describes a process for one given area may not do the same for another.

3.2.5 Annual net Sediment Transport

To quantify the annual net sediment transport in the study area, the calibrated model was run using the formula that best reproduces the bedload sediment transport in the study area. We assumed that the formula is also able to represent the suspended sediment transport. The year of 2014 was chosen because it encompasses most of the measured data (including calibration/validation periods) and therefore gives more confidence to the results. The input data (see Figure 11 for locations) presented the expected environmental conditions for the study area where north to northeast winds blow predominantly due to the presence of the South Atlantic Anticyclone which is frequently disturbed by the Polar Mobile Anticyclone (Nimer, 1989; Vintem et al. 2004; Truccolo and Schettini, 2009), especially during austral autumn and winter (March to August). The waves used as input for numerical modelling agrees with Araujo et al. (2003) where easterly sea (peak period of ~8s) conditions occur all year while south swell (peak period of ~12s) is more frequent during winter, bimodal wave conditions are also frequent. Although some changes can be expected over the years due to changes in atmospheric conditions (Siegle and Asp, 2007), the simulated year is considered to represent the average conditions at the study area.

For the annual sediment transport model a "brute force" (without any wave case reduction e.g. Daly et al. 2013; Walstra et al. 2013) model was run. Despite being less computer efficient (longer time to run) this approach reduces the simplification errors related to the case selection/schematization and it is expected to better reproduce the process and point out if and where the headland sediment bypassing occurs. The results presented for the annual sediment transport are derived from the mean total transport outputted by the model (m^2s^{-1}) and were simply multiplied by the average results by the time (in seconds) of the simulation, resulting in values of m^3yr^{-1} .

4 RESULTS

Following the two methods (sediment transport and numerical modelling), this section will be presented in two linked and complementary topics. 1) Sediment trapping measurements; and 2) Numerical modelling.

4.1 Sediment Trapping Experiment

FW1 was carried out under a northeast wind varying from 5 to 8 m/s during spring tides. Each sampling location encompasses a distinct set of tide, current and wave conditions (Figure 12). The sampling in Ponta das Canas took place during the flood tide. Lagoinha was sampled close to the highest tide just before the slack tide and finishing during the ebb tide. At Brava, the sampling was mainly during the low tide to the beginning of flood tide. The current conditions during the sediment transport measurement were no higher than 0.5 m s^{-1} and the wave condition vary between a lower H_s (1 m) with longer peak period (12 s) from east-southeast at Ponta das Canas and Lagoinha to a higher 1.5 m (H_s) and shorter peak wave period (7.5 s) also from east-southeast during Brava sampling period. The abrupt change in peak wave period (from 12 s to 7.5 s) is a result of a bimodal swell (12 s) and sea (7.5 s) where the swell slightly loses energy and the sea begins to be responsible for a higher amount of energy.

FW2 was accomplished under a calm north wind ranging from 2 to 4 m s^{-1} , at a very low amplitude tide (neap tides) during Brava and Ingleses measurements and slightly higher amplitudes during Lagoinha (flood) and Ponta das Canas (ebb) (Figure 12). Both zonal (U) and meridional (V) current velocities were very close to zero. The significant wave height was 0.95 m during Ingleses and Brava measurements and 0.7 m during Lagoinha and Ponta das Canas measurements. The peak period and direction were relatively constant during all measurements, respectively 7.8 s from east-southeast.

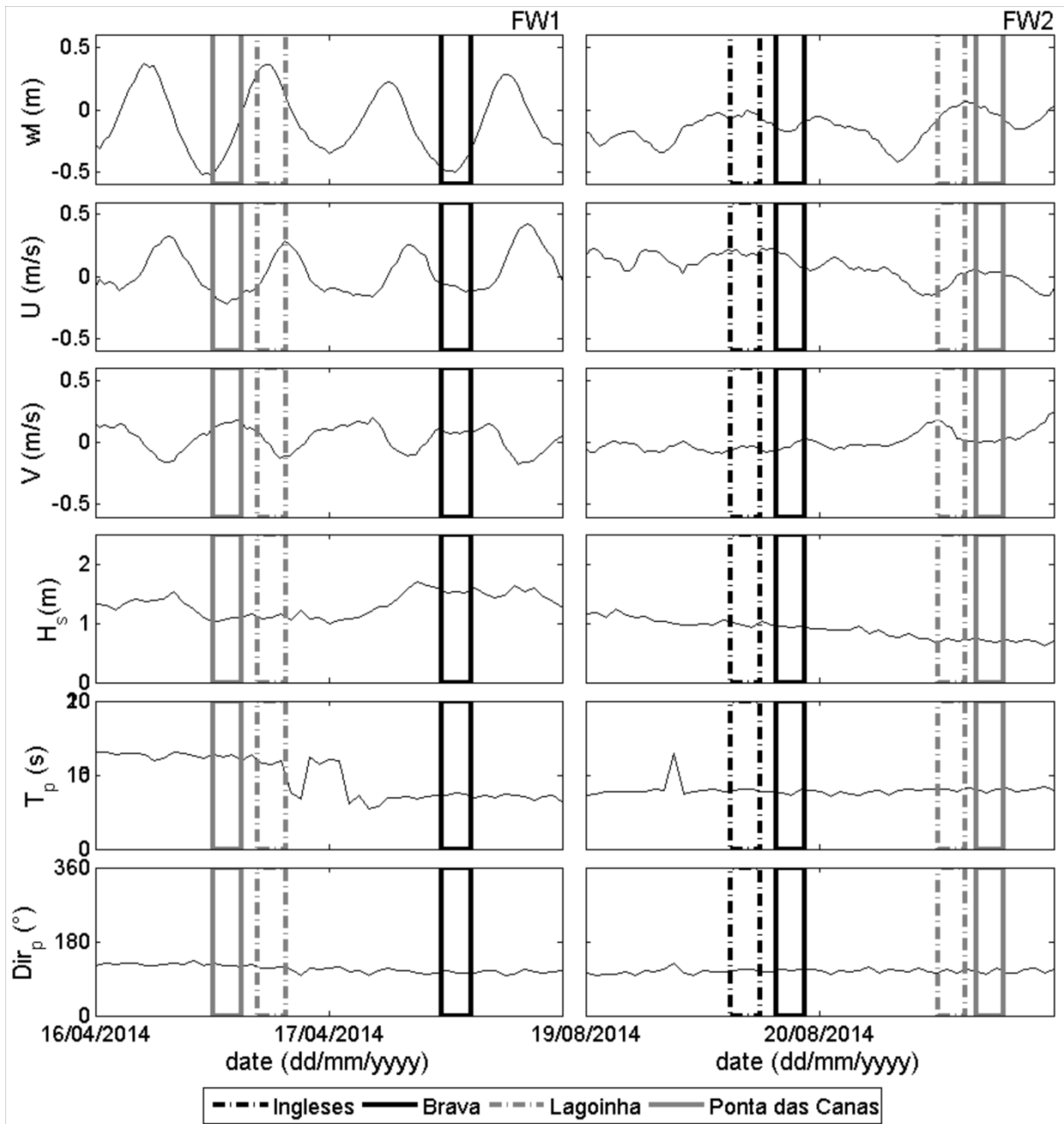


Figure 12: Environmental conditions measured at ST17 (see Figure 9) during the sediment trap experiment (wl: water level; U: zonal velocity; V: meridional velocity; Hs: significant wave height; Tp: peak wave period; Dirp: peak wave direction). The rectangles indicate the trapping period for each location - 20 samples were collected within the time encompassed by each rectangle.

The measured bedload sediment transport synthesis is presented in Figure 13. Ingleses and Brava beaches are located in an exposed area of the island (see Figure 9) (facing east-northeast) therefore receiving higher wave energy than Lagoinha (facing north) and Ponta das Canas (facing southwest). Sediment transport rates measured for the present paper around headlands are presented in $\text{m}^2 \text{s}^{-1}$ as a standard transport unity (or $\text{m}^3 \text{m}^{-1} \text{s}^{-1}$, representing the amount of cubic meters of sediment transported over a meter per second) and are in the order of magnitude of 10^{-7} to $10^{-6} \text{m}^2 \text{s}^{-1}$.

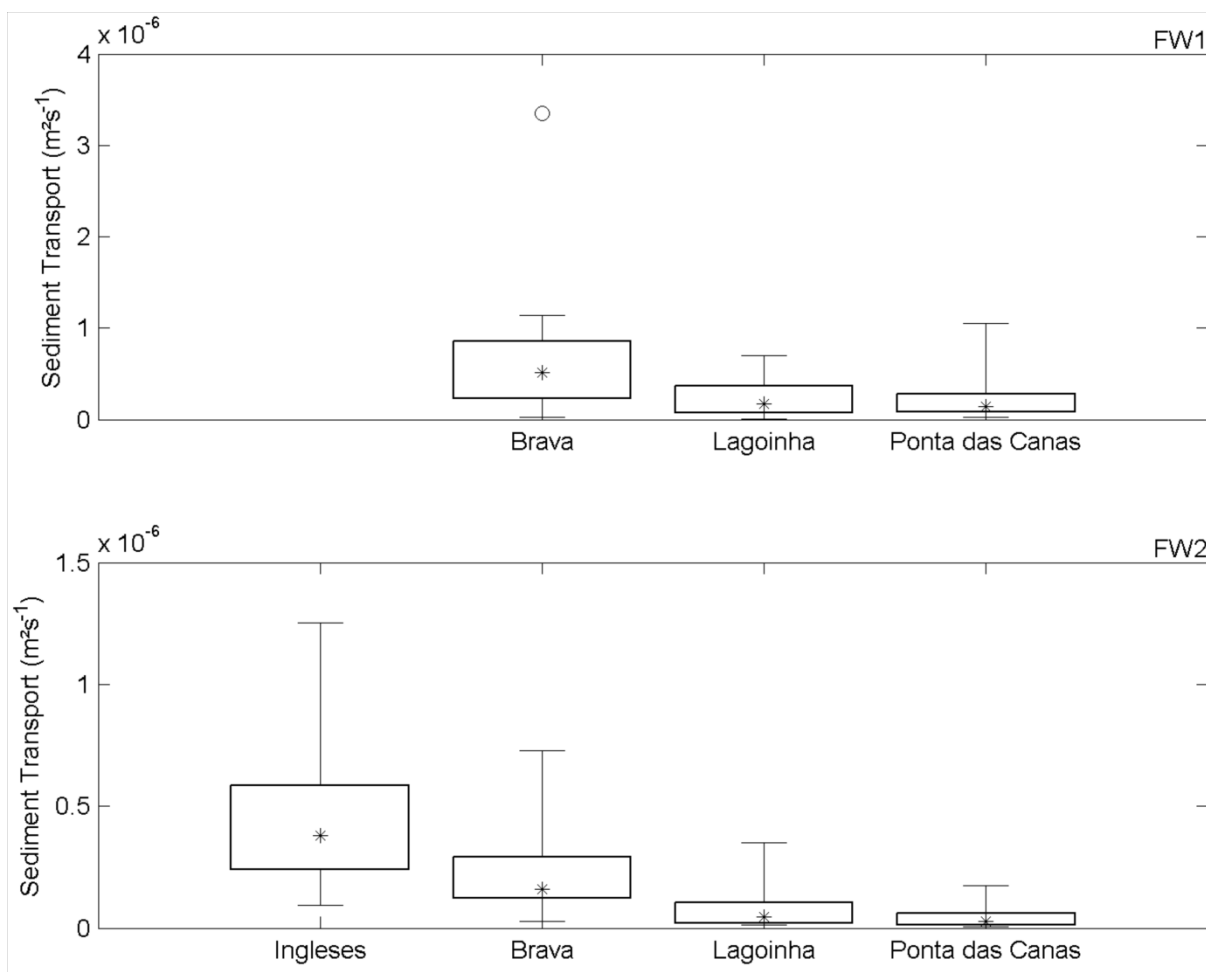


Figure 13: Measured sediment transport rates (m^2s^{-1}) for four locations at field work 1 (top panel) and field work 2 (bottom panel). * represent the median sediment transport, the rectangles are the quartiles (25 and 75%), the lines indicate the maximum values not considered outliers and the circle is the outlier value. Values presented here encompass all 140 samples (20 samples / location / FW). Note different vertical scales.

The trapped grain size distribution is homogeneous, composed mainly of fine sand ($D_{50} = 0.22 \text{ mm}$). A small percentage of very coarse to gravel was trapped at more energetic conditions such as FW1 (all locations) and Brava FW2. The presence of the coarser material is related to biodebitic (shell pieces) at the samples (Figure 14).

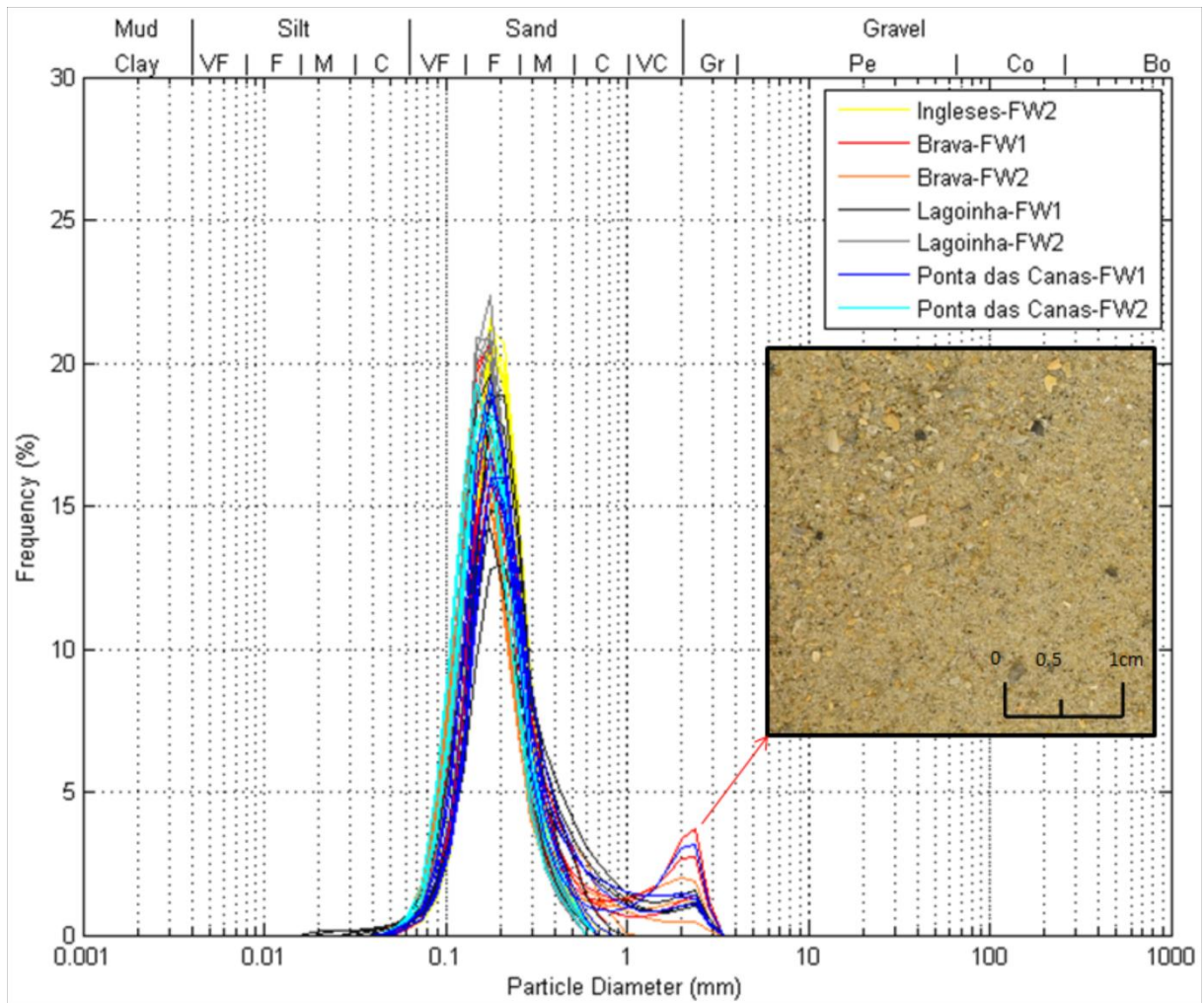


Figure 14: Grain size distribution for 6 samples of each location / field work. The highlighted picture shows the presence of coarser composition due biotrititic (shell pieces) material at Brava FW1.

4.2 Numerical modelling

During sensitivity testing of the model it was noted that bimodal sea-swell was very important in the study area, especially because of the variable orientation of the coastline. The exposed area (i.e. Brava and Ingleses beaches) receives both easterly and southerly waves, while, the southerly waves do not reach the protected area (Ponta das Canas - Daniela) since it would need to refract/diffract $\sim 180^\circ$. In this area, during bimodal wave conditions, the usually less energetic east conditions will become more important. Therefore, the full wave spectra time series is essential for wave calibration at the study area.

The model was calibrated during austral summer (22/01 -18/02/2014 - Figure 15) and validated during austral winter (01-29/07/2014 - Figure 16). Table 6 presents the percentage of error (MAE divided by the range of measured variable for the period times 100) for each analysed variables at each location for both calibration and validation runs. The model presents a very good representation of the environmental

conditions. Despite the peak wave direction at ST17 and the zonal velocity (U) during validation at ST15 all variables at different locations presented errors that correspond to less than 15% of the magnitude of the measured data for the analysed period. At ST17 the peak wave direction presented a fair-poor representation of the environment being 47% (35.6°) for calibration and 23% (23.6°) for validation that is explained by the location where ST17 is moored - surrounded by small islands as well as Santinho-Ingleses headland where the only available bathymetry is from low resolution nautical charts. The zonal current velocity (U) during validation at ST15 presented a fair representation of the environmental conditions and despite the 30% errors this corresponds to only 0.11 m s⁻¹. For all other locations, period and variables the representation of the environmental conditions contained errors equal or lower than 15 % of the magnitudes. Nonetheless the model provides a good representation of the waves, tides and currents and the average of all variables MAE represent only 11% of the magnitude range of measured data.

Table 6: Mean absolute error (MAE) in percentage. Note that excepting the peak wave direction on ST17 and zonal velocity during validation on ST15 (bold) all the errors are lower than 15%. Hs: Significant wave height; Tp: peak wave period; Dirp: peak wave direction; wl: water level; U: zonal current velocity; V: meridional current velocity.

	Calibration			Validation		
	ST15	ST16	ST17	ST15	ST16	ST17
Hs	4%	12%	7%	7%	10%	18%
Tp	7%	6%	7%	8%	5%	6%
Dirp	10%	4%	47%	13%	9%	23%
wl	5%	5%	5%	4%	4%	4%
U	9%	10%	10%	30%	9%	11%
V	4%	12%	13%	15%	12%	13%

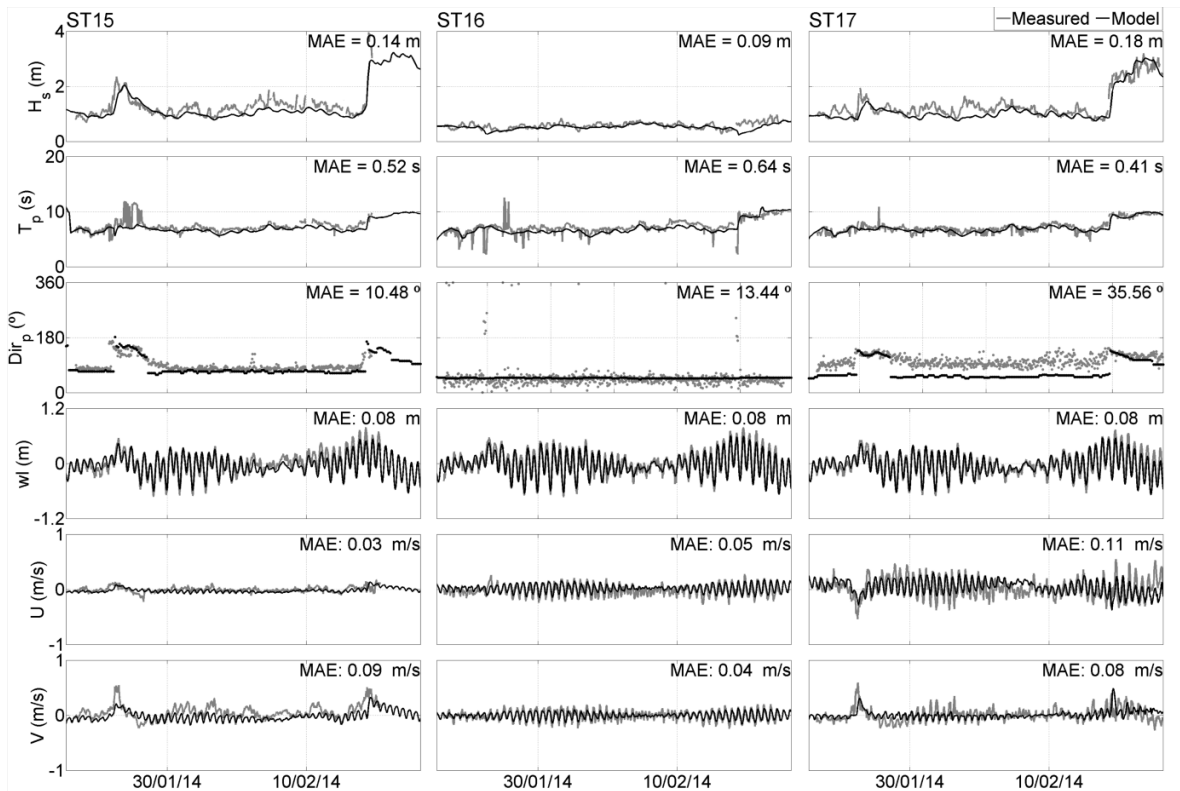


Figure 15: Hydrodynamic and wave model calibration and mean absolute error (MAE) - austral summer. From top to bottom: H_s : Significant wave height; T_p : peak wave period; Dir_p : peak wave direction; wl: water level; U: depth average zonal velocity; V: depth average meridional velocity. From left to right: ST15, ST16 and ST17 - see Figure 9.

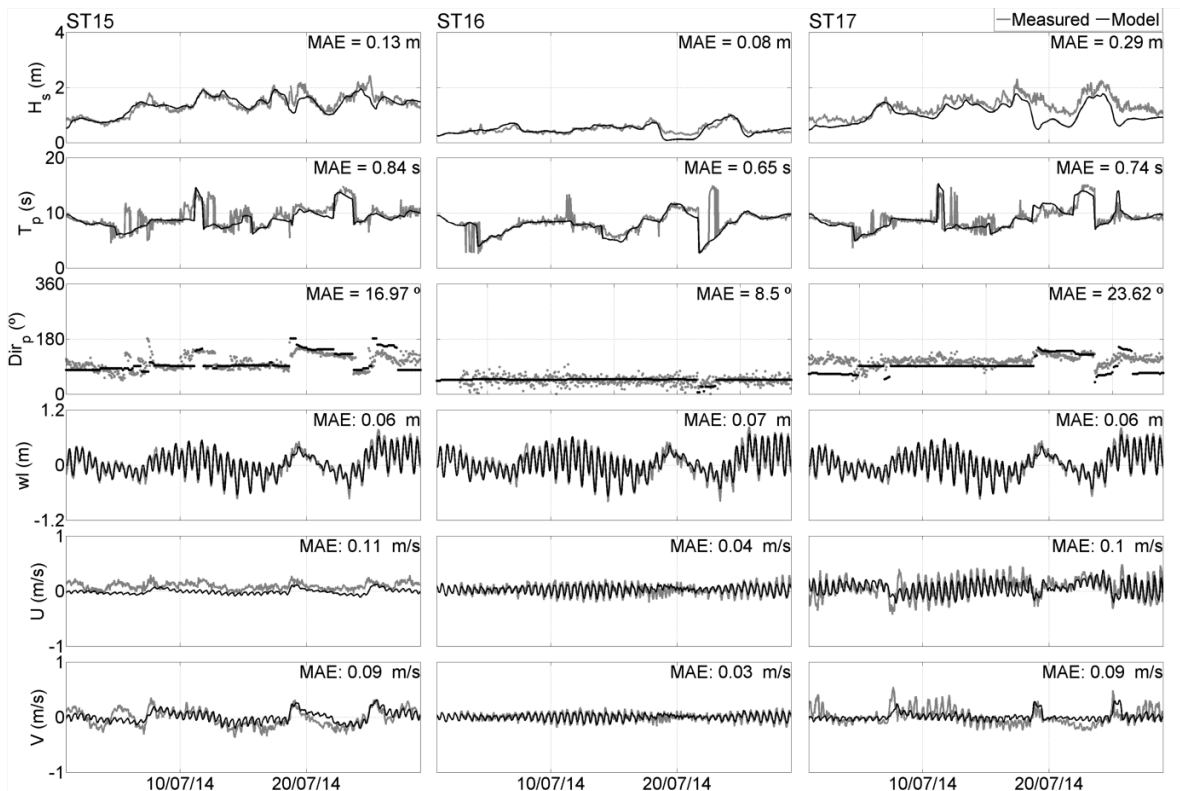


Figure 16: Hydrodynamic and wave model validation and mean absolute error (MAE) - austral winter. From top to bottom: H_s : Significant wave height; T_p : peak wave period; Dir_p : peak wave direction; wl: water level; U: depth average zonal velocity; V: depth average meridional velocity. From left to right: ST15, ST16 and ST17 - see Figure 9.

The comparison of effectiveness of the three sediment transport formulae is presented in Figure 17. The van Rijn and Soulsby formulae gave unsatisfactory rates of sediment transport during low transport conditions and presented a MAE of 2.53 and $1.78 \times 10^{-7} \text{ m}^2\text{s}^{-1}$, respectively on the other hand, the Bijker formula reproduced fairly well the measured sediment transport and its predictions are clearly closer to the diagonal solid line (perfect agreement). Bijker formula presented a MAE of $1.31 \times 10^{-7} \text{ m}^2\text{s}^{-1}$.

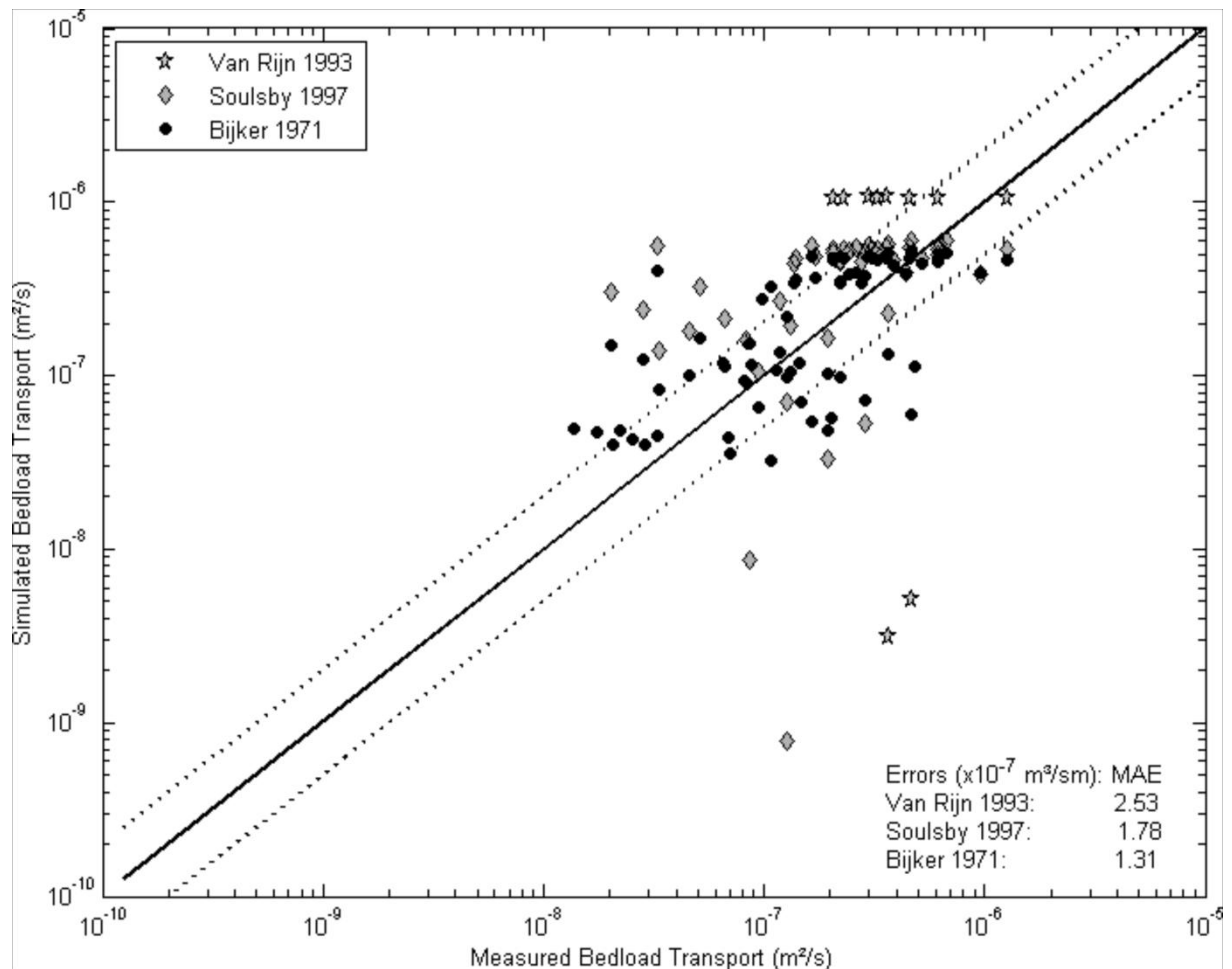


Figure 17: Sediment transport formula comparison. The diagonal solid line represent perfect agreement between measured and simulated bedload transport, the dashed lines represent a factor of 0.5 and 2 of the perfect agreement indicating a good agreement buffer as described by Camenen and Larroudé (2003).

The general results of the annual sediment transport model are presented in Figure 18 and the detailed results in Figure 19. The results as for the measured data are derived from the mean total transport (m^2s^{-1}) and are presented in $\text{m}^2 \text{yr}^{-1}$ (or $\text{m}^3 \text{m}^{-1} \text{yr}^{-1}$ representing the amount of sand in cubic meters that is transported over a meter per year). It was further was integrated in representative transects to quantify the total volume transported in a year at specific sections (i.e. at headlands, beaches inputs and outputs) to obtain values in $\text{m}^3 \text{yr}^{-1}$. The results indicate the complex

sediment transport pattern in the exposed areas and a uniform pattern in the protected areas (Figure10).

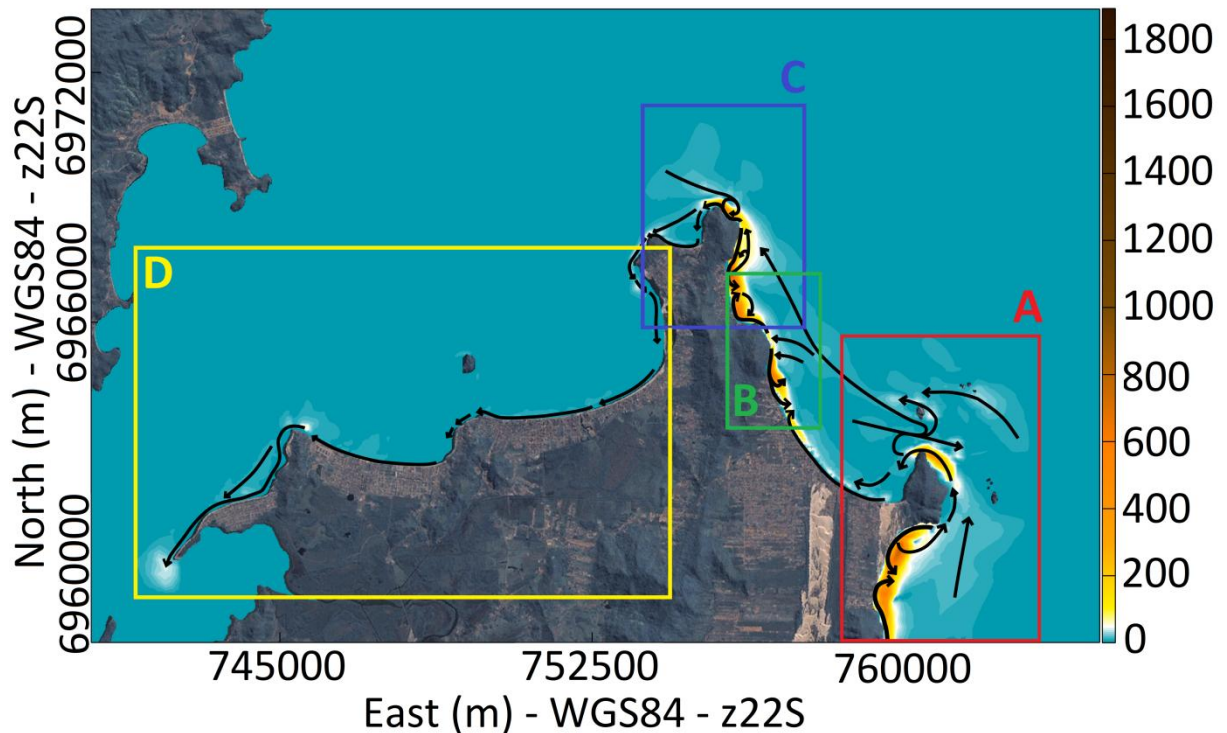


Figure 18: Mean direction of sand transport during the simulated year (2014). Arrows are indicative of the direction of transport, colours indicate the magnitude (m^2yr^{-1}). Background image source: Landsat 7.

Figure 19 is divided in four headland zones, the results are presented per headland/path of sediment transport and described below.

Santinho-Ingleses (Figure 19 A): this headland has the most complex sediment transport pattern for the study area. Beginning in the south part of the zone, Santinho beach has a cellular type sediment circulation where the sediment is transported from the headlands towards the centre of the beach and eventually to the inner shelf. Part of the sediment transported from the north headland to the centre of the bay is transported northward through the inner shelf and part is transported closer to the shoreline around the headland as a result of more energetic waves from south. The sediment transport between the island and the headland is predicted at $12,000 \text{ m}^3 \text{ yr}^{-1}$. At the tip of the headland the sediment splits in two directions, 1) transported towards Ingleses delivering $3,500 \text{ m}^3 \text{ yr}^{-1}$ to the beach and 2) turns its path $\sim 180^\circ$ and merge with an westerly offshore transport path between the headland and the island at a rate of $7,000 \text{ m}^3 \text{ yr}^{-1}$. The difference ($1,500 \text{ m}^3 \text{ yr}^{-1}$) is either deposited in front of the headland or redirected northward to the inner shelf.

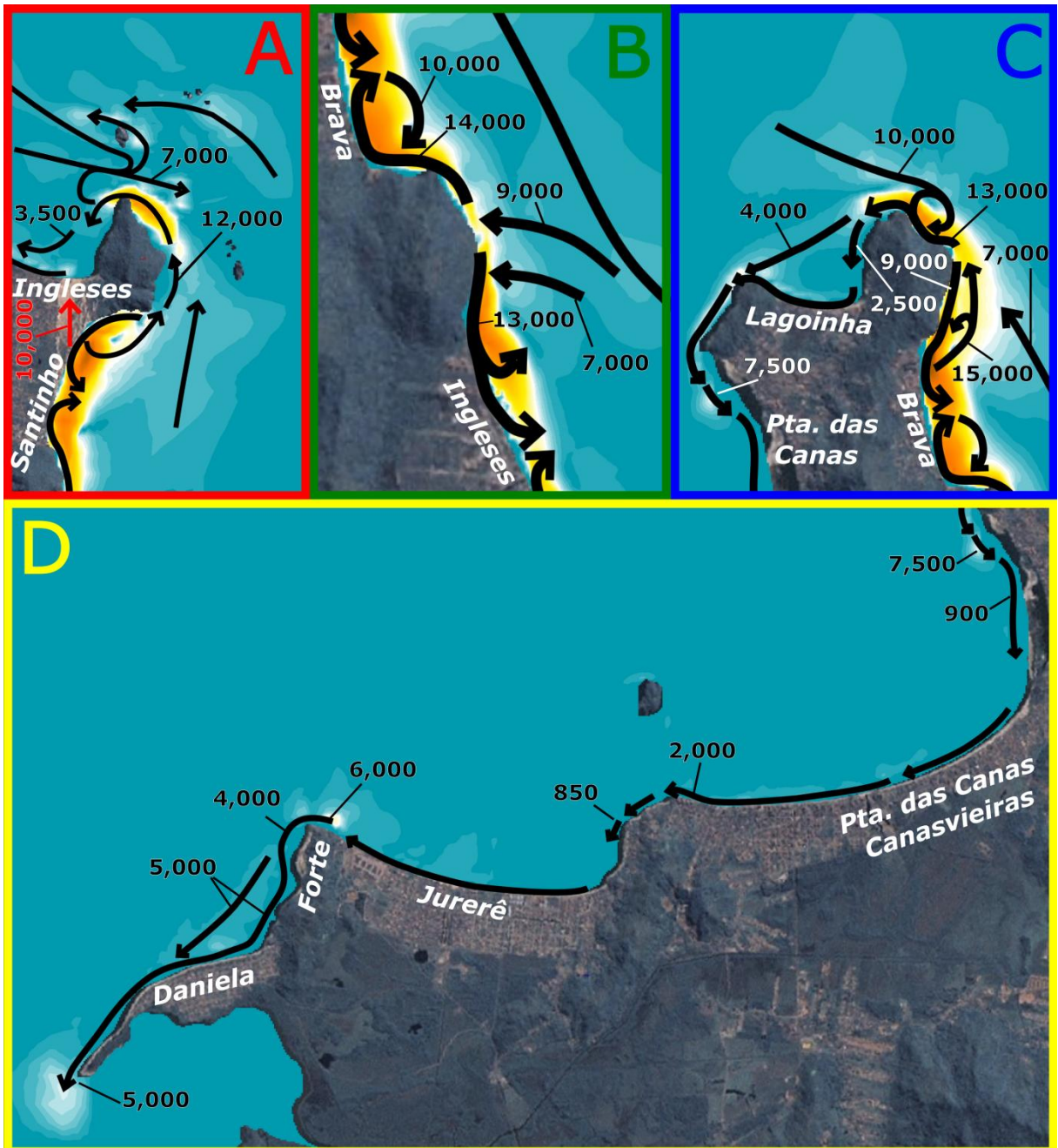


Figure 19: Predicted sediment transport in $\text{m}^3 \text{yr}^{-1}$ at the study area. A, B, C and D represent a zoom of the Figure 18 including the transport rates at specific locations. A) headland between Santinho (south) and Ingleses (north); B) headland between Ingleses (south) and Brava (north); C) headlands between Brava (east) and Lagoinha (north) and between Lagoinha (north) and Ponta das Canas (west) and; D) protected areas, including Ponta das Canas - Canasvieiras, Jurerê, Forte and Daniela beaches as well as the headland between them. Background image source: Landsat 7.

Ingleses-Brava (Figure 19 B): Ingleses beach has a longshore sediment transport gradient that increases northward as result of increasing wave exposure. At its northern headland (Ingleses-Brava) there is a split in the sediment transport direction. Due to the orientation of its southern headland, the sediment is transported towards Ingleses ($13,000 \text{ m}^3 \text{yr}^{-1}$), while to the north it is transported toward Brava ($14,000 \text{ m}^3 \text{yr}^{-1}$). The split point receives $9,000 \text{ m}^3 \text{yr}^{-1}$ of sand from the Santinho-

Ingleses headland via the inner shelf and by two circulation cells on north of Ingleses ($7,000 \text{ m}^3\text{yr}^{-1}$) and south of Brava ($10,000 \text{ m}^3\text{yr}^{-1}$) beaches. Therefore, the sand input via the inner shelf as well as the circulation cell at the north end of Ingleses beach are the responsible for the sediment input to Brava beach.

Brava - Lagoinha - Ponta das Canas (Figure 19 C): this headland also has a split point at the point of headland inflection (closer to Brava). From the split point, part of the sediment is transported towards Brava ($9,000 \text{ m}^3\text{yr}^{-1}$) and part of is towards Lagoinha ($13,000 \text{ m}^3\text{yr}^{-1}$). Similar to Brava-Ingleses headland, part of the sediment transported southwards is redirected northward into deeper water in this case forming transport cells that delivers $15,000 \text{ m}^3 \text{ yr}^{-1}$ of sediment. Besides the circulation cells at this point, $7,000 \text{ m}^3\text{yr}^{-1}$ of sediment is delivered from Santinho-Ingleses headland through the inner shelf (see Figure 18 for the complete path of sediment transport). North of the split point an important contribution of $10,000 \text{ m}^3\text{yr}^{-1}$ of sand from the inner shelf arrives from the northwest as a result of the deflection of currents from north. The sediment from the inner shelf merges with the northernmost part of the headland and is redirected towards Lagoinha. From the tip of the headland towards Lagoinha, where the wave energy becomes weaker and two distinct paths are observed: 1) close to the headland and beach towards Ponta das Canas ($2,500 \text{ m}^3\text{yr}^{-1}$); and 2) through the shelf ($4,000 \text{ m}^3\text{yr}^{-1}$) also towards Lagoinha Ponta das Canas headland.

Protected areas (Figure 19 D): finally, in the most protected area, including Ponta das Canas-Canasvieiras, Jurerê, Forte and Daniela, the net sediment transport is unidirectional towards the North Bay. In this zone, there are areas with higher and lower intensity of sediment transport. In the north the sediment transport is highest at a $7500 \text{ m}^3 \text{ yr}^{-1}$ where the Ponta das Canas spit is developing followed by an area of lower sediment transport ($900 \text{ m}^3 \text{ yr}^{-1}$). At the western end of Ponta das Canas-Canasvieiras the transport rate is of $2000 \text{ m}^3 \text{ yr}^{-1}$ of which $850 \text{ m}^3 \text{ yr}^{-1}$ reaches Jurerê Beach, while $1150 \text{ m}^3 \text{ yr}^{-1}$ deposited on an underwater bar in front of the headland. To the west of Jurerê, there is an increase of sediment transport ($6000 \text{ m}^3 \text{ yr}^{-1}$) due to sand accumulation at its end. From Forte, the sand is transported through the inner shelf and close to the beach ($5,000 \text{ m}^3 \text{ yr}^{-1}$) to nourish Daniela beach and the same amount of sand ($5,000 \text{ m}^3 \text{ yr}^{-1}$) is outputted to North Bay.

5 DISCUSSION

The discussion will be presented in two linked and complementary topics. 1) Sediment trapping measurements; and 2) Numerical modelling.

5.1 Sediment trapping measurements

According to Kraus et al. (1987), sediment traps offer a practical means to acquire point measurements of sand transport; however, they are normally limited by environmental conditions. For the present research, sediment trapping experiment also occur during relatively calm conditions (Figure 12). Wave conditions during FW2 were less energetic than observed during FW1. The peak wave direction did not varied significantly during the period because the measurement was made in shallower water (19.7 m) where the wave has already refracted over the shelf and around the headlands that partially protect from primarily southerly waves. Analysing the zonal (U) currents, it is clear there is a tide influence on currents (i.e. stronger currents occur during spring tides and weaker currents during neap tides). There was also a tidal signal on zonal currents (U), confirming the importance of the tide-induced currents at coasts where large bays such as North Bay is present as demonstrated by Lessa et al. (2001). As demonstrated by CPE (2010), the tidal currents are intensified at the entrance of North Bay and, therefore, the tidal influence is much stronger along the north-facing beaches (Lagoinha to Daniela). In contrast the east-facing part of the study area (Santinho, Ingleses and Brava) receive more energetic waves.

Despite being measured during periods of low sediment transport the values are coherent with the presence of the headland that partially blocks the sediment transport (Short and Masselink, 1999) as well as the low environmental conditions such as when the measurements occur. Therefore the sediment transport rates measured are expected to be lower than longshore sediment transport rates calculated for other beaches in Santa Catarina State (Siegle and Asp, 2007; Miot da Silva et al., 2012).

The trapped sediment contained biotritic material during more energetic conditions, although, no biotritic material was trapped at Ingleses. This leads to two possible conclusions: 1) the local conditions at Ingleses were calm enough not to transport this material or; 2) the biotritic material has been produced somewhere between Ingleses and Brava. Either way, the presence of this type material is small

and the grain size distribution is very similar for all locations or field work experiments, furthermore, it was proved that sediment is being transported around headlands, therefore, it is likely that the source of sediment is the same for all beaches. The beaches in the study area may be assumed to be part of a sediment path and that sand exchange is happening between them via headland bypassing. This finding verifies through measurements the insights presented by Vieira da Silva et al. (in press) of sediment transport around both headlands.

5.1 Numerical Modelling

Araujo et al. (2003) found that in the study area a bimodal sea-swell configuration occurs 31% of the time (i.e. sea from east and swell from south). Their findings were confirmed during the model calibration procedure. Model run with wave parameters as boundary conditions did not correlate well with the measured data (see STs on Figure 9), especially in the protected area (ST16). This is because the model derives a theoretical wave spectrum (such as JONSWAP - Hasselmann et al., 1973) and in the study area the second mode condition is suppressed. Consequently, use of full wave spectrum (energy in several frequency and direction) provides the best boundary condition when a bimodal wave condition is present.

Both, FLOW and WAVE models correlated with the environmental conditions at the study area (see Figure 15, Figure 16 and Table 6). Of the sediment transport formulae tested, van Rijn (van Rijn 1993; 2000), and Soulsby (Soulsby, 1997) provide poor correlation during calm conditions, while Bijker (Bijker 1967; 1971), was able to reproduce it fairly well for all conditions tested. While all formulae significantly improved their sediment transport predictions for rates higher than $\sim 5 \times 10^{-7} \text{ m}^2\text{s}^{-1}$ (Figure 17), the modal rather than very energetic (storm) events are expected to be responsible for onshore sediment transport in the surf zone as well as sand recovery from the lower shoreface (Hoefel and Elgar, 2003; Mortlock and Goodwin, 2015). Therefore the good representation during calmer condition is a key point for the headland bypassing and the numerical model using the Bijker formula is capable of doing so, and was used for estimating the net transport in the study area. The scattering around the perfect agreement line (Figure 17) can be explained by the sediment transport being calculated using as input the model results rather than in situ measurements. Nonetheless the good agreement between measured and simulated sediment transport for four different locations under two distinct

environmental conditions reaffirms the capacity of the model to reproduce the environmental conditions.

Santinho-Ingleses: the model results showed that the sediment transport pattern around Santinho-Ingleses headland is very complex (Figure 19 A). On the east side of the headland the sediment is transported northward while to the north of the headland the sand is transported eastward. The convergent transport paths are responsible for generating the shelf sand body described by Porpilho et al. (in press) and also shown by Vieira da Silva (in press). At the north tip of the headland there was an observed shift in transport direction as a result of a changing driving force (from wave to wind-driven currents). Between the headland and the island the depth increases, reducing the wave capacity to stir the bed and transport sand. Furthermore, currents from south are much calmer at that location due to the presence of the Santinho-Ingleses headland and the islands; on the other hand, currents from north are deflected eastwards (offshore) due to the shape of the coast and are also intensified as the water mass is squeezed between the headland and the island. Part of the sediment transported eastward is deflected to the left and transported through the inner shelf towards northwest eventually reaching both Ingleses-Brava and Brava-Lagoinha headlands. Also, part of the sand transported bypasses the headland and reaches Ingleses beach as presented conceptually by Evans, 1943; Short and Masselink, 1999; and Smith; 2001 as well as by Goodwin et al. (2013) based on field data. However, in the case of Ingleses beach, spit formation was not observed. In the south of Ingleses beach there is also an important ($10,000 \text{ m}^3 \text{ yr}^{-1}$) input of sand via overpassing (migrating dunefield) as presented by Boeyinga et al. (2010). Pinto et al. (2015) demonstrate that due to urbanization and increase in vegetation the input of sediment through the dunefield has reduced over the last ~60 years. According to the authors (Pinto, personal communication) the current sediment input is approximately half of the amount calculated by Boeyinga et al. (2010). The volume of sand input from the dunefield to Ingleses is still higher than the amount of sand that bypasses the headland ($3,500 \text{ m}^3 \text{ yr}^{-1}$) and is, therefore, the main source of sediment at the southern end of Ingleses beach.

Ingleses-Brava: the headland between Ingleses and Brava (Figure 19 B) is nourished by the inner shelf sediment path that begins at the headland between Santinho and Ingleses. Also, two circular cells are observed, one at north end of Ingleses and the other at south of Brava. The net sediment transport at this headland is also 3,000

$\text{m}^3/\text{yr}^{-1}$ towards Brava, which is another indication of the continuous anticlockwise sediment transport path.

Brava-Lagoinha-Ponta das Canas: at the next headland (Brava-Lagoinha - see Figure 19 C) there is an important contribution to sand supply from the inner shelf beginning at Santinho-Ingleses headland ($7,000 \text{ m}^3 \text{ yr}^{-1}$) as well as from north ($10,000 \text{ m}^3 \text{ yr}^{-1}$). The input from inner shelf increases the net transport around the headland to $6,500 \text{ m}^3 \text{ yr}^{-1}$, with $2,500 \text{ m}^3 \text{ yr}^{-1}$ transported to Lagoinha and $4,000 \text{ m}^3 \text{ yr}^{-1}$ to Lagoinha-Ponta das Canas headland. On the western side of this headland the waves are smaller than the exposed areas, however they are mainly unidirectional (H2, 2008) and transport the sand in the same direction. Also, as presented by CPE (2010), the tide-induced currents are stronger during flooding periods, this results in a net transport from the inner shelf towards the bay. Both paths merge together at Lagoinha-Ponta das Canas headland. The reduction in sediment transport from the exposed part of Brava-Lagoinha headland to the protected area (Lagoinha bay) results in sand accumulation that should be responsible for the delivery of sand to Lagoinha as well as Ponta das Canas spit. The build up of this submerged deposit may "trap" sediment that will eventually be transported to Ponta das Canas spit, nourishing the cyclically spit development and merging to the coast as happens in Ponta das Canas spit (Vieira da Silva et al., in press). This demonstrates numerically the insights raised by Vieira da Silva et al., (in press) that Ponta das Canas spit is being nourished by sand from both, Lagoinha and from Brava-Lagoinha headland via headland bypassing.

Lagoinha-Ponta das Canas: from Lagoinha-Ponta das Canas headland (Figure 19 C), the total transport is increased to $7,500 \text{ m}^3/\text{yr}^{-1}$ also corroborating with Vieira da Silva et al. (in press) findings that Ponta das Canas spit builds/migrates at $7,000 \text{ m}^3/\text{yr}^{-1}$. The authors also showed that at the north portion of Ponta das Canas a spit develops and migrates cyclically, indicating the final part of the headland bypassing process as described by other authors (Evans, 1943; Short and Masselink, 1999; Smith; 2001; Ab Razak, 2015).

Protected area: in the most protected sector of the study area (Ponta das Canas-Daniela), the sediment transport occurs close to the beaches in very shallow water as a result of unidirectional oblique waves, corroborating the observations of H2 (2008). The reduction of sand transport to the north of Ponta das Canas (Figure 19

D) will result in the development of Ponta das Canas spit as described by Vieira da Silva et al. (in press). As the sand builds the spit and the sediment transport continues downdrift it is expected that a lack of sediment will lead to possible retreat of the shoreline as observed by Vieira da Silva et al. (in press) will occur. During the modelled year (2014), the headland between Ponta das Canas - Canasvieiras and Jurerê inputted $2,000 \text{ m}^3 \text{ yr}^{-1}$ of sediment from east and outputted $850 \text{ m}^3 \text{ yr}^{-1}$, with the difference in sediment transport rates resulting in an accumulation of the sand in front of the headland that will build the minor spit described by Vieira da Silva et al. (in press), and which will eventually migrate and merge with Jurerê beach. To the west of Jurerê an increase of sediment transport is observed and the transported sand will be responsible for building Forte and Daniela spits as indicated by Vieira da Silva et al. (in press). This finding corroborates the observations of Diehl (1997) and Almeida et al. (1991) that net transport is occurring into North Bay. Silveira et al. (2010) classified the plan view of Daniela as dynamic equilibrium where the shoreline is offshore of its equilibrium position due to the input of sediment from east. The distinct rates of sediment transport in key locations (both ends of headlands) may indicate a dependence of sand availability and supports corroborates the cyclic pattern described by Short and Masselink (1999) for headland bypassing as well as the Ponta das Canas spit sand dependence of the downdrift beaches described by Vieira da Silva et al. (in press).

The foregoing describes the sediment path (for one year timescale) along the north shore of Santa Catarina Island. The development of Daniela spit (the end of the path) as well as the sediment budget of all updrift beaches is highly dependent on sand of: 1) headland bypassing; 2) inner shelf that re-enters in the system through Ingleses-Brava and Brava-Lagoinha headlands; and 3) Ingleses dunefield overpassing. The transported sand reaches Lagoinha-Ponta da Canas headland from where it is continuously transported westward towards Daniela due to continuous wave obliquity as well as net tidal currents. Any interruption of the sand transport at the updrift beaches will lead to a leak of sediment to downdrift beaches. The results showed that the beaches are connected via both headland bypassing and overpassing and through the inner shelf and that such transport paths must be incorporated into any study of the beaches of Santa Catarina Island north shore.

6 CONCLUSIONS

This paper presented a comprehensive study of headland bypassing at the north end of Santa Catarina Island, southern Brazil, including complementary methodologies to access the process. In situ measurements are very important and reliable while generally covering a small scale both in time and space. Therefore, the use of numerical models is helpful to understand the "big picture". Nonetheless, numerical modelling must rely on measured data to calibrate and validate its results.

The presence of cyclic development and migrating spits together with measurements and model results are evidence of headland sand bypassing in the area and collaborate the conceptual model of the process. However, it did observed sediment transport around headlands (headland bypassing) without the spit development on the lee side of some headlands. Therefore, despite being a good indication of headland bypassing, the absence of spits does not imply the non-occurrence of the process.

In the study area the major contribution of sand to headland bypassing is longshore sediment transport. In addition, sand input from the inner shelf make an important contribution to the sediment budget for the area. Another important sediment path in the study area are via overpassing (dunefield migration) since the contribution of sand to the system is higher than the headland bypassing at Ingleses beach.

This paper has demonstrated there is a sediment transport connection between the headland embayed-beaches of the study area. Therefore, any interruption of the sand transport at the updrift beaches will lead to a leakage of sediment to downdrift beaches, via the headland. Therefore, the inputs and outputs of sediment through headland bypassing and inner shelf transport should be considered in any intervention. This is an important finding of the present research, and has a broad application worldwide where headland bay beaches are considered closed cells rather than interconnected as demonstrated here.

Acknowledgments

The authors would like to acknowledge the support of Prof. Carla Bonetti with statistics; Cultura Subaquática dive center as well as LOC divers Charline Dalinghaus, Diego Porpilho, Maiara Werner, Paula Gomes and; Fundo Clima – MMA (Process number 3520120), CNPQ (Process number 400302/2012-8 and

303550/2012-0), PRH-PB240 (Process number 48610.002443/2013-14), CAPES (Process number: 005809/2014-02), SMC-BRASIL (MMA-IHC), CASAN and CB&I Brasil.

References

Ab Razak, 2015. Natural Headland Sand Bypassing: Towards Identifying and Modelling the Mechanisms and Processes. Ph.D. Thesis. Delft University of Technology. CRC Press/Balkema. the Netherlands. ISBN 9781138028647.

Ab Razak, M.S., Dastgheib, A., Roelvink, D. 2013. Sand bypassing and shoreline evolution near coastal structure comparing analytical solution and XBeach numerical modelling, Proceedings 12th International Coastal Symposium (Plymouth, England), Journal of Coastal Research, Special Issue No. 65, pp. 2083-2088, ISSN 0749-0208.

Almeida, E.S., Abreu de Castilhos, J. J., Simon, A.F., Avila, E.L., Aumond, J.J., Pinto, N.L.C. dal Santo, N.A. e Infante, N., 1991. Observações Geomorfológicas na Praia do Forte - Ilha da Santa Catarina, Município de Florianópolis - SC. Geosul 11, 38-54.

Amoudry, L, 2008. A Review on Coastal Sediment Transport Modelling. Proudman Oceanographic Laboratory. Natural Environment Research Council -Internal Document, N. 189.

Araújo, C.E.S.; Franco, D.; Melo Filho, E., and Pimenta, F. 2003. Wave Regime Characteristics of Southern Brazilian Coast. Proceedings of the 6^o International Conference on Coastal and Port Engineering in Developing Countries, COPEDEC. Colombo, Sri Lanka, Paper 97, 15p.

Battjes, J. and J. Janssen, 1978. Energy loss and set-up due to breaking of random waves,. In Proceedings 16th International Conference Coastal Engineering, ASCE, 569-587.

Bayram, A., Larson, M, Miller, H., Kraus, N. C., 2001 Cross-shore distribution of longshore sediment transport comparison between predictive formulas and field measurements. Coastal Engineering 44, 79-99.

- Bruun, P., 1954. Coast erosion and the development of beach profiles. U.S. Army Beach Erosion Board Technical Memorandum 44, 79 pp.
- Bijker, E. W., 1967. Some considerations about scales for coastal models with moveable bed. Technical Report. 50, WL j Delft Hydraulics, Delft, The Netherlands.
- Bijker, E. W., 1971. Longshore Transport Computations. Journal of Waterways, Harbors and Coastal Engineering Division, American Society of Civil Engineers, Volume 97(4), 687-701.
- Boeyinga, J.; Dusseljee, D.W.; Pool, A.D.; Schoutens, P.; Verduin, F.; Van Zwicht, B.N.M., and Klein, A.H.F., 2010. The effects of a bypass dunefield on the stability of a headland bay beach: A case study. Coastal Engineering 57(1), 152–159.
- Camenen, B., Larroudé, P., 2003. Comparison of sediment transport formulae for the coastal environment. Coastal Engineering 48, 111 -132.
- Cartier, A., Larroudé, P., & Héquette, A. 2012. Comparison of Sediment Transport Models With in-situ Sand Flux Measurements and Beach Morphodynamic Evolution. Coastal Engineering Proceedings, 1(33), sediment.19. doi: <http://dx.doi.org/10.9753/icce.v33.sediment.19>
- Cheung, K. F., Gerritsen, F. Cleveringa, j., 2007. Morphodynamics and sand bypassing at Ameland Inet, The Netherlands. Journal of Coastal Research 23, 106-118.
- CPE (Coastal Planning and Engineering do Brazil), 2010. Análise de Alternativas para o Terminal de Cruzeiros de Florinaópolis - Possíveis Alterações nos Padrões de Circulação e Taxa de Sedimentação no Canal de Acesso ao Porto de Canasvieiras. Florianópolis, SC Brazil. Technical Report. Florianópolis, 55p.
- Daly, C. J., Bryan, K. R., Gonzalez, M. E., Klein, A. H.F., and Winter C., 2013. Wave Climate Control Of Embayed Beach Equilibrium Bathymetry. Proceedings of Coastal Dynamics 2013. 397 - 408, Arcachon - France.
- Dean, R.G., 1977. Equilibrium beach profiles: U.S. Atlantic and Gulf coasts. Department of Civil Engineering, Ocean Engineering Report No. 12, University of Delaware, Newark, DE. 45p.

Diehl, F. L. Aspectos geoevolutivos, morfodinâmicos e ambientais do Pontal da Daniela, Ilha de Santa Catarina, Brasil. Master thesis Geography. Universidade Federal de Santa Catarina, Florianópolis, 1997.

Duarte, J. Taborda, R., Ribeiro, M., Cascalho, J. Silva, A., Bosnic, I., 2014. Evidences of Sediment Bypassing at Nazaré Headland Revealed by a Large Scale Sand Tracer Experiment. Proceedings of 3^{as} Jornadas de Engenharia Hidrográica. Lisboa. 2014. pp 289-292.

Egbert, G. D. e Erofeeva, S. Y., 2002. Efficient inverse modeling of barotropic ocean tides. *Journal of Atmospheric and Oceanic Technology*, 19, 183-204.

Egbert, G.D., Bennett, A.F., Foreman, M.G.G, 1994. TOPEX/POSIDON tides estimated using a global inverse model. *Journal of Geophysical Research* 99 (C12), 24821-24852.

Eslami, S., van Rijn, L., Walstra, D., Luijendijk, A., AND Stive, M., 2010. A Numerical Study on Design of Coastal Groins. in: *Scour and Erosion*: pp. 501-510.

Evans, O. F., 1943. The relation of the action of waves and currents on headlands to the control of shore erosion by groynes. *Academy of Science for 1943* 9-13.

Fitzgerald, D. M. Krauss, N. C., Hands, E. B. , 2000. Natural Mechanisms of Sediment Bypassing at Tidal Inlets. ERDC/CGL CHETN-IV -30 US Army Corps of Engineering.

Fitzgerald, D. M. E Pendleton, E., 2002 Inlet formation and evolution of the sediment bypassing system: New Inlet Cape Cod, Massachusetts. *Journal of Coastal Research*. SI 36, 290-299.

FitzGerald, D.M., Cleary, W.J., Buynevich, I.V., Hein, C.J., Klein, A.H.F., Asp, N., and Angulo, R, 2007. Strandplain Evolution along the Southern Coast of Santa Catarina, Brazil. *Journal of Coastal Research*, SI 50 (Proceedings of the 9th International Coastal Symposium), 152 – 156. Gold Coast, Australia, ISSN 0749.0208

Fontoura, 2004. Hidrodinâmica Costeira e Quantificação do Transporte Longitudinal de Sedimentos não Coesivos na zona de Surfe das Praias Adjacentes aos Molhes da Barra do Rio Grande, RS, Brasil. Ph.D. Thesis. Universidade Federal do Rio grande do Sul - UFRGS. Porto Alegre, 2000.

- Godin, G., 1972, *The Analysis of Tides*, University of Toronto Press, Toronto.
- Goodwin, I. D., Freeman, R., Blackmore, K., 2013, An insight into headland sand bypassing and wave climate variability from shoreface bathymetric change at Byron Bay, New South Wales, Australia. *Marine Geology*, 341, 29-45.
- H2 Engenharia. 2008. *Estrutura de Apoio à Navegação - Canasvieiras, Florianópolis, SC*. Technical Report. Florianópolis, 423 p.
- Hasselmann, K., T. P. Barnett, E. Bouws, H. Carlson, D. E. Cartwright, K. Enke, J. Ewing, H. Gienapp, D. E. Hasselmann, P. Kruseman, A. Meerburg, P. Müller, D. J. Olbers, K. Richter, W. Sell and H. Walden, 1973. Measurements of wind wave growth and swell decay during the Joint North Sea Wave Project (JONSWAP)." *Deutsche Hydrographische Zeitschrift* 8 (12).
- Helley, E. J. e Smith, W., 1971. *Development and Calibration of a Pressure-Difference Bedload Sampler*. Relatório técnico. USGS, Menlo Park, California.
- Hoefel, F., Elgar, S., 2003. Wave-Induced Sediment Transport and Sandbar Migration. *Science*. 299, 1185-1187.
- Klein, A. H. F., Ferreira, Ó., Dias, J. M. A., Tessler, M. G., Silveira, L. F., Benedet, L., Menezes, J. T., Abreu, J. G. N., 2010. Morphodynamics of structurally controlled headland-bay beaches in southeastern Brazil: A review. *Coastal Engineering* 57, 98-111.
- Klein, A.H.F., Prado, M.F.V., Dalinghaus, C., Camargo, J.M., 2015. Metodologia para quantificação de perigos costeiros e projeção de linhas de costa futuras como subsídio para estudo de adaptação das zonas costeiras: Litoral norte da Ilha de Santa Catarina e entorno. Final Report. Ministério do Meio Ambiente. 206 pp.
- Klein, A. H. F., Short, A. D., Bonetti, J. in press. Santa Catarina beach Systems. in: Short, A. D and Klein, A. H. F. (eds) *Brazilian Beach Systems*. Springer Coastal Research Library.
- Kraus, M.C., 1987. Application of Portable Traps for Obtaining Point Measurements of Sediment Transport Rates in the Surf Zone. *Journal of Coastal Research* 3(2), 139-152.

Kraus N.C., Larson M., Kriebel D.L., 1991. Evaluation of beach erosion and accretion predictors. Proc. Co. Sediments'91, ASCE, Seattle, pp.527-587.

Komen, G., S. Hasselmann and K. Hasselmann, 1984. On the existence of a fully developed wind-sea spectrum. *Journal of Physical Oceanography* 14, 1271-1285.

Larson, M., Rosati, J. D., Kraus, N., 2003 Overview of Regional Coastal Sediment Processes and Controls. US Army Corps of Engineers. ERDC/CHL CHETN - XIV -4.

Lessa, G. C.; Dominguez, J. M. L.; Bittencourt, A. C.S.P. and Brichta, Arno. 2001 The tides and tidal circulation of Todos os Santos Bay, Northeast Brazil: a general characterization. *Anais da Academia Brasileira de Ciências* 73 (2), 245-261.

Lesser, G. R., Roelvink, J. A., van Kester J. A. T. M., Stelling, G. S., 2004. Development and Validation of a Three-Dimensional Morphological Model. *Coastal Engineering* 51, 883-915.

Mariani, A., Carley, J. T., and Miller, B. M., 2010, Infilling and Sand Bypassing of Coastal Structures and Headlands by Littoral Drift. 19^o NSW Coastal Conference, Batemans Bay NSW.

Masselink, G. and Short, A. D., 1993. The Effect of Tide Range on Beach Morphodynamics and Morphology: A Conceptual Beach Model. *Journal of Coastal Research* 9 (3), 785-800.

Miot da Silva, G., Mousavi, S. M., S., Jose, F. 2012 Wave-driven sediment transport and beach-dune dynamics in a headland bay beach. *Marine Geology* 323-325, 29-46.

Mortlock, T. R., and Goodwin, I. 2015 Directional Wave Climate and Power Variability Along Southeast Australian Shelf. *Continental Shelf Research* 98. 36-53.

Nimer, E., 1989: *Climatologia do Brasil*. Instituto Brasileiro de Geografia e Estatística, Rio de Janeiro.

Nobre, C. A.; Cavalcanti, M. A. G.; Nobre, P.; Kayano, M. T.; Rao, V. B.; Bonatti, J. P.; Satyamurti, P.; Uvo, C. B., and Cohen, J. C. 1996. Aspectos da climatologia dinâmica do Brasil. *Climanálise Special Issue* (no number), 65p.

Pinto, M. W.; Meireles, R.; Cooper, A., and Klein, A. H. F. 2015. Santinho/Ingleses Transgressive Dunefield system - Santa Catarina Island (Brazil): Temporal Variability in Vegetation, Manmade Structures and Dune Migration. Proceedings of Coastal Sediments'15 (San Diego, CA, USA), 14p.

Porpilho, D., Klein, A.H.F, de Camargo, R. S. V., Prado, M. F. V., Short, A. D., Vieira da Silva, G. inpress. Santinho-Ingleses headland bedform characterization through interferometric data, Santa Catarina Island, southern Brazil. Proceedings of ICS 2016.

Ribeiro, M., Taborda, R., Lira, C., Bizarro, A., Oliveira, A., 2014. Headland Sediment Bypassing and Beach Rotation in a Rocky Coast: An Example at the Western Portuguese Coast. Geophysical Research Abstracts. 16. EGU2014-14602.

Roelvink, J. A. and D. J. R. Walstra, 2004. Keeping it simple by using complex models. In: Proceedings of the 6th International Conference on Hydro-Science and Engineering. Advances in Hydro-Science and Engineering, vol. VI, page p. 12. Brisbane, Australia. 217, 219.

Saha, S., Moorthi,S., Wu, X., Wang, J., Nadiga, S., Tripp, P., Behringer, D., Hou, Y., Chuang, H., Iredell, M., Ek, M., Meng, J., Yang, R., Mendez, M. P., van den Dool, H., Zhang, Q., Wang, W., Chen, M., and Becker, E., 2014. The NCEP Climate Forecast System Version 2. J. Climate, 27, 2185–2208.doi: <http://dx.doi.org/10.1175/JCLI-D-12-00823.1>

Short, A. D. and Masselink, G. Eds. 1999. Embayed and structurally controlled beaches, In:Short, A.D. (ed).,Handbooks of Beach and Shoreface Hydrodynamics. John Wiley & Sons, Chicester.

Siegle, E. and Asp, N. E., 2007 Wave Refraction and Longshore Transport Patterns Along the Southern Santa Catarina Coast. Brazilian Journal of Oceanography 55(2), 109-120.

Silva, P. A., Bertin, X., Fortunato, A. B. and Oliveira, A., 2009. Intercomparison of Sediment Transport Formulas in Current and Combined Wave-Current Conditions. Journal of Coastal Research. SI 56 Proceedings of the 10th International Coastal Symposium, 559-563. Lisbon, Portugal, ISSN 0749-0258.

Silveira, L. F., Klein, A. H. F., Tessler, M. G., 2010. Headland-Bay Beach Planform Stability of Santa Catarina State and of the Northern Coast of São Paulo State. *Brazilian Journal of Oceanography* 58 (2) 101-122.

Silveira, L. F., Klein, A. H. F., Tessler, M. G., 2011. Classificação Morfodinâmica das Praias do Estado de Santa Catarina e do Litoral Norte do Estado de São Paulo Utilizando Sensoriamento Remoto. *Brazilian Journal of Aquatic Science and Technology* 15 (2), 13-28.

Silvester, R., 1985. Sediment By-Passing Across Coastal Inlets by Natural Means. *Coastal Engineering* 9, 327-346.

Smith, A.W., 2001. Headland bypassing. *Coasts & Ports 2001: Proceedings of the 15th Australasian Coastal and Ocean Engineering Conference, the 8th Australasian Port and Harbour Conference*, Institution of Engineers, Australia, Barton, A.C.T., pp. 214–216.

Soulsby, R., 1997. *Dynamics of marine sands, a manual for practical applications*. Thomas Telford, London.

Tolman, H.L. 1991. A third-generation model for wind waves on slowly varying, unsteady and inhomogeneous depths and currents. *Journal of Physical Oceanography* 21, 782–797.

Tolman, H.L. 1997. User manual and system documentation of WAVEWATCH-III version 1.15 NOAA/NWS/NCEP/OMB, United States (1997).

Tolman, 2009 H.L. User manual and system documentation of WAVEWATCH-III Tech. rep., NOAA/NWS/NCEP/OMB (2009).

Truccolo, E.C., 2011. Assessment of the Wind Behaviour in the Northern Coast of Santa Catarina. *Revista Brasileira de Meteorologia* 26(3), 450-460.

Truccolo, E.C.; Franco, D., and Schettini, C.A.F., 2004. The Low Frequency Sea Level Oscillations in the Northern Coast of Santa Catarina, Brazil. In: Klein et al. (ed.), *Proceedings of International Coastal Symposium*. *Journal of Coastal Research*, Special Issue No. 39, pp. 547-552.

Truccolo, E. C. & Schettini, C. A. F. 2009. Condições meteo-oceanográficas costeiras na região do estuário o Rio Itajaí-Açú. In: Joaquim Olinto Branco; Maria José

Lunardon-Branco & Valéria Regina Bellotto (Org.). Estuário do Rio Itajaí-Açú, Santa Catarina: caracterização ambiental e alterações antrópicas. Editora UNIVALI, Itajaí, SC. pp 75-90.

Tukey, J. W. 1977. Exploratory Data Analysis. Addison-Wesley, London.

Van Rijn, L.C., 1993 Principles of sediment transport in rivers, estuaries and coastal seas. Aqua Publications: Amsterdam.

Van Rijn, L.C., 2000. General view on sand transport by currents and waves. Report Z2899.20/Z2099.30/Z2824.30. Delft Hydraulics, Delft, The Netherlands

Vieira da Silva, G., Muler, M., Prado, M. F. V., Short, A. D., Toldo Jr., E. E., Klein, A. H. F., inpress, Shoreline changes Analysis and Insights into Sediment Transport Path - Example of Santa Catarina Island North Shore, Brazil. Journal of Coastal Research Accepted for publication.

Vintem, G.; Tomazelli L. J. and Klein, A. H. F, 2006. The effect of sand grain size in the aeolian transport processes of transgressive dunefields of the coast of the Santa Catarina State Brazil. Journal of Coastal Research, SI 39 (Proceedings of the 8th International Coastal Symposium), 102 - 106. Itajaí, SC, Brazil, ISSN 0749-0208.

Walstra, D.J.R, Hoekstra, R., Tonnon, P.K. and Ruessink, B.G., 2013. Input reduction for long-term morphodynamic simulations in wave-dominated coastal settings, Journal of Coastal Engineering 77, 57–70.

Wang, P.; Kraus, N. C., and Davis, R. A. Jr., 1998. Total Longshore Sediment Transport Rate in the Surf Zone: Field Measurements and Empirical Predictions. Journal of Coastal Research 14(1), 269-282. Royal Palm Beach (Florida), ISSN 0749-0208

Willmott, C. J., and Matsuura, K., 2005. Advantages of the mean absolute error (MAE) over the root mean square error (RMSE) in assessing average model performance. Climate Research 30, 79-82.

IDENTIFICATION OF DRIVING FORCES AND THEIR IMPORTANCE FOR HEADLAND SAND BYPASSING ON THE NORTH SHORE, SANTA CATARINA ISLAND, SOUTHERN BRAZIL

Este capítulo apresenta o conteúdo terceiro artigo que compõe esta tese e foi enviado à revista *Coastal Engineering* em 04/02/2016. A seguir o conteúdo submetido é apresentado com ajustes na formatação a fim de melhorar a apresentação do mesmo.

IDENTIFICATION OF DRIVING FORCES AND THEIR IMPORTANCE FOR HEADLAND SAND BYPASSING ON THE NORTH SHORE, SANTA CATARINA ISLAND, SOUTHERN BRAZIL

Guilherme VIEIRA DA SILVA ^a, Elírio E. TOLDO JR. ^a, Antonio H. da F. KLEIN ^b, Andrew D. SHORT ^c

^a Centro de Estudos de Geologia Costeira e Oceânica, Instituto de Geociências, Universidade Federal do Rio Grande do Sul. Campus do Vale Av. Bento Gonçalves, 9500 Porto Alegre, RS, Brazil. CEP: 91501-970.

^b Laboratório de Oceanografia Costeira, Departamento de Geociências, Centro de Filosofia e Ciências Humanas Universidade Federal de Santa Catarina. Beco dos Coroas, Fundos, Barra da Lagoa - Florianópolis SC, Brazil – CEP: 88062-601.

^c School of Geosciences, University of Sydney, Sydney, NSW, Australia, 2006.

Corresponding author: Guilherme VIEIRA DA SILVA, e-mail: oc.guilhermevs@gmail.com

Elírio E. TOLDO JR., e-mail: toldo@ufrgs.br

Antônio H. da F. KLEIN, e-mail: antonio.klein@ufsc.br

Andrew D. SHORT, e-mail: andrew.short@sydney.edu.au

ABSTRACT

This paper presents a sediment transport numerical model results aimed at understanding the contribution of tides, winds and waves to headland sand bypassing; at identifying the environmental conditions that allow the process to occur; and finally generating a conceptual model for processes in the study area. The study area comprises a series of six headlands with different degrees of wave exposure due to shoreline orientation and tidal influence due to proximity next to a relatively large bay. To achieve the aims of this paper, a calibrated and validated process-based model (Delft3D) was used to simulate a series of scenarios including spring and neap tides during flood and ebb conditions and a range of wind and wave scenarios under different directions during both average and extreme conditions. The results indicate that the waves are the main driving force for the headland bypassing in the study area as they transport sand at rates up to three orders of magnitude

higher than tide or wind driven sediment transport. The magnitude of the wave-induced sediment transport around headlands can reach $4.64 \times 10^5 \text{ m}^3 \text{ y}^{-1}$ while the tide-induced sediment transport can reach $4.03 \times 10^3 \text{ m}^3 \text{ y}^{-1}$ and wind-induced sediment transport around the headlands have maximum magnitude of $3.91 \times 10^3 \text{ m}^3 \text{ y}^{-1}$. It was also observed that waves had their greatest influence on the most exposed section of the area with a reduction in importance towards the entrance of the bay. Tides showed an inverse pattern, with the exposed parts of the study area not influenced by tides, while at the entrance of the bay the tide-induced sediment transport is observed during spring tides, while neap tides do not produce currents capable of transporting sediments in the study area. In most cases wind-driven currents do not produce enough speed to transport sediment, except during extreme N, S and SW conditions. It has been demonstrated that the headland sand bypassing can occur in both directions around most headlands of the study area. Anticlockwise (westerly) is, however, the preferable direction of the sediment transport. On the exposed eastern coast most of anticlockwise headland bypassing occur when waves from east to south are present, while along the protected northern coast the northeast waves dictates the transport around headlands. This is the first time the contribution of tide, wind and wave-generated sediment transport to headland bypassing has been modelled.

key words: Sediment budget; numerical modelling; wave-induced; wind-induced; tide-induced; sediment transport.

1 INTRODUCTION

Sand bypassing is a major interest of coastal researchers, engineers and coastal managers because it is a component of longshore sand transport and influences sediment budgets. The process was conceptually described by Evans (1943), Short and Masselink (1999) and Smith (2001). Due to their economic importance most bypassing studies have focused on manmade structures or inlets (Silvester, 1985; FitzGerald et al., 2000; FitzGerald and Pendleton, 2002; Cheung et al., 2007; Mariani, 2010; Eslami et al. 2010; Ab Razak et al. 2013; Garel et al. 2015). More recently new studies have focused on understanding the process based on field data and numerical modelling. These include shoreface bathymetric changes (Goodwin et al. 2013) which related headland sand bypassing to wave climate variability; use of satellite images and RTK-GPS data (Ribeiro et al. 2014); using sand tracers (Duarte

et al 2014); statistical analysis of shoreline changes (Vieira da Silva et al. 2016); George et al. (2015) developed a classification of headlands as well as investigating the cell boundaries associated with distinct headland types; Ab Razak (2015) reproduced and studied the process based on numerical modelling; Vieira da Silva et al (*in press*) measured sand transport around headlands and used numerical model tools to quantify the magnitude of the process. Despite of growing of interest in headland sand bypassing topic, George et al. (2015) highlight that studies connecting oceanographic processes to sediment transport rates and morphological change are still lacking.

Most of studies however infer that the main driving force for headland sand bypassing is waves (i.e. Evans, 1943; Short and Masselink, 1999, Smith, 2001, Goodwin et al., 2013 Ab Razak, 2015), and while the effect of winds and tidal currents has never been tested they may also be important to sediment transport around headlands. Masselink and Pattiaratchi (1998) described the importance of winds on low energy environments while Lessa et al. (2001) suggest that tidal currents are important components of longshore sediment transport close to large embayments. Therefore, rather than assume winds and tidal currents have little influence the present paper intends to quantify the importance of each driving force using a process-based model. The aim of the present paper is to 1) understand the importance of each driving force (waves, tides and wind) on the bypassing process around both protected and exposed headlands under variable tidal influence; 2) identify the environmental conditions that allow the headland sand bypassing to occur; and 3) to generate a conceptual model of the conditions that generate the headland sediment bypassing in the study area.

2 REGIONAL SETTINGS

The study area encompasses seven beaches (Ingleses, Brava, Lagoinha, Ponta das Canas - Canasvieiras, Jurerê, Forte and Daniela) separated by headlands located on the north shore of Santa Catarina Island, southern Brazil (Figure 20). The coast is classified as rugged bedrock-controlled strand plain coast by Klein et al. (2010). FitzGerald et al. (2007) described it as having relatively narrow discontinuous coastal plain that is bordered by crystalline rocks and where exposed granitic plutons form numerous low-relief headlands that dominate this section of the coast.

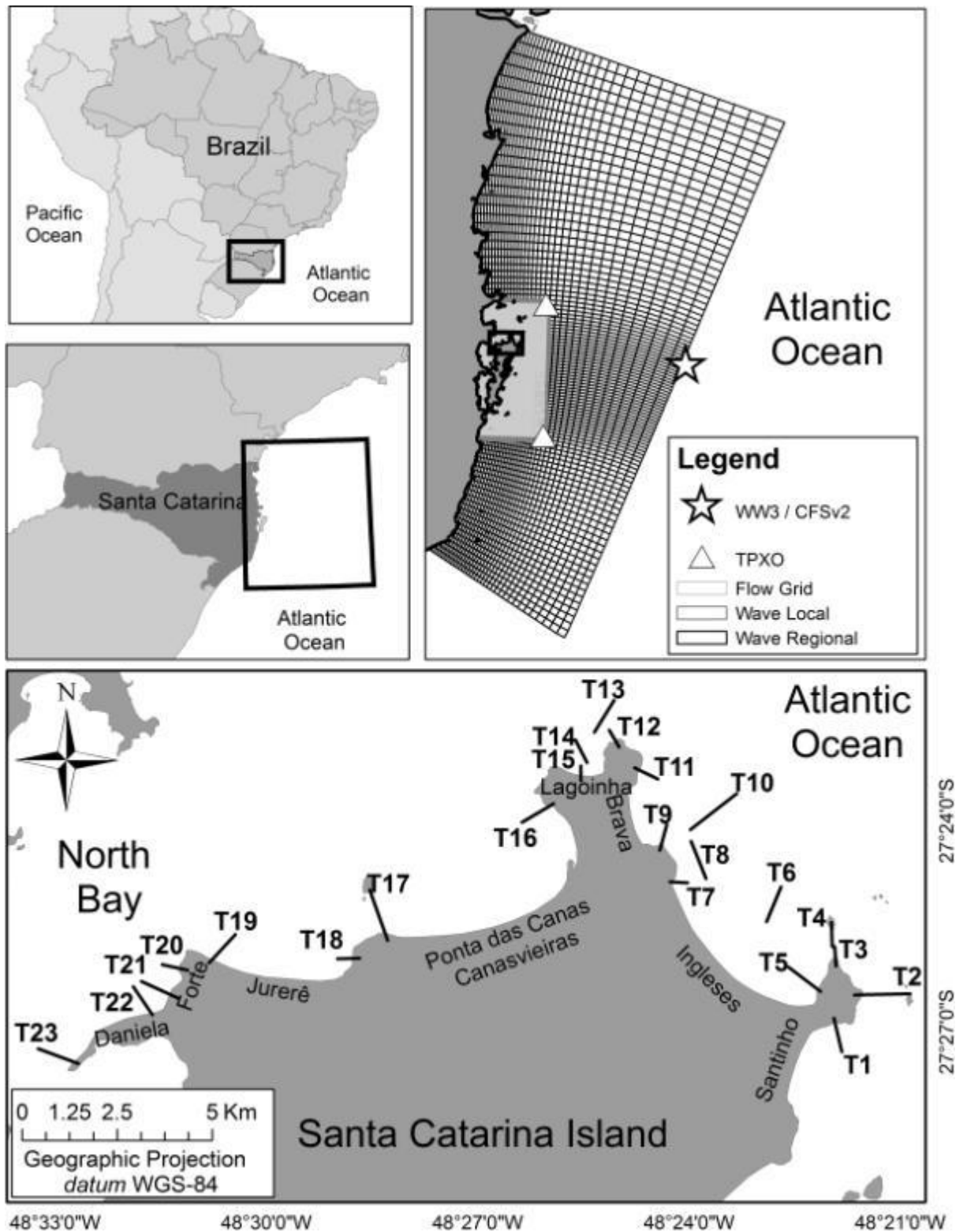


Figure 20: Study area, dataset location, numerical grids, transect location where the transport rates were integrated for every simulation.

Santa Catarina Island has a microtidal regime with astronomical tides ranging between 0.4 to 1.2 m at neap and spring tides, respectively. Truccolo et al. (2004) showed that Santa Catarina State is influenced by low frequency water level oscillations caused by meteorological forcing that can reach up to 1 m. Winds are

predominantly northwest with stronger southerly winds associated with the passage of cold-front systems (Nobre et al., 1996; Truccolo, 2011).

Waves arrive mainly from south with periods of 12 s followed by waves from east with periods of 8 s while 30% of the time bimodal sea conditions occur. The height averages 1 to 1.5 m with highest waves from south. The deepwater wave height and period can exceed 4 m, and 12 s respectively (Araújo et al., 2003). Swell from south prevail during austral autumn and winter (March to August) while there is a balance between them during the summer (December to February) and a predominance of easterly seas occur during spring. The main wave, tide and wind conditions in the study area are summarized in Table 7.

Table 7: Summary of physical settings (Truccolo et al., 2004; Nobre et al., 1996; Truccolo, 2011 and Araújo et al., 2003).

Physical settings	Characteristic
Tides	0.4 - 1.2 m (neap-spring)
Low frequency water level oscillations	Up to 1m
Main wind direction	Northwest
Extreme wind direction	South
Main wave direction and period	South 12 s / east 8 s
Average wave height	1 - 1.5 m
Extreme wave conditions	Up to 4m / > 12 s

The north shore of Santa Catarina Island is mainly wave-dominated based on Masselink and Short (1993) relative tide range (RTR) classification. However, as presented by Vieira da Silva et al. (*in press*) when breaker wave height (H_b) is lower than 0.4 m it becomes tide-modified. According to the authors, this scenario usually does not occur at the exposed east-facing beaches, but can occur along the protected north-facing area.

The beach face sediment is homogeneous with an average diameter of 0.22 mm (Martins and Eichler, 1969; Horn Filho, 2006; Vieira da Silva et al., 2016) and Vieira da Silva et al (*in press*) found that the same size of sediment is transported around the headlands. Also a very similar (0.23 mm) median grain size was found by Vintem et al., (2006) in the Santinho-Ingleses dunefield. Porpilho et al. (2016) showed that the inner shelf has similar sediments together with patches of coarser sediments.

Beaches are classified as sheltered reflective on the north coast while on the east the beaches are predominately rip-dominated transverse bar and rip to rhythmic bar and beach (TBR-RBB) (Klein, Short, and Bonetti, *in press*). The east-facing beaches are

more exposed to waves than north and west-facing beaches that receive only refracted/attenuated waves (H2, 2008; Vieira da Silva et al, *in press*).

CPE (2010) observed the intensification of tidal currents near headlands especially during flood tide conditions between Lagoinha and Ponta das Canas. The dunefield between Santinho and Ingleses migrates northward and delivers $\sim 10,000 \text{ m}^3 \text{ yr}^{-1}$ to Ingleses beach via headland overpassing (Boeyinga et al. 2010). Pinto et al. (2015) showed a reduction on the dunefield rate of migration during the last 60 years due to urbanization and increased vegetation coverage. Vieira da Silva et al (2016) identified an anticlockwise sediment transport path at the study area and Vieira da Silva et al (*in press*) confirmed the path of sediment showing the longshore sediment transport including headland sand bypassing at the study area.

3 MATERIALS AND METHODS

To assess the importance of each driving force on headland sand bypassing as well as to identify the environmental conditions that allow it to occur the present paper used a process-based (Deflt3D) numerical model. The setup of the model is the same as presented by Vieira da Silva et al (*in press*) and included both Wave and Flow modules. The wave model used two nested numerical grids, the first (Regional) is a curvilinear grid covering an area of 410 x 240 km resulting in varying resolution from deep (10 x 6 km) to shallow water (1.7 x 1.7 km). A higher resolution (Local) grid covering an area of 50 x 95 km was nested on Regional grid and also gave resolution from 1.5 x 1.2 km offshore to 30 x 30 m at the study area. The Flow module was run with a very similar grid as Wave Local. The differences are: 1) the Flow grid is two lines/rows smaller than Wave Local avoiding boundary instability and 2) the Flow module was run in 3D mode with five sigma vertical layers.

The model was calibrated (waves, currents and water level) in three locations for approximately a month representing austral summer and validated for a month during winter period. According to the authors, the model well represented the environment with overall mean absolute errors (MAE) corresponding to 11% of the magnitude of the measured data. After calibration and validation of waves, currents and water levels, the authors tested three of the most used sediment transport formulae (Bijker, 1967; 1971; van Rijn 1993; 2000; and Soulsby, 1997) to identify the one that best describes the process against data from sediment trap experiment with Bijker (1967; 1971) providing the best results (Vieira da Silva et al. *in press*). Therefore it was used

by the authors as well as for the present study. For a detailed description of the model refer to Vieira da Silva et al (*in press*).

A series of scenarios for waves, tides and wind were simulated (Table 8) to identify which ones were capable of transporting sediment around the headlands. To simplify the analysis we assume that the nonlinearity effects between tides, winds and waves are small compared to the magnitude of each forcing separate. The tide scenarios were obtained from a 29 days simulation including two neap and two spring tides forced using predicted tides from TPXO 7.2 model (Egbert et al. 1994; Egbert and Erofeeva, 2002 - see location of the tidal constants in Figure 20). Representative conditions during flooding and ebbing tides were choose to demonstrate the tide effect on sediment transport. For both, waves and winds a Wave Watch III (WW3 - Tolman, 1991; Tolman, 1997 and Tolman, 2009) / NCEP Climate Forecast System Version 2 (CFSv2 - Saha et al. 2014) timeseries (from 1979 to 2015) was analyzed (see location of the timeseries in Figure 20). The series were split into eight directions (N, NE, E, SE, S, SW, W and NW) and the frequency of each direction was calculated. For each direction an average and an extreme scenario was defined. The average scenario correspond to the 50% quartile of the wind magnitude or significant wave height (H_s) and the extreme scenario correspond to the 95% quantile. The associated peak wave period (T_p) for each selected H_s was defined according to Kamphuis (2010). Winds from W were not considered in the analysis since it only occurs 3.6% of the time. Waves from SW, W, NW and N occur during less than 3% of the time and are likely to propagate offshore, therefore these directions were not propagated.

Overall, 26 scenarios encompassing a range of tides (4 scenarios), winds (14 scenarios) and wave (8 scenarios) conditions were simulated and their characteristics are presented in Table 8. The results were analysed in specific locations based on the results presented by Vieira da Silva et al. (*in press*).

Table 8: Modelled scenarios.

Number	Scenario #	Tides	Wind	Waves
1	Flood Neap Tide	Flood Neap	-	-
2	Ebb Neap Tide	Ebb Neap	-	-
3	Flood Spring Tide	Flood Spring	-	-
4	Ebb Spring Tide	Ebb Spring	-	-
5	NW average wind	-	NW 5.2 m/s	-
6	NW extreme wind	-	NW 9.8 m/s	-
7	N average wind	-	N 6.4 m/s	-
8	N extreme wind	-	N 9.9 m/s	-
9	NE average wind	-	NE 6.4 m/s	
10	NE extreme wind		NE 10.1 m/s	
11	E average wind		E 5.8 m/s	
12	E extreme wind		E 9.8 m/s	
13	SE average wind		SE 5.6 m/s	
14	SE extreme wind		SE 10.5 m/s	
15	S average wind		S 7.2 m/s	
16	S extreme wind		S 12.6 m/s	
17	SW average wind		SW 7.4 m/s	
18	SW extreme wind		SW 14.5 m/s	
19	NE average wave			Hs 1.6 m / Tp 6.8 s
20	NE extreme wave			Hs 2.7 m / Tp 7.7 s
21	E average wave			Hs 1.6 m / Tp 7.8 s
12	E extreme wave			Hs 2.7 m / Tp 8.5 s
23	SE average wave			Hs 1.7 m / Tp 9.3 s
24	SE extreme wave			Hs 3.1 m / Tp 9.9 s
25	S average wave			Hs 2 m / Tp 10.6 s
26	S extreme wave			Hs 3.7 m / Tp 11.1 s

4 RESULTS

This section presents the results of the modelling. It is divided in three subsections (tides, winds and waves) to facilitate the interpretation/discussion since each forcing parameter in a different order of magnitude of sediment transport.

The tide scenarios are presented Figure 21. Negative signs represent anticlockwise direction of transport while positive sign refer to clockwise direction, with the location of each transect (T) presented in Figure 20 and follow the anticlockwise sediment transport path presented by Vieira da Silva (*in press*). The tidal simulations indicate that during neap tides sediment transport does not exceed $50 \text{ m}^3 \text{ y}^{-1}$ in the study area. While, during spring tides, the transport can reach $10^3 \text{ m}^3 \text{ y}^{-1}$ at the entrance of

the North Bay (T20 and T23). It was also observed that tide-induced sediment transport at the northernmost portion of the Santa Catarina Island (T12) during spring ebb tides is a result of the water exiting the bay. The results indicate the anticlockwise direction of the transport during flood conditions (water entering the bay) while the clockwise transport occur during the ebb. The highest magnitude of the transport was observed in T23 during flood conditions ($4.03 \times 10^3 \text{ m}^3 \text{ y}^{-1}$) while the maximum sediment transport during ebb conditions was observed in the same location with a much lower transport rate ($1.43 \times 10^3 \text{ m}^3 \text{ y}^{-1}$).

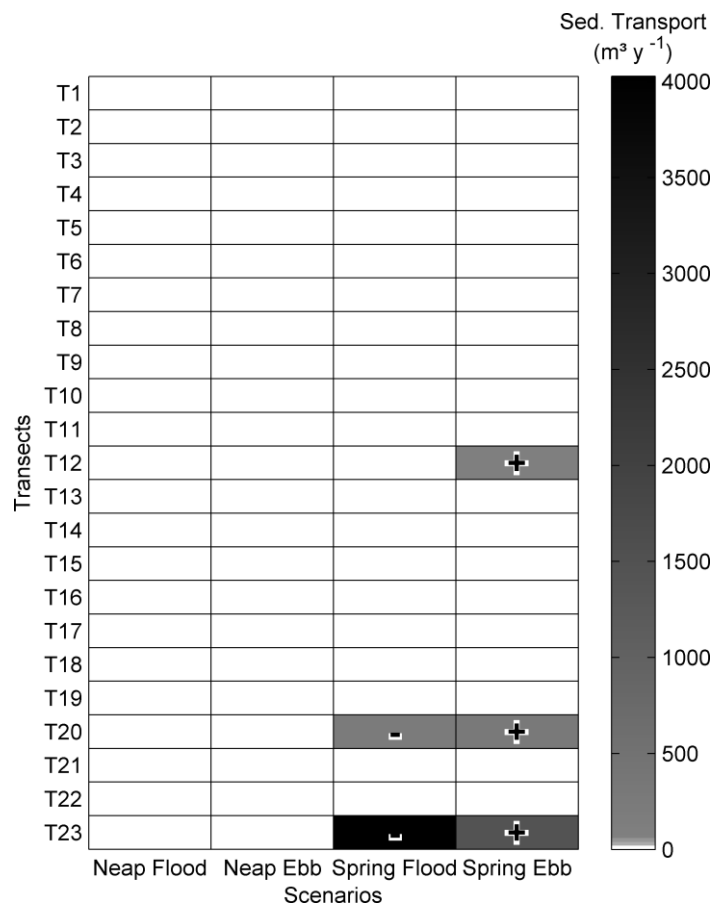


Figure 21: Transport ($\text{m}^3 \text{ yr}^{-1}$) during tide scenario simulation per location (see Figure 20). + indicate sediment transport in clockwise direction (exiting bay); - indicate anticlockwise direction of sediment transport (towards the bay). Magnitudes lower than $50 \text{ m}^3 \text{ y}^{-1}$ are suppressed of the figure.

Figure 22 presents the sediment transport modelling results for wind simulation (+ and - signs indicate clockwise and anticlockwise sediment transport, respectively), with location of each transect (T) presented in Figure 20. The results indicate that that wind-generated currents only induce sediment transport during extreme conditions with a maximum rate of $3.91 \times 10^3 \text{ m}^3 \text{ y}^{-1}$ (anticlockwise) at T2 during extreme south winds. At this point (T2) the water mass is compressed between the headland and the small island thereby intensifying the currents and consequently the

sediment transport. At T16 the maximum transport ($1.74 \times 10^3 \text{ m}^3 \text{ y}^{-1}$) occurs during extreme southwest wind and is clockwise. This scenario generates currents moving out of the bay, which on reaching T16 are intensified by the presence of the headland between Ponta das Canas - Canasvieiras and Lagoinha beaches. At T20 extreme southwest winds can transport $\sim 100 \text{ m}^3 \text{ y}^{-1}$ of sediment. Most of the wind-induced sediment transport higher than $50 \text{ m}^3 \text{ y}^{-1}$ occurs in clockwise direction (extreme north at T12, extreme south at T16 and extreme southwest at T16 and T20) however, the highest sediment transport occur in anticlockwise direction (extreme south at T2). During extreme south and especially southwest winds T16 and T23 are influenced by the wind-generated currents in clockwise direction as a result of the exiting of the water from North Bay to the ocean as the wind pushes the water in this direction. During extreme N winds sediment is transported at T12 as a result of the eastward deflection (towards the ocean) of the wind-driven currents as they approach Santa Catarina Island. T2 has anticlockwise sediment transport as north (to the north) currents generated by extreme south and southwest winds are compressed between the headland and the island intensifying the sediment transport.

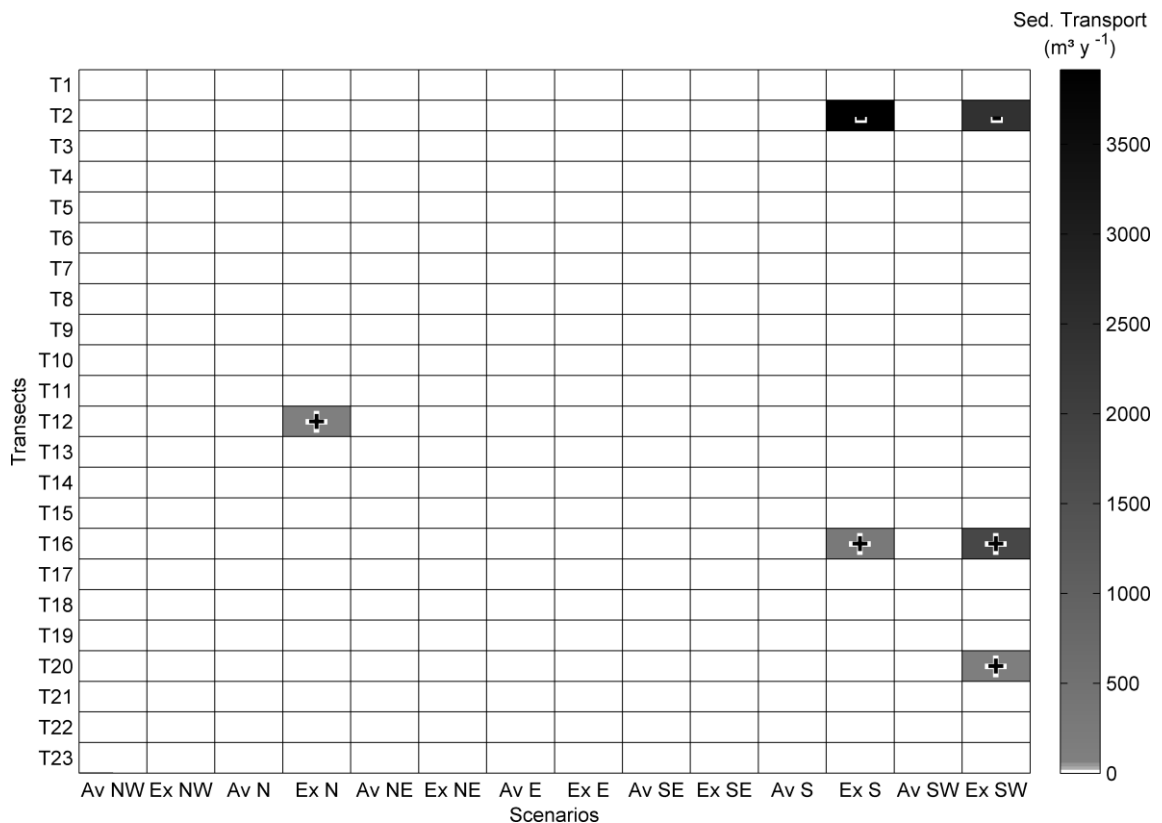


Figure 22: Transport ($\text{m}^3 \text{ yr}^{-1}$) during wind scenario simulation per location (see Figure 1). Av=Average; Ex=extreme; NW=Northwest; N=North; NE=Northeast, E=East, SE Southeast; S=South and SW=Southwest. + indicate sediment transport in clockwise direction (exiting bay); - indicate anticlockwise direction of sediment transport (towards the bay). Magnitudes lower than $50 \text{ m}^3 \text{ y}^{-1}$ are suppressed of the figure.

Wave-induced sediment transport reaches $10^5 \text{ m}^3 \text{ y}^{-1}$ as shown in Figure 23 (the direction of the transport is represented in the figure by + and - signs indicating clockwise and anticlockwise sediment transport, respectively). The highest sediment transport rates are found during extreme easterly waves. T3 has the highest anticlockwise sediment transport rate ($4.56 \times 10^5 \text{ m}^3 \text{ y}^{-1}$) while the highest clockwise transport rate occurred at T11 ($4.64 \times 10^5 \text{ m}^3 \text{ y}^{-1}$).

Northeast waves tend to transport sediment in clockwise direction in the exposed area (T1 to T13) and anticlockwise direction at protected area (T14 to T23). For average waves the exceptions are T5, located at the protected south portion of Ingleses beach and T8 indicating the waves transport sand towards Brava-Ingleses headland and T12 because of wave obliquity at this point pushes sand towards Lagoinha beach. For extreme northeast waves anticlockwise transport occurs at the exposed area (T4 and T6) due to a vortex formation generated by the presence of the island as well as the headland, this vortex widens during these conditions changing the direction of the transport in these locations. In the protected area, T17 and T19 an inversion of the sediment transport also occurs, however, at this point the magnitude of the transport is lowest for this scenario ($< 800 \text{ m}^3 \text{ y}^{-1}$).

East waves produced a general trend of anticlockwise transport sediment (towards the bay) in both exposed and protected portion of the study area. Exceptions for average conditions are: T1, T7 and T11 that due their location in the northern portion of the beaches tend to transport sediment back along the beach; T2 and T17 are affected by the presence of small islands that increase the refraction and diffraction processes changing the wave direction and consequently the sediment transport at these points; T19 where the sediment transport magnitude close to zero ($< 60 \text{ m}^3 \text{ y}^{-1}$). Extreme waves from east also produce anticlockwise sediment transport in the study area, however with higher rates than average conditions. Despite the higher transport rates during extreme scenarios, a difference between extreme and average east conditions is found in T2, where extreme waves transport sediment anticlockwise while average transport clockwise.

Southeast waves affect mainly the exposed portion of the study area. Average waves can transport sediment from T1 to T12 (from T13 the sediment transport rate is $< 55 \text{ m}^3 \text{ y}^{-1}$), extreme waves can transport sediment ($> 50 \text{ m}^3 \text{ y}^{-1}$) from T1 to T15. For both scenarios, with the direction of the transport mainly anticlockwise. Exceptions are T1

during average conditions, T5 and T15 for extreme conditions. At T1 a sediment circulation cell is generated where sand is transported back to Santinho close to the headland and offshore (towards T2) at the end of the transect. During average conditions, the sediment can be more effectively transported close to the headland, on the other hand, during extreme conditions, the outer part of the circulation cell became stronger and transports more sand towards T2. At T5, wave diffraction generates a difference in wave height that results in a current moving from the middle of Ingleses to the south, consequently transporting sand in clockwise direction. The maximum magnitude of sediment transport is found in T3 during extreme conditions reaching $3.22 \times 10^5 \text{ m}^3 \text{ y}^{-1}$.

Waves from south are capable of transporting sediment only in exposed areas. The transport is limited to T1 to T4 during average conditions and from T1 to T13 during extreme conditions. However, it also can transport significant amounts of sediment reaching $2.67 \times 10^5 \text{ m}^3 \text{ y}^{-1}$ during extreme conditions at T1.

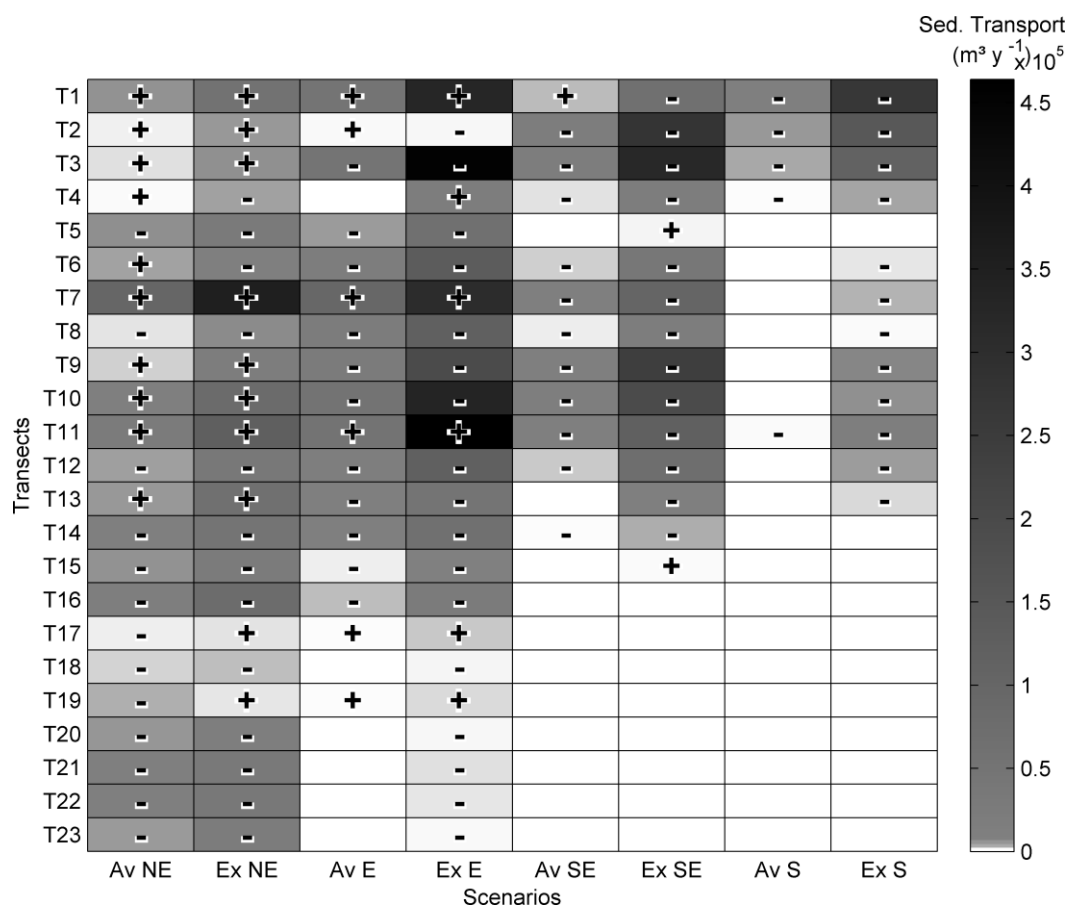


Figure 23: Transport ($\text{m}^3 \text{ yr}^{-1}$) during wave scenario simulation per location (see Figure 1). Av=Average; Ex=extreme; NE=Northeast, E=East, SE Southeast and S=South. + indicate sediment transport in clockwise direction (exiting bay); - indicate anticlockwise direction of sediment transport (towards the bay). Magnitudes lower than $50 \text{ m}^3 \text{ y}^{-1}$ are suppressed of the figure.

5 DISCUSSION

The discussion section is divided into eight sub-sections covering the seven headlands (east to west) in the bypassing process, followed by a conceptual model of the driving forces that generate headland sediment bypassing in the study area.

5.1 Santinho - Ingleses (T1 to T5)

This headland was described by Vieira da Silva (*in press*) as the headland that has the most complex sediment transport pattern in the study area. According Boeyinga et al.(2010) and Pinto et al. (2015), the sand overpasses the headland over a dunefield located between both beaches (overpassing). Vieira da Silva (*in press*) indicated that the rates calculated by Boeyinga et al.(2010) and Pinto et al. (2015) for headland overpassing are two to three times higher than the net headland bypassing at this location. It was observed at T2 that extreme south and southwest winds as well as waves from east, southeast and south generates a northward current, which is intensified by the presence of the headland and small islands. These are the driving forces that generates the northward migrating asymmetrical, catenary megaripples identified by Porpilho et al. (2016) through interferometric data. The authors also identify similar bedforms at the T4, in this case, migrating offshore (anticlockwise/eastward), this finding is related to the waves from northeast (average) and east (extreme) that generate sediment transport in the same direction. Vieira da Silva et al (*in press*) identified a transport path at T3 in anticlockwise direction, which is mainly driven by waves from east, to south. Continuing its path the sand arrives at south of Ingleses beach (T5), driven by waves from northeast to east. The headland bypassing scheme presented here is similar to the model presented by Goodwin et al. (2013) for Byron Bay, Australia, where the sand is pushed to the beach by northeast (east-northeast in Australian case) and east (both cases) waves. Goodwin et al. (2013) also presented a similar sediment pathway of sand through the inner shelf to downdrift areas. Byron bay and Ingleses are located at similar latitudes (difference of ~ one degree), both in the southern hemisphere.

5.2 Ingleses - Brava (T7-T9)

Ingleses - Brava headland receives sediment from the inner shelf that is transported from Santinho-Ingleses headland (Vieira da Silva et al., *in press*). This delivery, computed at T8, indicates that all simulated wave directions transported sediment toward the headland, except the south average scenario. Again, this pathway of sediment through the inner shelf is similar to that the presented by Goodwin et al

(2013) for Byron Bay, Australia. Sediment is pushed back to Ingleses (T7) during northeast and east wave conditions and pushed offshore during SE (average and extreme) and S (extreme) scenarios. The transport of sediment to Brava beach occurs during E and SE during average and extreme scenarios and S during extreme conditions. Northeast waves push it back offshore, with the net bypassing transport anticlockwise as presented by Vieira da Silva et al. (*in press*).

5.3 Brava - Lagoinha (T10-T14)

This headland also receives sediment from the inner shelf (Vieira da Silva et al., *in press*) as computed by T10 (see Figure 20 and Figure 24). Extreme waves from east to south as well average waves from east and southeast transport sediment clockwise towards Brava-Lagoinha headland. Average and extreme waves from northeast also deliver sediment from the inner shelf to the headland (T13). At T11 sand is transported clockwise back to Brava during northeast and east waves while southeast and south waves transport sand anticlockwise towards the tip of the headland (Figure 24 C). At T12, tides can transport sediment during spring ebb conditions (clockwise) and extreme north winds are able to transport sand back to the tip of the headland. The waves transport sediment anticlockwise during most simulated scenarios, exception of average south waves where no transport higher than $50 \text{ m}^3 \text{ y}^{-1}$ is observed. At T14 there is a sediment path that delivers sand to Lagoinha - Ponta das Canas headland (Vieira da Silva et al., *in press*). According to the model results presented here, this path driven by waves from northeast to southeast. Headland sand bypassing around this headland and does not follow a classic pulsating model such as Short and Masselink (1999) but rather works as a continuous longshore sediment transport path.

5.4 Lagoinha-Ponta das Canas - Canasvieiras - (T14-T16)

At this headland the tidal influence on sediment transport is close to zero (Figure 21) and wind-driven currents are only capable of transporting sediment during extreme south or southwest conditions in an anticlockwise direction (T16). Therefore, waves are the main driving force, following the classic model of pulsating headland sand bypassing presented by Evans (1943); Short and Masselink (1999) and Smith (2001) including the spit development (Ponta das Canas spit). The pulsating spit cycle controls the availability of sediment to the downdrift areas (Vieira da Silva et al., 2016) and the sediment source for Ponta das Canas spit are both Lagoinha beach (T15) and sand that travels through the inner shelf from the tip of Brava-Lagoinha

headland (T14) and are driven by waves as described by other authors in different locations (Evans, 1943; Short and Masselink, 1999; Smith; 2001; Ab Razak, 2015).

5.5 Ponta das Canas - Canasvieiras - Jurerê (T17-T18)

Sediment is transported from Ponta das Canas - Canasvieiras towards Jurerê (T17) by average northeast waves while the transport is in the opposite direction during extreme northeast and east scenarios. However, average northeast waves occur twice as frequently as extreme northeast and east waves together, indicating a net transport anticlockwise. At the eastern end of Jurerê, Vieira da Silva et al. (2016) also described a cyclic development of a minor spit indicating an anticlockwise net sediment transport driven by average and extreme northeast and extreme east waves. Tide and wind transport is negligible ($<50\text{m}^3 \text{y}^{-1}$).

5.6 Jurerê - Forte (T19-T20)

Around this headland (T20) the tidal influence starts to become important and sediment can be transported towards the bay (anticlockwise) or towards the ocean (clockwise) during spring flood and ebb tides, respectively with similar magnitudes (see Figure 21), resulting in a net tide-induced sediment transport close to zero. Winds can transport sediment only during extreme SW conditions at T20 in clockwise direction. At this headland, once again, the wave-induced sediment transport is the main driving force for headland bypassing. Almeida et al. (1991) indicates that the net sediment transport at Forte beach is towards the bay. At western end of Jurerê (T19) the average northeast waves drives the sediment towards Forte (anticlockwise) while (less frequent) extreme northeast and east as well as average northeast waves transport sediment to Forte (T20). At the northern end of Forte beach (T20), Vieira da Silva et al. (2016) identify the cyclic development of a minor spit, indicating the pulsative net sediment transport in anticlockwise direction.

5.7 Forte - Daniela - North Bay (T21-T23)

Daniela spit has the highest level of tide-induced sediment transport of the study area, especially at the southwest end of the spit, towards the bay (T23) where transport rates during spring flood tides ($4 \times 10^3 \text{m}^3 \text{y}^{-1}$) are three time higher than during spring ebb tides ($1.4 \times 10^3 \text{m}^3 \text{y}^{-1}$), indicating a net tide-induced sediment transport towards the bay. Wind-driven currents do not transport sediment at this location (T21 to T23). And waves at this point can only transport sediment during northeast conditions (both average and extreme) and extreme east waves, showing

the importance of the wave condition and especially its direction in the protected part of the study area. These conditions are responsible for the development of Daniela spit as a result of the net sediment transport into the bay (Diehl, 1997). The author suggests that the source of sediment to Daniela spit is from the exposed beaches of Santa Catarina Island (i.e. Ingleses, Brava) as demonstrated here. Silveira et al. (2010) classified Daniela as being in dynamic equilibrium with a shoreline seaward of its equilibrium position, indicating a positive sediment budget for the spit. Vieira da Silva et al. (2016), based on shoreline changes analysis showed the dynamic behaviour of Daniela spit shoreline position is controlled by sediment availability from Ponta das Canas spit, and Vieira da Silva et al. (*in press*) confirmed the anticlockwise sediment transport towards the bay.

5.8 Conceptual model of headland bypassing

Vieira da Silva et al. (2016) analysed the shoreline changes in the study area and suggested that headland sediment bypassing occurs in a net anticlockwise direction from the exposed eastern coast area to the North Bay entrance. Afterwards, Vieira da Silva et al. (*in press*) using sediment trap data and numerical modelling demonstrated that the assumptions raised by Vieira da Silva et al. (2016) were right. The present paper uses numerical simulations to generate the conditions that drive the headland bypassing in the study area. A conceptual model of the conditions that generate the headland sand bypassing in both anticlockwise (net) and clockwise directions are shown in Figure 24.

Despite of the findings of Lessa et al. (2001) on tidal currents and Masselink and Pattiaratchi (1998) on the importance of winds on low energy environments, the waves are the main driving force for headland sand bypassing in the study area. This is the first time the importance of each driving force has been tested and confirms the assumptions of several authors (Evans, 1943; Short and Masselink, 1999, Smith, 2001, Goodwin et al., 2013 Ab Razak, 2015) that waves are the main driving force for headland sand bypassing. The magnitude of sediment transport around headlands due to waves can reach $10^5 \text{ m}^3 \text{ y}^{-1}$, while wind and tide-induced currents can transport two orders of magnitude lower than waves ($10^3 \text{ m}^3 \text{ y}^{-1}$). While waves decrease their sediment transport capacity as the area becomes more protected (towards T23), the tides can only transport sediment at the entrance of the bay (T20 and T23) where the entrance narrows and the tide-induced currents are stronger. A similar process of currents intensification was described by Lessa et al. (2001) in

northeast coast of Brazil. It was also observed that wind-induced currents can transport sediment during extreme conditions, especially for winds from north (T12), south (T2 and T16) and southwest (T2, T16 and T20) as similarly described by Masselink and Pattiaratchi (1998) for a low energy coast.

Figure 24 indicates that wave direction is very important for headland sand bypassing in the study area. In the exposed areas (T1 to T12) waves from southeast and east are the driving force. Easterly wave scenarios generate the highest transport rates from T1 to T17. This is because waves from the east lose less energy during wave refraction (when compared to the other directions). On the other hand, in the protected areas (T13 to T23), northeast wave conditions are necessary to transport sand anticlockwise.

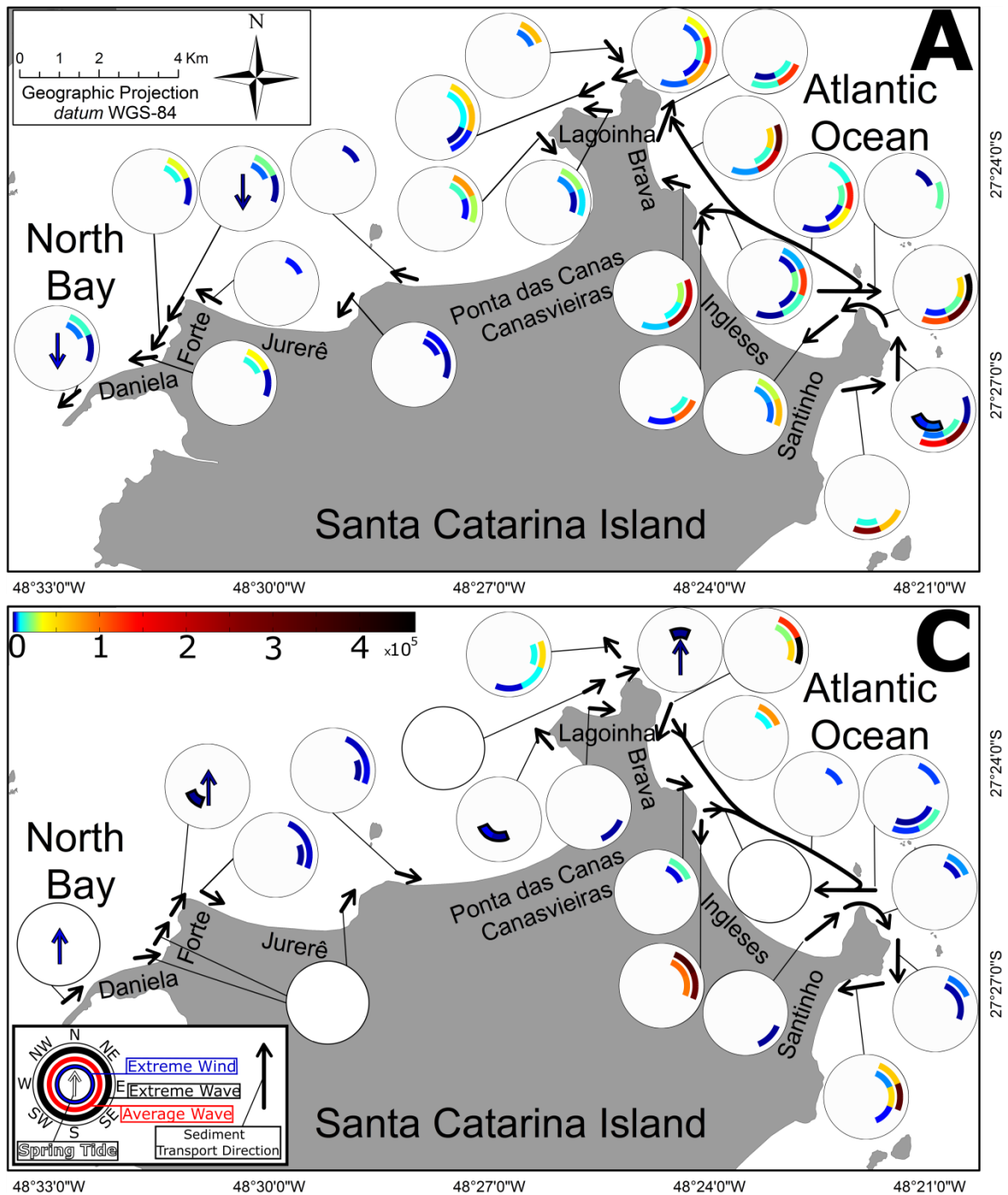


Figure 24: Conceptual model of conditions that generate headland sand bypassing in anticlockwise (A) and clockwise directions (C) press. Hollow circles indicate that sediment transport does not occur in this direction. The arrows represent the sediment transport based on Vieira da Silva (*in press*) for anticlockwise (net) and the opposite of the authors suggestions for clockwise. Colours represent the magnitude of the sediment transport for each scenario in $\text{m}^3 \text{y}^{-1}$.

6. CONCLUSIONS

This paper presented a numerical study assessing the importance of tides, winds and waves on sediment transport around headlands on northern Santa Catarina Island, southern Brazil. Previous headland sediment bypassing studies have always assumed waves are the sole agent of transport and have not tested the influence of tides and winds. This paper has, for the first time, separately tested each driving

forcing to assess their role in the process. It was undertaken using a calibrated and validated numerical model and the results were used to develop a conceptual model for the sediment transport around the headlands and long the beaches.

Tide-driven currents can only transport sediment during spring tides and in very specific locations: T12 (during ebb tides) which is located at the northern tip of Santa Catarina Island where the currents are intensified as the water exits North Bay and flows seaward; T20 and T23, where the entrance of the bay narrows and the tide-currents are intensified. T20 had similar transport rates for both ebb and flood tides while at T23 the ebb tides has a higher rates of sediment transport, indicating a anticlockwise sediment transport at this point.

Wind influence on sediment transport is limited to specific locations: i.e. between a headland and small islands (T2), at the tip of Santa Catarina island (T12); at the northernmost portion of the protected area (T16) and, close to a headland (T20). At all these places the currents are intensified and so is the sediment transport, however only at T2 the transport is in anticlockwise direction, demonstrating the minor influence of winds for sediment transport at the study area.

The waves are the main driving force for headland sediment bypassing in both exposed and protected areas. Waves can transport sediment on the order of $10^5 \text{ m}^3 \text{ y}^{-1}$ while tides and winds can transport up to $10^3 \text{ m}^3 \text{ y}^{-1}$. The more exposed the headland, higher is the sediment transport, and as the coast becomes protected, the magnitude of wave-induced sediment transport reduces, however the wave driven sediment transport remains always higher than tide or wind driven. For headland bypassing to occur the right wave direction is crucial. It has been demonstrated that the headland sand bypassing can occur in either directions at most headlands of the study area. Exceptions are east of Jurerê (T18), south of Forte (T21) and east of Daniela (T22) where bypassing occurs only in an anticlockwise. Anticlockwise is, therefore, the preferable direction of the transport and the direction of the net sediment transport of the study area. On the exposed eastern coast most of headland bypassing occur when waves from east to south are present, while along the protected northern coast the northeast waves dictates the transport around headlands. The harmony between different wave directions is, accordingly, important for the balance for the whole system and its temporal variability may be the cause of

the pulsating cycle of headland sand bypassing observed on the development of Ponta das Canas, Jurerê and Forte spits.

The results also pointed out that because of the varying orientation of the coast, for headland sand bypassing to occur in the exposed area, a combination of different wave directions is needed. First the sand must be transported offshore (from south to northeast depending on the orientation of the coast) followed by a change in wave direction (from south to east) to transport sand to the next beach. In the protected area, on the other hand, northeast waves are required to both transport the sand out of one beach and transport it back to the next. In some locations this can occur during east and southeast wave directions, however with lower transport rates as presented in the conceptual model.

Acknowledgments

The authors would like to acknowledge the support of Fundo Clima – MMA (Process number 3520120), CNPQ (Process number 400302/2012-8 and 303550/2012-0), PRH-PB240 (Process number 48610.002443/2013-14), CAPES (Process number: 005809/2014-02), CASAN and CB&I Brasil.

References

Ab Razak, M.S., Dastgheib, A., Roelvink, D. 2013. Sand bypassing and shoreline evolution near coastal structure comparing analytical solution and XBeach numerical modelling, Proceedings 12th International Coastal Symposium (Plymouth, England), Journal of Coastal Research, Special Issue No. 65, pp. 2083-2088, ISSN 0749-0208.

Ab Razak, 2015. Natural Headland Sand Bypassing: Towards Identifying and Modelling the Mechanisms and Processes. Ph.D. Thesis. Delft University of Technology. CRC Press/Balkema. the Netherlands. ISBN 9781138028647.

Almeida, E.S., Abreu de Castilhos, J. J., Simon, A.F., Avila, E.L., Aumond, J.J., Pinto, N.L.C. dal Santo, N.A. e Infante, N., 1991. Observações Geomorfológicas na Praia do Forte - Ilha da Santa Catarina, Município de Florianópolis - SC. Geosul 11, 38-54.

Araújo, C.E.S.; Franco, D.; Melo Filho, E., and Pimenta, F. 2003. Wave Regime Characteristics of Southern Brazilian Coast. Proceedings of the 6^o International

Conference on Coastal and Port Engineering in Developing Countries, COPEDEC. Colombo, Sri Lanka, Paper 97, 15p.

Bijker, E. W., 1967. Some considerations about scales for coastal models with moveable bed. Technical Report. 50, WL j Delft Hydraulics, Delft, The Netherlands.

Bijker, E. W., 1971. Longshore Transport Computations. Journal of Waterways, Harbors and Coastal Engineering Division, American Society of Civil Engineers, Volume 97(4), 687-701.

Boeyinga, J.; Dusseljee, D.W.; Pool, A.D.; Schoutens, P.; Verduin, F.; Van Zwicht, B.N.M., and Klein, A.H.F., 2010. The effects of a bypass dunefield on the stability of a headland bay beach: A case study. Coastal Engineering 57(1), 152–159.

Cheung, K. F., Gerritsen, F. Cleveringa, j., 2007. Morphodynamics and sand bypassing at Ameland Inet, The Netherlands. Journal of Coastal Research 23, 106-118.

CPE (Coastal Planning and Engineering do Brazil), 2010. Análise de Alternativas para o Terminal de Cruzeiros de Florianópolis - Possíveis Alterações nos Padrões de Circulação e Taxa de Sedimentação no Canal de Acesso ao Porto de Canasvieiras. Florianópolis, SC Brazil. *Technical Report*. Florianópolis, 55p.

Diehl, F. L. Aspectos geoevolutivos, morfodinâmicos e ambientais do Pontal da Daniela, Ilha de Santa Catarina, Brasil. Master thesis Geography. Universidade Federal de Santa Catarina, Florianópolis, 1997.

Duarte, J. Taborda, R., Ribeiro, M., Cascalho, J. Silva, A., Bosnic, I., 2014. Evidences of Sediment Bypassing at Nazaré Headland Revealed by a Large Scale Sand Tracer Experiment. Proceedings of 3^{as} Jornadas de Engenharia Hidrográica. Lisboa. 2014. pp 289-292.

Egbert, G. D. e Erofeeva, S. Y., 2002. Efficient inverse modeling of barotropic ocean tides. Journal of Atmospheric and Oceanic Technology, 19, 183-204.

Egbert, G.D., Bennett, A.F., Foreman, M.G.G, 1994. TOPEX/POSIDON tides estimated using a global inverse model. Journal of Geophysical Research 99 (C12), 24821-24852.

Eslami, S., van Rijn, L., Walstra, D., Luijendijk, A., AND Stive, M., 2010. A Numerical Study on Design of Coastal Groins. in: Scour and Erosion: pp. 501-510.

Evans, O. F., 1943. The relation of the action of waves and currents on headlands to the control of shore erosion by groynes. Academy of Science for 1943 9-13.

Fitzgerald, D. M. Krauss, N. C., Hands, E. B. , 2000. Natural Mechanisms of Sediment Bypassing at Tidal Inlets. ERDC/CGL CHETN-IV -30 US Army Corps of Engineering.

Fitzgerald, D. M. E Pendleton, E., 2002 Inlet formation and evolution of the sediment bypassing system: New Inlet Cape Cod, Massachusetts. Journal of Coastal Research. SI 36, 290-299.

FitzGerald, D.M., Cleary, W.J., Buynevich, I.V., Hein, C.J., Klein, A.H.F., Asp, N., and Angulo, R, 2007. Strandplain Evolution along the Southern Coast of Santa Catarina, Brazil. Journal of Coastal Research, SI 50 (Proceedings of the 9th International Coastal Symposium), 152 – 156. Gold Coast, Australia, ISSN 0749.0208

Garel, E., Sousa, C., Ferreira, Ó., 2015. Sand bypass and updrift beach evolution after jetty construction at an ebb-tidal delta, Estuarine, Coastal and Shelf Science.

George, D.A, Largies, J.L., Storlazzi, C.D., Barnard. P.L., 2015. Classification of rocky headlands in California with relevance to littoral cell boundary delineation. Marine Geology, 369, 137-152.

Goodwin, I. D., Freeman, R., Blackmore, K., 2013, An insight into headland sand bypassing and wave climate variability from shoreface bathymetric change at Byron Bay, New South Wales, Australia. Marine Geology, 341, 29-45.

H2 Engenharia. 2008. Estrutura de Apoio à Navegação - Canasvieiras, Florianópolis, SC. *Technical Report*. Florianópolis, 423 p.

Horn Filho, N. O., 2006. Granulometria das Praias Arenosas da Ilha de Santa Catarina. GRAVEL. Porto Alegre. (4). 1-21.

Kamphuis, J.W., 2010. Introduction to Coastal Engineering and Management. Advanced Series on Ocean Engineering - Vol 30. World Scientific Press, 2nd ed. Singapore. 525p.

- Klein, A. H. F., Ferreira, Ó., Dias, J. M. A., Tessler, M. G., Silveira, L. F., Benedet, L., Menezes, J. T., Abreu, J. G. N., 2010. Morphodynamics of structurally controlled headland-bay beaches in southeastern Brazil: A review. *Coastal Engineering* 57, 98-111.
- Klein, A. H. F., Short, A. D., Bonetti, J. *in press*. Santa Catarina beach Systems. in: Short, A. D and Klein, A. H. F. (eds) *Brazilian Beach Systems*. Springer Coastal Research Library.
- Lessa, G. C.; Dominguez, J. M. L.; Bittencourt, A. C.S.P. and Brichta, Arno. 2001 The tides and tidal circulation of Todos os Santos Bay, Northeast Brazil: a general characterization. *Anais da Academia Brasileira de Ciências* 73 (2), 245-261.
- Martins L.R., and Eichler, B.B., 1969. Propriedades texturais dos sedimentos litorâneos de Santa Catarina. 11: areias de praia e dunas, trecho Laguna-Imbituba. *Notas e Estudos*. Escola de Geologia, Universidade Federal do Rio Grande do Sul, 2(1):27-44
- Mariani, A., Carley, J. T., and Miller, B. M., 2010, Infilling and Sand Bypassing of Coastal Structures and Headlands by Littoral Drift. 19^o NSW Coastal Conference, Batemans Bay NSW.
- Masselink, G. and Short, A. D., 1993. The Effect of Tide Range on Beach Morphodynamics and Morphology: A Conceptual Beach Model. *Journal of Coastal Research* 9 (3), 785-800.
- Masselink, G., Parriaratchi, C. B., 1998. The Effect of Sea Breeze on Beach Morphology, Surf Zone Hydrodynamics and Sediment Resuspension. *Marine Geology*. 146. p. 115- 135.
- Nobre, C. A.; Cavalcanti, M. A. G.; Nobre, P.; Kayano, M. T.; Rao, V. B.; Bonatti, J. P.; Satyamurti, P.; Uvo, C. B., and Cohen, J. C. 1996. Aspectos da climatologia dinâmica do Brasil. *Climanálise Special Issue* (no number), 65p.
- Pinto, M. W.; Meireles, R.; Cooper, A., and Klein, A. H. F. 2015. Santinho/Ingleses Transgressive Dunefield system - Santa Catarina Island (Brazil): Temporal Variability in Vegetation, Manmade Structures and Dune Migration. *Proceedings of Coastal Sediments'15* (San Diego, CA, USA), 14p.

Porpilho, D., Klein, A.H.F, de Camargo, R. S. V., Prado, M. F. V., Short, A. D., Vieira da Silva, G. 2016. Santinho-Ingleses headland bedform characterization through interferometric data, Santa Catarina Island, southern Brazil. Proceedings of ICS 2016.

Ribeiro, M., Taborda, R., Lira, C., Bizarro, A., Oliveira, A., 2014. Headland Sediment Bypassing and Beach Rotation in a Rocky Coast: An Example at the Western Portuguese Coast. Geophysical Research Abstracts. 16. EGU2014-14602.

Saha, S., Moorthi,S., Wu, X., Wang, J., Nadiga, S., Tripp, P., Behringer, D., Hou, Y., Chuang, H., Iredell, M., Ek, M., Meng, J., Yang, R., Mendez, M. P., van den Dool, H., Zhang, Q., Wang, W., Chen, M., and Becker, E., 2014. The NCEP Climate Forecast System Version 2. *J. Climate*, 27, 2185–2208.doi: <http://dx.doi.org/10.1175/JCLI-D-12-00823.1>

Short, A. D. and Masselink, G. Eds. 1999. Embayed and structurally controlled beaches, In:Short, A.D. (ed).,Handbooks of Beach and Shoreface Hydrodynamics. John Wiley & Sons, Chicester.

Silveira, L. F., Klein, A. H. F., Tessler, M. G., 2010. Headland-Bay Beach Planform Stability of Santa Catarina State and of the Northern Coast of São Paulo State. *Brazilian Journal of Oceanography* 58 (2) 101-122.

Silvester, R., 1985. Sediment By-Passing Across Coastal Inlets by Natural Means. *Coastal Engineering* 9, 327-346.

Smith, A.W., 2001. Headland bypassing. *Coasts & Ports 2001: Proceedings of the 15th Australasian Coastal and Ocean Engineering Conference, the 8th Australasian Port and Harbour Conference*, Institution of Engineers, Australia, Barton, A.C.T., pp. 214–216

Soulsby, R., 1997. Dynamics of marine sands, a manual for practical applications. Thomas Telford, London.

Tolman, 2009 H.L. User manual and system documentation of WAVEWATCH-III Tech. rep., NOAA/NWS/NCEP/OMB (2009).

Tolman, H.L. 1991. A third-generation model for wind waves on slowly varying, unsteady and inhomogeneous depths and currents. *Journal of Physical Oceanography* 21, 782–797.

Tolman, H.L. 1997. User manual and system documentation of WAVEWATCH-III version 1.15 NOAA/NWS/NCEP/OMB, United States (1997).

Truccolo, E.C., 2011. Assessment of the Wind Behaviour in the Northern Coast of Santa Catarina. *Revista Brasileira de Meteorologia* 26(3), 450-460.

Truccolo, E.C.; Franco, D., and Schettini, C.A.F., 2004. The Low Frequency Sea Level Oscillations in the Northern Coast of Santa Catarina, Brazil. *In: Klein et al. (ed.), Proceedings of International Coastal Symposium. Journal of Coastal Research, Special Issue No. 39, pp. 547-552.*

Van Rijn, L.C., 1993 Principles of sediment transport in rivers, estuaries and coastal seas. Aqua Publications: Amsterdam.

Van Rijn, L.C., 2000. General view on sand transport by currents and waves. Report Z2899.20/Z2099.30/Z2824.30. Delft Hydraulics, Delft, The Netherlands

Vieira da Silva, G, Toldo Jr.,E.E., Klein, A.H.F., Short,A.D., Woodroffe,C.D. *inpress*. Headland Sand Bypassing - Quantification of Net Sediment Transport in Embayed Beaches, Santa Catarina Island North Shore, Southern Brazil. Submitted to *Marine Geology*.

Vieira da Silva, G., Muler, M., Prado, M. F. V., Short, A. D., Toldo Jr., E. E., Klein, A. H. F., 2016, Shoreline changes Analysis and Insights into Sediment Transport Path - Example of Santa Catarina Island North Shore, Brazil. *Journal of Coastal Research* Accepted for publication.

Vintem, G.; Tomazelli L. J. and Klein, A. H. F, 2006. The effect of sand grain size in the aeolian transport processes of transgressive dunefields of the coast of the Santa Catarina State Brazil. *Journal of Coastal Research, SI 39 (Proceedings of the 8th International Coastal Symposium),102 - 106. Itajaí, SC, Brazil, ISSN 0749-0208.*

TRABALHOS FUTUROS

O presente trabalho analisou o processo de transposição sedimentar incluindo distintas metodologias (i.e. análise de variação de linha de costa, medições de campo e modelagem numérica), contudo, alguns processos foram simplificados e, por isso, sugerem-se alguns tópicos para a continuidade deste estudo.

- **Análise dos efeitos de mares bi ou multimodais:** Sabe-se que no estado de Santa Catarina a presença de mares bi ou por vezes multimodais ocorre com frequência (30% do tempo de acordo com Araujo et al., 2003). Como demonstrado nesta tese, na parte exposta, ondas entre sul e leste são responsáveis pelo transporte de sedimentos no sentido preferencial do transporte, por outro lado, ondas de nordeste são as responsáveis pela continuidade do transporte na porção abrigada. Além disso, a propagação espectral de ondas (incluindo mares bi ou multimodais), como realizado no artigo II, permite que os mares secundários (normalmente leste ou nordeste) atuem como agente gerador do transporte de sedimentos - importantes para a porção abrigada da área de estudo. No caso de simulações paramétricas (sem a inclusão de mares secundários), acredita-se, ocorreria redução das previsões de taxas de transporte na área abrigada. Apesar de terem sido incluídos nas propagações do artigo II, para simplificação, estas condições não foram testadas no artigo III.

- **Análise dos efeitos das ondas de infragravidade:** a escolha do modelo numérico é parte fundamental do processo de modelagem numérica. Dependendo o objetivo e da escala espacial e temporal do estudo, alguns processos/forçantes podem ser simplificados ou desconsiderados. Nesta tese, o modelo Delft3D foi selecionado por ser capaz de simular longos intervalos de tempo (ano), incluindo o efeito de ventos, marés e ondas. Entre os processos desconsiderados pelo modelo utilizado está a ação das ondas de infragravidade. Alguns estudos, porém, indicam que a ação dessas ondas pode estar relacionada com o transporte de sedimentos em direção ao mar, conseqüentemente, disponibilizando sedimento para a transposição de sedimentos. Sugere-se como trabalhos futuros a análise da ação das ondas de infragravidade no processo de transposição sedimentar nos promontórios com modelos capazes de reproduzir esse processo (e.g. XBeach). Ressalta-se que, neste caso, as escalas temporal e espacial devem ser reduzidas em virtude da maior demanda computacional desse tipo de modelo.

CONSIDERAÇÕES FINAIS

Esta tese teve como objetivo estabelecer uma compreensão do processo de transposição de sedimentos (*bypassing*), entre promontórios, tendo como área de estudo a costa norte da Ilha de Santa Catarina. Para atingir esse objetivo, a tese foi estruturada em três partes: 1) o transporte de sedimentos foi inicialmente inferido a partir da análise da variação da linha de costa das praias adjacentes aos promontórios estudados; 2) foi realizada a medição do transporte de sedimentos no entorno de dois promontórios considerados chave para este estudo: a) entre as praias Ingleses e Brava com alta exposição às ondas e; b) entre as praias Lagoinha e Ponta das Canas (onde se desenvolve ciclicamente um pontal arenoso) e um modelo numérico baseado nos processos (*process based*) foi configurado, as ondas, correntes e marés foram calibrados e validados e foi identificada a equação de transporte de sedimentos que melhor reproduz esta dinâmica. Foram simuladas as condições ambientais durante um ano e os resultados apontaram a magnitude e direção do transporte líquido de sedimentos; e 3) foram simulados 26 cenários de ondas, ventos e marés para identificar os processos e condições que causam a transposição de sedimentos e gerar um modelo conceitual do mesmo para a área de estudo. A hipótese da pesquisa que a ação das ondas é a principal forçante da transposição de sedimentos nos promontórios foi confirmada, porém, foi observado que a influência de marés e ventos é mais restrita que se supunha. Esta é apenas observada durante condições extremas de vento ou maré de sizígia em locais onde a corrente é intensificada em função da presença de promontórios ou ilhas.

A partir dos resultados apresentados foi possível compreender a dinâmica sedimentar de forma abrangente e a partir de distintas metodologias, incluindo, variação de linha de costa, medições de transporte de sedimentos e modelagem numérica. As principais conclusões que foram obtidas a partir desta tese são:

1) A análise de variação de linha de costa tradicional aliada a métodos estatísticos geram resultados com maior grau de confiabilidade sendo possível identificar (embora os processos ocorram em escalas distintas) a rotação praial; a importância da presença das dunas entre Ingleses e Santinho para o balanço sedimentar de ambas as praias; o controle sedimentar das praias a oeste de Ponta das Canas pelo pontal que ali ciclicamente se desenvolve atuando como fonte (quando o pontal se une à costa e o sedimento é distribuído) ou sumidouro (quando o pontal está em

desenvolvimento) de sedimento; e, por fim, foi identificado o transporte de sedimentos no sentido anti-horário nas praias estudadas. Contudo, a partir desse tipo de análise não foi possível identificar conexões entre algumas praias bem como o volume de sedimentos que é transportado entre elas.

2) O terceiro capítulo desta tese (segundo artigo) apresentou um estudo que incluiu metodologias complementares para avaliar o processo de transposição de sedimentos nos promontórios. Medidas de campo são muito importante e confiáveis, porém, sua abrangência temporal e espacial é limitada, por outro lado o uso de modelos numéricos é muito útil para compreender a dinâmica sedimentar como um todo, contudo são dependentes de medidas de campo para que esse seja calibrado e validado. Os resultados demonstraram que o processo de transposição de sedimentos pode ocorrer também sem a formação cíclica de um pontal arenoso como descrito na literatura, sendo o transporte ao longo da costa o principal contribuinte para esta dinâmica. Foi também observado o transporte através da plataforma interna. A conexão entre as praias da área de estudo foi demonstrada e quantificada a partir de medições de campo e modelagem numérica. Portanto, ao invés de serem consideradas células fechadas é recomendado que as entradas e saídas de sedimentos nas praias estudadas seja considerada em qualquer intervenção (i.e. obras costeiras), e se for o caso, que seja conduzida de modo planejado e sustentável. Essa é uma importante conclusão com ampla aplicação global onde praias são consideradas células fechadas.

3) Por fim, o estudo numérico de cenários foi apresentado e a importância das marés, ventos e ondas no transporte de sedimentos no entorno dos promontórios do norte da Ilha de Santa Catarina foi apresentada e quantificada. Este é o primeiro registro na literatura sobre a importância das forçantes no processo de transposição de sedimentos nos promontórios. As correntes geradas por marés são capazes de transportar sedimentos apenas durante marés de sizígia em locais específicos onde as correntes são intensificadas devido à presença e costões ou da proximidade da Ilha de Santa Catarina com o continente. Os ventos também geram correntes capazes de transportar sedimentos durante condições extremas em locais específicos (e.g. entre um promontório e pequenas ilhas, no extremo norte da ilha, ou próximo a promontórios). Nesses lugares ocorre a intensificação das correntes e conseqüentemente do transporte de sedimentos. Como demonstrado, a transposição de sedimentos pode ocorrer em ambas as direções (dependendo da

incidência das ondas). Exceções são o leste de Jurerê, sul do Forte e leste da Daniela, onde a transposição ocorre apenas na direção anti-horária (predominante). Por fim, foi demonstrado que as ondas são as principais forçantes da transposição de sedimentos na área de estudo tanto nas partes abrigadas, quanto nas protegidas. Ondas são capazes de transportar sedimento em uma ordem de magnitude de 10^5 m^3 ano⁻¹ enquanto marés e ventos transportam até 10^3 m^3 ano⁻¹. Para ocorrer a transposição de sedimentos nos promontórios a direção de aproximação da onda é crucial. Para o estabelecimento da condição predominante do transporte de sedimentos (anti-horário), na parte exposta (leste) da área de estudo é necessária a atuação de ondas de sudeste e sul, enquanto na área abrigada (norte) é necessária a atuação de ondas de nordeste. Portanto, a harmonia entre diferentes direções de ondas é importante para o balanço do sistema e a variabilidade temporal dessas direções pode ser a causa dos ciclos "pulsantes" de transposição de sedimentos observados no desenvolvimento dos pontais de Ponta das Canas, Jurerê e Forte. A partir dos resultados apresentados um modelo conceitual sobre as condições necessárias para o transporte de sedimentos entre as praias, tanto no sentido horário, quanto anti-horário, foi proposto a fim de facilitar a compreensão do processo na costa norte da Ilha de Santa Catarina.

REFERÊNCIAS BIBLIOGRÁFICAS

Ab Razak, M.S., Dastgheib, A., Roelvink, D. 2013. Sand bypassing and shoreline evolution near coastal structure comparing analytical solution and XBeach numerical modelling, Proceedings 12th International Coastal Symposium (Plymouth, England), Journal of Coastal Research, Special Issue No. 65, pp. 2083-2088, ISSN 0749-0208.

Ab Razak, 2015. Natural Headland Sand Bypassing: Towards Identifying and Modelling the Mechanisms and Processes: Delft University of Technology. CRC Press/Balkema. the Netherlands. Ph.D. Thesis. 186 p.

Araújo, C.E.S.; Franco, D.; Melo Filho, E., and Pimenta, F., 2003. Wave regime characteristics of southern Brazilian coast. *Proceedings of the 6^o International Conference on Coastal and Port Engineering in Developing Countries, COPEDEC* (Colombo, Sri Lanka), Paper 97, 15p.

Cheung, K.F.; Gerritsen, F., and Cleveringa, J., 2007. Morphodynamics and sand bypassing at Ameland Inlet, The Netherlands. *Journal of Coastal Research*, 23(1), 106-118.

CPE, 2010. *Análise de alternativas para o terminal de cruzeiros de Florianópolis - possíveis alterações nos padrões de circulação e taxa de sedimentação no canal de acesso ao porto de canasvieiras*. Florianópolis, SC Brazil: Coastal Planning and Engineering do Brazil, 55p.

Duarte, J. Taborda, R., Ribeiro, M., Cascalho, J. Silva, A., Bosnic, I., 2014. Evidences of Sediment Bypassing at Nazaré Headland Revealed by a Large Scale Sand Tracer Experiment. Proceedings of 3^{as} Jornadas de Engenharia Hidrográfica. Lisboa. 2014. pp 289-292.

Eslami, S.; Van Rijn, L.; Walstra, D.; Luijendijk, A., and Stive, M., 2010. A Numerical study on design of coastal groins. *Proceedings of International Conference on Scour and Erosion* (San Francisco, CA, USA), pp. 501-510.

Evans, O. F., 1943. The relation of the action of waves and currents on headlands to the control of shore erosion by groynes. *Academy of Science for 1943* 9-13.

FEMAR, 2000. Catálogo de Estações Maregráficas Brasileiras, página 267. disponível *online* em: <http://www.fundacaofemar.org.br>. Acessado em 02/04/2013.

Fitzgerald, D.M. and Pendleton, E., 2002. Inlet formation and evolution of the sediment bypassing system: New Inlet Cape Cod, Massachusetts. *In: Cooper and Jackson (eds.), Proceedings of International Coastal Symposium*. Journal of Coastal Research, Special Issue No. 36, pp. 290-299.

Fitzgerald, D.M., Krauss, N.C., and Hands, E.B., 2000. *Natural Mechanisms of Sediment Bypassing at Tidal Inlets*. Vicksburg, Mississippi: US Army Corps of Engineering, Report ERDC/CGL CHETN-IV-30,10p.

GAPLAN. 1986. Atlas de Santa Catarina. Gabinete de Planejamento e Coordenação Geral, Rio de Janeiro.

Garel, E., Sousa, C., Ferreira, Ó., 2015. Sand bypass and updrift beach evolution after jetty construction at an ebb-tidal delta, *Estuarine, Coastal and Shelf Science*.

George, D.A, Largies, J.L., Storlazzi, C.D., Barnard. P.L., 2015. Classification of rocky headlands in California with relevance to littoral cell boundary delineation. *Marine Geology*, 369, 137-152.

Goodwin, I.D., Freeman, R., and Blackmore, K., 2013. An insight into headland sand bypassing and wave climate variability from shoreface bathymetric change at Byron Bay, New South Wales, Australia. *Marine Geology*, 341(1), 29-45.

Horn Filho, N. O., 2006. Granulometria das Praias Arenosas da Ilha de Santa Catarina. GRAVEL. Porto Alegre. (4). 1-21.

IBGE, 2010. Cidades@: dados do censo demográfico 2010 por cidade. acesso *online* < <http://www.ibge.gov.br/cidadesat/topwindow.htm?1>>. acessado em: 02/04/2013.

Lessa, G. C.; Dominguez, J. M. L.; Bittencourt, A. C.S.P. and Brichta, Arno. 2001 The tides and tidal circulation of Todos os Santos Bay, Northeast Brazil: a general characterization. *Anais da Academia Brasileira de Ciências* 73 (2), 245-261.

Mariani, A.; Carley, J.T., and Miller, B.M., 2010, Infilling and sand bypassing of coastal structures and headlands by littoral drift. *Proceedings of 19º NSW Coastal Conference* (Batemans Bay, NSW, Austrália), 8p.

Masselink, G., Pattiaratchi, C.B., Seasonal changes in beach morphology along the sheltered coastline of Perth, Western Australia. *Marine Geology*. 172, 243-263.

MONTEIRO, M. A. 1992. Avaliação das condições atmosféricas de Florianópolis para controle da qualidade do ar. Florianópolis. Monografia. Curso de Geografia, Universidade Federal de Santa Catarina.

Ribeiro, M., Taborda, R., Lira, C., Bizarro, A., Oliveira, A., 2014. Headland Sediment Bypassing and Beach Rotation in a Rocky Coast: An Example at the Western Portuguese Coast. Geophysical Research Abstracts. 16. EGU2014-14602.

Short, A.D. and Masselink, G. Eds. 1999. Embayed and structurally controlled beaches, *In: Short, A.D.(ed), Handbooks of Beach and Shoreface Hydrodynamics*. New York: John Wiley and Sons, pp. 230–249.

Silveira, L.F.; Klein, A.H.F., and Tessler, M.G., 2010. Headland-bay beach planform stability of Santa Catarina state and of the northern coast of São Paulo state. *Brazilian Journal of Oceanography*, 58 (2), 101-122.

Silvester, R., 1985. Sediment by-passing across coastal inlets by natural means. *Coastal Engineering*, 9, 327-346.

SIMÓ, D. H. e, HORN FILHO, N. O., 2004. Caracterização e Distribuição Espacial das Ressacas e Áreas de Risco na Ilha de Santa Catarina, SC, Brasil., GRAVEL. 2. p. 96-103.

Smith, A.W., 2001. Headland bypassing. *Coasts & Ports 2001: Proceedings of the 15th Australasian Coastal and Ocean Engineering Conference, the 8th Australasian Port and Harbour Conference*, Institution of Engineers, Australia, Barton, A.C.T., pp. 214–216.